T.C.

AYDIN ADNAN MENDERES UNIVERSITY

GRADUATE SCHOOL OF NATURAL AND APPLIED SCIENCES

MASTER'S PROGRAMME IN CIVIL ENGINEERING

2022-YL-004

DELAMINATION ANALYSIS OF LAMINATED GLASS PLATE STRUCTURES

FULYA OYAR

MASTER'S THESIS

SUPERVISOR

Assoc. Prof. Dr. Ebru DURAL

AYDIN–2022

ACKNOWLEDGEMENTS

I wish to express her deepest gratitude to my supervisor Assoc. Prof. Dr. Ebru DURAL for her guidance, advice, criticism, encouragements and insight throughout the research.

Words cannot describe my gratitude towards the person dearest to me Hülya; my mother. Her belief in me, although at times irrational, has been vital for this work. I dedicate this thesis to her.

TABLE OF CONTENTS

LIST OF SYMBOLS AND ABBREVATIONS

ϕ : Angle undergone by an originally horizontal fiber of the interlayer

θ : Angle undergone by an originally vertical fiber of the interlayer

μ : Poisson's ratio for the glass

α,β : Interpolation parameters

$\{w\}$: Lateral displacement vector

γ_{xz}, γ_{yz} : Shear strain components of the interlayer

$\overline{U}_b^{(2)}$: Bending strain energy for the bottom plate

$\overline{U}_b^{(1)}$: Bending strain energy for the top plate

$\overline{\Omega}$: Load potential energy function

$\overline{U}_m^{(2)}$: Membrane strain energy for the bottom plate

$\overline{U}_m^{(1)}$: Membrane strain energy for the top plate

$\overline{U}_{xz}^{(I)}, \overline{U}_{yz}^{(I)}$: Shear strain energy for the interlayer due to γ_{xz}, γ_{yz}, respectively

e_{2x}, e_{2y}, e_{2xy} : Strain components of the bottom plate

e_{1x}, e_{1y}, e_{1xy} : Strain components of the top plate

[A] : Matrix containing linear terms of the lateral displacement field equation

{RHS} : Vector containing the right hand side of the lateral displacement field equation.

$\mathbf{D_1}$: Flexural Rigidity of the top plate

$\mathbf{D_2}$: Flexural Rigidity of the bottom plate

E : Glass Young's modulus

G : Glass shear modulus

h_1 **:** Thickness of the top plate

h_2 **:** Thickness of the bottom plate

h_x **:** Finite difference mesh length in the x direction

hy **:** Finite difference mesh length in the y direction

nx, ny **:** Number of subdivisions in the x and y directions, respectively.

q **:** Uniform applied lateral pressure

t **:** Thickness of the interlayer

u_1 **:** In plane displacement for the top plate in the x direction.

u_2 **:** In plane displacement for the bottom plate in the x direction.

V **:** Total potential energy of the system

v_1 **:** In plane displacement for the top plate in the y direction.

v_2 **:** In plane displacement for the bottom plate in the y direction

w **:** Lateral deflection of the top and bottom plate

w_{max} **:** Maximum lateral deflection

x,y,z **:** Rectangular coordinates

LIST OF FIGURES

LIST OF TABLES

ÖZET

LAMİNE CAM PLAK YAPILARININ DELAMİNASYON ANALİZİ

Oyar F. Aydın Adnan Menderes Üniversitesi, Fen Bilimleri Enstitüsü, İnşaat Mühendisliği Programı, Yüksek Lisans Tezi, Aydın, 2022.

Amaç: Bu çalışmada amaç, lamine cam plak yapılarının delaminasyon analizi için matematiksel bir model geliştirmektir.

Materyal ve Yöntem: Bu çalışmada, lamine bir cam tabakada delaminasyon incelenmiştir. Deformasyon ve gerilme denklemleri varyasyonel yaklaşım, minimum potansiyel enerji teoremi ve sonlu elemanlar yöntemi ile elde edilir. Geliştirilen matematiksel modelde kullanılan varsayımların doğrulanması için lamine cam levha bir sonlu eleman yazılımı kullanılarak modellenmiştir.

Bulgular: Lamine cam, iki kat camın PVB (Polivinil butiral) veya farklı bir yapıştırıcı ile ısı ve basınç yardımı ile birleştirilmesiyle oluşturulan bir cam türüdür. Herhangi bir darbe yükü ile karşılaşıldığında etrafa yayılmaz ve örümcek ağı şeklinde çatlaklar oluşur. Bu çalışmanın konusu, lamine cam levha yapıların delaminasyon analizidir. Delaminasyon, kompoziti oluşturan katmanların ayrılması olarak tanımlanır. Kompozit katmanlar arasındaki düşük mukavemet nedeniyle en yaygın hasar türüdür.

Sonuç: Malzeme sertliği kaybı ve malzeme ömrünün kısalması gibi sonuçlar verebildiği için önemli bir çalışma konusudur.

Anahtar Kelimeler: Delaminasyon Analizi, Lamine Cam Plak, Matematiksel Modelleme, Sonlu Elemanlar Yöntemi, Varyasyonel Yaklaşım, Doğrusal Olmayan Davranış.

ABSTRACT

DELAMINATION ANALYSIS OF LAMINATED GLASS PLATE STRUCTURES

Oyar F. Aydın Adnan Menderes University, Graduate School of Natural and Applied Sciences, Civil Engineering Program, Master Thesis, Aydın, 2022.

Objective: The object of this study is to improve a mathematical model for delamination analysis of laminated glass plate structures. In this study, delamination is investigated in a laminated glass plate.

Material and Methods: Deformation and stress equations are obtained by the variational approach, finite element method and minimum potential energy theorem. For the verification of assumptions used in the developed mathematical model the laminated glass plate is modeled using a finite element software.

Results: Laminated glass defined as a type of glass created by combining two layers of glass with PVB (polyvinyl butyral) or a different adhesive with the help of heat and pressure. When faced with any impact load, it does not spread around and cracks in the form of spider webs occur. The subject of this study is delamination analysis of laminated glass plate structures. Delamination is defined as the separation of the layers that make up the composite. It is the most common type of damage due to low strength between composite layers.

Conclusion: It is an important study subject because it can produce results such as loss of material hardness and shortened material life.

Keywords: Delamination Analysis, Finite Element Method, Laminated Glass Plate, Mathematical Modelling, Variational Approach, Nonlineer Behavior.

1. INTRODUCTION

1.1. Glass

Since ancient times, glass has been used as both construction and ornamental items. Today, it still has a very common usage area, from the simplest tools to communication and space technologies. Glass is a material that is always encountered in daily life.

Glass is used as the main material in many sectors in a wide range of products, from the window to the drinking glass, from the lid of the washing machine to the glasses. It is a fluid material formed by the dissolution of instantly cooled alkali and alkaline earth metal oxides and some other metal oxides, and its main material is silicon. Glass solidifies, preserving its amorphous structure. Due to rapid cooling during production, an amorphous structure is formed instead of a crystalline structure. This structure gives the glass strength and transparency.

The most classic explanation of glass production is explained by Paul (1990) as follows:

When the liquid freezes, its fluidity decreases, and at a certain degree below the freezing point, this fluidity approaches almost zero. Thus, the liquid becomes solid.

In general, glass production process consists the following stages:

Raw Material: Mostly silica-based materials such as sand, limestone, feldspar, dolomite, soda, sodium sulfate are made suitable for melting, cleaned and stocked.

Blend: According to the glass to be produced, the above-mentioned materials are mixed according to certain recipes.

Melting: The blend is melted by heating up to 1500-1600ºC in special furnaces using natural gas, fuel-oil or electricity.

Shaping: Melted glass shaping, again according to the product's feature taken into sections. Blowing, pressing, rolling, flotation, tossing, flowing etc. It is put into the desired form by one of the methods.

Cooling: Glass, which is a very fragile material in its natural state, is reheated and cooled in a controlled manner and is relieved of internal tension. This makes the material more durable.

Storage: Depending on the characteristics such as organization, market and product, the glass product is stored with special packaging and storage equipment.

Shipping: Since glass is not a bulk and rough cargo, its transportation also requires special vehicles. Glass is transported with trucks and transport equipment produced for this purpose.

Glass, which passes through these stages, is used as auxiliary material or raw material in many sectors. For example, glass is widely used in the packaging industry, as it does not react chemically with the various substances put into it. The fact that it is environmentally friendly and a highly recyclable material makes glass both useful and preferable. This feature also means raw material and energy savings for manufacturers.

It would not be wrong to say that there are different types of glass in terms of glass types. Glasses, each of which has different features in itself, also bring different advantages for users. In fact, it is possible to say that the advantages and features it provides are effective in glass selection. While some of them are in an important position in terms of durability, some of them add difference to their environment with their aesthetic appearance. For this reason, it is useful to dwell on some of the glass types. Now, let us give information about the most curious glasses among the varieties.

Tempered Glass: It is among the structurally very durable glass models. Tempered glass, also known as reinforced or toughened glass, does not break into small pieces when broken, minimizing the risk of injury. Due to its durable structure, it is often preferred on the exterior.

Reflective Glasses: It is one of the very effective glasses for breaking the heat from the sun. It is produced by applying a metallic coating to the surface. The metallic coating applied to the surface also creates a mirror effect and thus makes the interior visible. It is generally seen on the exterior of buildings.

Double Glazing: It may consist of two or three flat panes. In double glazing, it consists of spaces filled with vacuum or gas between the layers. In addition, double glazing, which offers effective solutions for energy saving, is also used a lot for sound insulation.

Laminated Glass: Combination of at least two or more glass plates. PVB (Polyvinyl Butyral) is used in the production of these glasses, and the glasses are brought together by heat and pressure. In addition to its durable structure, laminated glasses are glass models that stand out in sound insulation with their acoustic types. The areas where they are generally used are safety and automobile windows. By tempering laminated glasses, it is possible to increase their strength to higher levels.

1.1.1. Laminated Glass

Laminated glass defined as a material obtained by combining two or more layers of glass with one or more PVB interlayers under high temperature (145ºC) and pressure (13 bar) and with very high mechanical strength properties. It has taken its place in our daily life as a modern building material that can be used easily in places where all kinds of safety and security precautions are desired, by removing all the borders related to the use of glass.

Laminated glass provides the building with strength and beauty, durability and openness while meeting its design needs. In addition to being long-lasting, its ability to meet many functions is provided only with laminated glasses, where the durability and strength of the glass and the flexibility of the plastic material meet. The strong, harmonious glass material, obtained as a result of the combination, offers a material that provides a wide range of design possibilities and has eye-catching properties to meet every need.

Figure 1.1. Laminated glass unit.

Depending on the design needs, laminated glasses can be made using softened glass layers, tempered, chemically or thermally reinforced glasses, which are obtained by softening slowly after cooling. It is very easy to work with laminated glasses in buildings

and to replace them.

Laminated glass has become a very important material among the contemporary building materials with the opportunities it provides to the building industry in terms of providing important structural performance features and benefits.

Laminated glasses are for human and human safety. The way to be able to use it, is to know and learn about laminated glass. Laminated glass, the use of which is increasing rapidly in the world, is now in the world standards and specifications for human safety, life and property safety, etc. It has become a modern building material that has been made compulsory for many reasons. In other words, the use of laminated glass is obligatory wherever there is the slightest possibility of harming people. With the recognition of the intermediate layer material PVB (Polyvinyl Butyral), which gives laminated glasses all mechanical strength properties, it is now the first material that comes to mind in designs.

Universities that provide technical training in this regard also have a great job to do. All materials, such as laminated glass, should be transferred to the students immediately, and students should be guided to the most appropriate use of these new materials even in their designs, and they should be made aware of the business. In this way, a student with up-to-date material knowledge will always be able to choose and apply the most appropriate material with a choice ability to decide for the better.

Since our subject is laminated glass, lectures and seminars should be given and spread at universities with the help of the authorities of the companies, if necessary, so that the core structure of engineering is recognized by the students.

Even if these things are not fulfilled, the use of laminated glass with PVB will become a necessity as a result of the imposition of living standards and living conditions, and will become widespread.

Conditions and experiences will in the process make laminated glass necessary for the building and especially for the human being. In addition, laminated glass will gain its importance in our daily life as a mandatory modern building material over time.

1.1.1.1. Benefits of Laminated Glass

Benefits of laminated glass can be listed as:

- It doesn't disintegrate in case of breakage, the parts stay in situ, and prevents the danger of injury, protect life and property.
- It prevents or delays entry in attacks and theft attempts with tools like stones and sticks.
- With its low UV transmittance, it prevents the passage of UV rays by 97-99%,
- It ensures that the natural colors of the things are preserved for a extended period of your time.
- It contributes to noise control. Internal partitions, doors, windows, curtain facades, showcases, overhead and skylight glasses, windbreakers, railings are some examples of using areas of laminated glass.

There are some important issues to be considered during the processing, stocking and application of shatterproof glass and they can be summarized as:

The edges of the shatterproof glass shouldn't be left exposed in reality with water, but should be protected.

There's a risk of thermal breakage in safety glass. Micro and macro cracks that will occur during edge cutting of shatterproof glass increase this risk. One of the ways to eliminate the danger is to deburring or grinding the sides of the glass.

Laminated glass storage conditions should lean maximum attention. Care should be taken to not be plagued by humidity and temperature conditions.

Corrosion may occur if safety glass is replaced after cutting without being washed and completely dried. For this reason, if glass is to be installed as one unit, it should be installed after washing and drying.

Glasses that compose safety glass (perforated glasses, etc.) could also be tempered or partially tempered because of static reasons.

1.1.1.2. Delamination

Delamination is defined as the separation of the layers that make up the composite. It is the most common type of damage due to low strength between composite layers. It is an important study subject because it can produce results such as loss of material hardness and shortened material life.

Delamination is a failure mode due to the loss of adhesion between the layers of laminated composites. Delamination may be due to breakage or separation in adhesive or resin, fracture in reinforcement. It tends to degrade the durability and strength as well as the aesthetic appearance of the material. Including laminate composites, concrete and composite materials many materials can fail due to delamination.

As mentioned delamination is caused by poor bonding. Therefore, delamination is an insidious type of failure as it develops inside the material without being visible on the surface.

The delamination error can be detected in the material by its sound. While a solid composite has a bright sound, layered part has a dull sound.

2. LITERATURE REVIEW

As the usage of laminated glass is increasing research studies about laminated glass structures is increasing day by day.

Hooper(1973) examined the basic behavior of laminated glass in bending. For this purpose, theoretical and experimental studies were carried out on the four-point bending motion of laminated glass beams. Data on tests conducted on small laminated glass beams subjected to both temporary and long-term loading at various ambient temperatures were presented. It has been shown that the degree of bonding between the two layers of glass is found to be a function of the loading time and the ambient temperature and is mainly depend on the shear modulus of the PVB interlayer.

Phillip Davies and Robert Cadwallader (1983) worked on delamination issues with laminated glass. In their study, they have analyzed causes of delamination and the ways of prevention of it. Test data on the edge stability of laminated glass in their products has been provided and detailed the various delamination problems that can occur if proper glass handling and installation practices are not followed.

Vallabhan (1983) used Von Karman equations for symbolize the behavior of rectangular thin glass units under lateral pressures. It was supposed that the glass plate is simply supported for in-plane deflections in supports. Using the iterative finite difference technique, nonlinear equations were solved. The number of repeats was reduced by using an insufficient relaxation parameter.

Vallabhan et al. (1985) investigated the behavior of laminated glass units subjected to lateral pressure symbolizing wind loads. It has been found that the laminated glass unit like a solid sheet of glass of the same nominal thickness at room temperature. It was concluded that at higher temperatures [170 °F (77 °C)] the behavior differs and approaches the laminated glass unit without an interlayer. Experimental stress analyzes designed to differentiate the behavior of laminated glass and monolithic glass were compared with the results of theoretical stress analyzes.

Behr et al. (1986) investigated the impact of loading time and interlayer thickness on laminated glass. Full-scale laminated glass laboratory specimens were tested. Effects caused

by long-term loads and varying interlayer thicknesses were observed. It has been noticed that the interlayer thickness effects on the structural response of the laminated glass unit are not large.

Vallabhan et al. (1993) made a research of laminated glass units by calculus of variations and the minimum potential energy theorem. Five nonlinear differential equations with suitable boundary conditions were had and solved numerically. Experiments were performed to measure stresses and lateral displacements at various positions above and below the units to verify the mathematical model. The experimental results were compared with the results from the mathematical model.

F. Shen et al. (2001) modeled delamination growth in laminated composites. It was relevant to the estimation of delamination growth and computational modeling of delamination in laminated composites. The experimental results were compared and it was predicted that the fatigue cycle and the delamination front would grow together. Evolution criteria based on total strain energy release rate predicted slower delamination growth rate than evolution criteria based on components of stress energy release rate.

Valeria La Saponara et al. (2001), for the delamination growth in double cantilever laminated beams conducted an experimental and numerical analyze. Using experiments and finite element models, delamination crack growth in laminated composites was investigated. For multilayer double cantilever beam laminates under plane stress conditions, it has been shown that it is sufficient to calibrate the binder elements from experimental load displacement data. In addition, dynamic crack growth was observed in notched laminates in the finite element model.

Z. Zou et al. (2002) modeled continuous media damage for delaminations in laminated composites. In the context of the sustained damage mechanics in the article, delamination, a typical mode of interface damage in laminated composites, was tackled. The model was also applied to estimate the failure strength of the overlapping layer blocking samples. The results were compared with the available experimental and alternative theoretical results and discussed.

Z. Zou et al. (2002) applied a delamination model to laminated composite structures. A model is presented for staged lamination layers in laminated composite structures. A study on the effect of mesh size was found to give sufficiently accurate results in a relatively coarse mesh. It was also concluded that these examples are a useful indicator of the

versatility and applicability of the current approach for real structural applications.

Timothy J. Saxe et al. get. (2002) examined the effects of glass type and missile size on the impact resistance of "sacrificial floor" laminated glass. Experiments were conducted to improve the "sacrificial floor" design concept for laminated glass. The concept authorizes the effects of wind-induced debris to break through the outer laminated glass floor, while the inner layer is protected to carry the wind pressure inside while maintaining wind-induced residual effects in the wind. Regardless of the outer glass floor type, it was found that laminated glass made of fully tempered or heat strengthened inner glass sheets has a significantly higher average minimum fracture rate than laminated glass made with tempered glass units. On the contrary, it has been found that converting the outer glass layer from tempered to fully tempered glass reduces the average minimum fracture rate regardless of the type of the inner glass layer.

Aşık (2003) made a study to reveal the nonlinear behavior of laminated glass plate units. For in-plane and lateral displacements which are obtained by the variational approach, nonlinear behavior of laminated glass unit was symbolized by five nonlinear partial differential equations. Linear algebraic equations were had by using the finite difference method by typing differential equations on the separate points of the glass plate units. The results showed that maximum stress is traveling and complex stress areas are developing.

L. R. Dharani and J. Yu (2004) examined the failure modes of glass units exposed to soft missile effects. The stress response and onset of fracture of glass units affected by a huge soft missile were analyzed using the finite element method. Energy release rate criteria were developed to determine crack initiation location and time for crack initiation. The effects of different loading, geometric and material parameters on maximum failure and stress modes were investigated.

D. Coutellier et al. (2005) presented a method for delamination detection within laminated structures. A methodology aimed at evaluating the behavior of delaminated composite structures has been developed. His work consisted of two parts: First, the detection of delamination in damaged thin laminated structures was discussed. These layered structures are modeled using multilayer shell elements in the finite element method (FEM) computation code. Second, the impacts of delamination on the general behavior of the structure was gaged. Satisfactory consistency was demonstrated for damage mechanisms and delamination patterns in different samples. Different aspects of the delamination

approach are presented.

Shuangmei Zhao et al. (2005) analyzed the damage to laminated automotive glass subjected to a simulated head impact. The impact and failure resistance of laminated automotive glass exposed to simulated head impact, a structural model based on Continuity Damage Mechanics (CDM) was developed and applied to an axisymmetric finite element model. Different geometric values were researched for determining the effects of laminated glass on impact resistance.

Aşık and Tezcan (2005) improved a model for the behavior of laminated glass beams. In the development of the model suppose that huge displacement for a laminated composite beam, the minimum total potential energy principle was used. The mathematical model was verified by finite element and experimental models for fixed and simply supported beams. It has been observed that the behavior of laminated glass beams huge displacements can be linear or nonlinear under constraints or boundary conditions.

Foraboschi (2007) examined the behavior and failure resistance of laminated glass beams. In the research, an analytical model is symbolized which presages the stress and strength development of laminated glass beams, which includes a multi-layer system that authorizes displacements in the shear-flexible intermediate layer. No specific simplifying assumption was made when formulating the work, so the theoretical model has been proven by comparison test results with predictions. The closed form of the model authorizes both to explain to correlate structural performance with mechanical and geometric parameters and the behavior of laminated glass.

Paolo Foraboschi (2012) developed an analytical model for laminated-glass plate. He solved the equations for the rectangular plate, which was simply supported under a static charge uniformly distributed laterally.

Laura Galuppi and Gianni Royer-Carfagni (2012) investigated laminated beams with viscoelastic interlayer. They analytically solved the time-dependent problem of a simply supported laminated beam, consisting of two elastic layers bonded with a viscoelastic interlayer and modeled with a series of Prony's Maxwell elements. They emphasized that there was a remarkable difference between the results obtained by numerical analysis of a full 3-D viscoelastic finite element and the stress state calculated in the full viscoelastic state or equivalent elastic problem and stress.

Foraboschi (2012) presented an analytical model of laminated glass unit. Mechanical

behavior is explained by three complete and explicit systems of equations. The equations are solved for the rectangular plate that is simply supported under the laterally homogeneously distributed static load. Because the model is both analytical and open, the mechanical behavior of the laminated glass sheet can be better understood.

Hooper et al. (2017) researched the delamination properties of laminated glass windows under blast loading. The delamination process was studied at realistic deformation rates to understand the resulting reaction force response. Experimental tensile tests were performed on previously cracked laminated glass samples to investigate the delamination behavior. The experiments confirmed the presence of a plateau in the force deflection graphs and showed that the delamination process absorbs a significant amount of energy. The laboratory results were then used to calibrate the FEA models of the delamination process to determine the delamination energy of the glass layers and polyvinyl butyral (PVB) and its relationship to the deformation rate.

In the past few decades, a growth in the use of laminated glass units in various industrial areas such as civil engineering, aerospace engineering, marine and automotive has been noticed. Correspondingly, an increase in the demand to analyze the mechanical behavior of laminated glass has been realized. As seen in the mentioned studies, the existing research on laminated glass is mainly analyze behavior of laminated unit, and the relevant research about delamination is rarely mentioned. Moreover, the related theoretical research which analyze nonlinear behavior of delaminated glass unit is relatively less and it is far behind its application in engineering. The present research is aimed to anallyze delamination, which is one of the most common problems in the use of laminated glass.

3. MATERIAL AND METHODS

3.1. A New Mathematical Model for Laminated Glass Plate Units Subjected to Initial Delamination

Laminated glass plate is composed of interlayer and glass plates connected to each other at specific conditions. Laminated glass plate exhibit nonlinear behavior under applied lateral loads since it makes very large lateral deflections according to its thickness and there is a huge difference between the mechanical properties of glass and intermediate layer. The classical assumption that "the plane portion before deformation remains plane after deformation" cannot be accepted for a laminated glass sheet due to non-linear behavior. Consequently, a new and more practical model is needed and this model is developed by Vallabhan, Magdi, Das (1990). The mentioned new model is based on derived using variational methods and minimum potential energy theorem.

Laminated glass plate that is considered in this study is shown in Figure 3.1. In the derivation process, to be able to use the advantage of symmetry only quarter of the plate is analyzed.

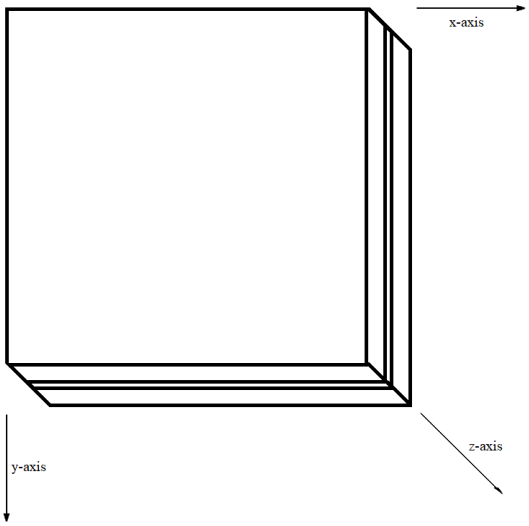

Figure 3.1. Axes of reference.

The mathematical formulation and solution technique which is used by Vallabhan,

Magdi and Das (1990) and Magdi (1990) are given below;

The total potential energy of the system (V) be expressed using glass units and the assumptions given for the interlayer as follows:

$$V = \overline{U}_m^{(1)} + \overline{U}_b^{(1)} + \overline{U}_m^{(2)} + \overline{U}_b^{(2)} + \overline{U}_{xz}^{(I)} + \overline{U}_{yz}^{(I)} + \overline{\Omega} \tag{3.1}$$

where,

$\overline{U}_m^{(i)}$ = membrane strain energy for the glass plate (i),

$\overline{U}_b^{(i)}$ = bending strain energy for the glass plate (i); i=1,2 for the top and bottom units,

$\overline{U}_{xz}^{(I)}, \overline{U}_{yz}^{(I)}$ = shear strain energy for the interlayer due to the shear strains γ_{xz} and γ_{yz},

$\overline{\Omega}$ = potential energy function due to applied loads.

The bending strain energy function found by Langhaar (1962) is given as:

$$\overline{U}_b^{(i)} = \int_{-b}^{b}\int_{-a}^{a} U_b^{(i)} dxdy = \int_{-b}^{b}\int_{-a}^{a} \frac{Eh_i^3}{24(1-\mu^2)}$$

$$\left[\left(\frac{\partial^2 w}{\partial x^2}\right)^2 + \left(\frac{\partial^2 w}{\partial y^2}\right)^2 + 2\mu\left(\frac{\partial^2 w}{\partial x^2}\right)\left(\frac{\partial^2 w}{\partial y^2}\right) + 2(1-\mu)\left(\frac{\partial^2 w}{\partial x \partial y}\right)^2\right] dxdy \tag{3.2}$$

The membrane strain energy functions, which be expressed in terms of strains found by Langhaar (1962), are given as:

$$\overline{U}_m^{(i)} = \int_{-b}^{b}\int_{-a}^{a} U_m^{(i)} dxdy = \int_{-b}^{b}\int_{-a}^{a} \frac{Eh_i}{2(1-\mu^2)}\left[e_{ix}^2 + e_{iy}^2 + 2\mu e_{ix} e_{iy} + \frac{1}{2}(1-\mu)e_{ixy}^2\right] dxdy \tag{3.3}$$

where, i=1,2 indicates the top and bottom plates.

e_{ix}, e_{iy}, e_{ixy} are the non-linear membrane strains and which can be expressed in terms of the displacements as,

$$e_{ix} = \frac{\partial u_i}{\partial x} + \frac{1}{2}\left(\frac{\partial w}{\partial x}\right)^2 \tag{3.4}$$

$$e_{iy} = \frac{\partial v_i}{\partial y} + \frac{1}{2}\left(\frac{\partial w}{\partial y}\right)^2 \tag{3.5}$$

and

$$e_{ixy} = \frac{\partial u_i}{\partial y} + \frac{\partial v_i}{\partial x} + \left(\frac{\partial w}{\partial x}\right)\left(\frac{\partial w}{\partial y}\right) \tag{3.6}$$

a = length of the unit in the x direction,

b = length of the unit in the y direction,

h_i = thickness of each glass layer,

E = Young's modulus of the glass units,

μ = Poisson's ratio of the unit,

$$\gamma_{xz} = \varphi_x + \theta_x$$

The average shear strains, γ_{xz} and $\gamma_{yz.}$, are

$$= -\frac{\partial w}{\partial x} + \frac{\partial u}{\partial z} = -\frac{\partial \omega}{\partial x} + \left[u_1 - u_2 - \frac{\partial \omega}{\partial x}\left(\frac{h_1}{2} + \frac{h_2}{2}\right)\right]/t \tag{3.7}$$

$$\gamma_{xz} = \left[u_1 - u_2 - \frac{\partial \omega}{\partial x}\left(\frac{h_1}{2} + \frac{h_2}{2} + t\right)\right] / t$$

$$\gamma_{yz} = \varphi_y + \theta_y$$

Similarly,

$$= -\frac{\partial w}{\partial y} + \frac{\partial v}{\partial z} = -\frac{\partial \omega}{\partial y} + \left[v_1 - v_2 - \frac{\partial w}{\partial y}\left(\frac{h_1}{2} + \frac{h_2}{2}\right)\right] / t \tag{3.8}$$

$$\gamma_{yz} = \left[v_1 - v_2 - \frac{\partial w}{\partial y}\left(\frac{h_1}{2} + \frac{h_2}{2} + t\right)\right] / t$$

Here, t is the thickness of the PVB interlayer.

w = lateral deflection of the laminated glass plate, for the top and bottom units.

$u_{i,}$,$v_{i,}$ and h_i (i=1,2) = in-plane displacements and thicknesses of top and bottom glass

units.

The interlayer shear strain energy expressions are written by using the previous two equations as follows;

$$\overline{U}_{xz}^{(I)} = \int_{-b}^{b}\int_{-a}^{a} U_{xz}^{(I)} dxdy = \int_{0}^{t}\int_{-b}^{b}\int_{-a}^{a} \frac{1}{2} G_I \gamma_{xz}^{2} dV$$

$$U_{xz} = \int_{-b}^{b}\int_{-a}^{a} \frac{G_I}{2t}\left[(u_1 - u_2) - \frac{\partial w}{\partial x}\left(\frac{h_1}{2} + \frac{h_2}{2} + t\right)\right]^2 dxdy \qquad (3.9)$$

and

$$\overline{U}_{yz}^{(I)} = \int_{-b}^{b}\int_{-a}^{a} U_{yz}^{(I)} dxdy = \int_{0}^{t}\int_{-b}^{b}\int_{-a}^{a} \frac{1}{2} G_I \gamma_{yz}^{2} dV$$

$$U_{yz} = \int_{-b}^{b}\int_{-a}^{a} \frac{G_I}{2t}\left[(v_1 - v_2) - \frac{\partial w}{\partial y}\left(\frac{h_1}{2} + \frac{h_2}{2} + t\right)\right]^2 dxdy \qquad (3.10)$$

In these equations, G_I is the interlayer shear modulus

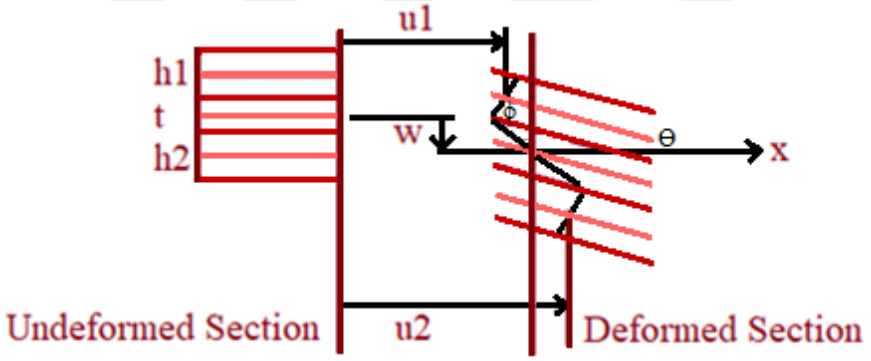

Figure 3.2. Laminated glass plate unit: undeformed and deformed sections.

The plate is subject to uniform pressure and $\overline{\Omega}$ is called as the load potential function and it is given as,

$$\overline{\Omega} = \int_{-b/2}^{b/2}\int_{-a/2}^{a/2} \Omega \, dxdy = \int_{-b}^{b}\int_{-a}^{a} -qw dxdy \qquad (3.11)$$

Substituting equations 3.2, 3.3, 3.9, 3.10 and 3.11 into Equation 3.1, the total potential energy of the system can be written as follows;

$$V = \int_{-b}^{b}\int_{-a}^{a}\left[\overline{U}_m^{(1)} + \overline{U}_b^{(1)} + \overline{U}_m^{(2)} + \overline{U}_b^{(2)} + \overline{U}_{xz}^{(I)} + \overline{U}_{yz}^{(I)} + \Omega\right] dxdy = \int_{-b}^{b}\int_{-a}^{a} F dxdy \qquad (3.12)$$

Here, F can be expressed as,

$$F=\frac{Eh_1}{2(1-\mu^2)}\left[e_{1x}^{\ 2}+e_{1y}^{\ 2}+2\mu e_{1x}e_{1y}+\frac{1}{2}(1-\mu)e_{1xy}^{\ 2}\right]$$

$$+\frac{Eh_2}{2(1-\mu^2)}\left[e_{2x}^{\ 2}+e_{2y}^{\ 2}+2\mu e_{2x}e_{2y}+\frac{1}{2}(1-\mu)e_{2xy}^{\ 2}\right]$$

$$+\frac{E\left(h_1^3+h_2^3\right)}{24(1-\mu^2)}\left[\left(\frac{\partial^2 w}{\partial x^2}\right)^2+\left(\frac{\partial^2 w}{\partial y^2}\right)^2+2\mu\left(\frac{\partial^2 w}{\partial x^2}\right)\left(\frac{\partial^2 w}{\partial y^2}\right)+2(1-\mu)\left(\frac{\partial^2 w}{\partial x\partial y}\right)^2\right]$$

$$+\frac{G_1}{2t}\left[u_1-u_2-\frac{\partial w}{\partial x}\left(\frac{h_1}{2}+\frac{h_2}{2}+t\right)\right]^2+\frac{G_1}{2t}\left[v_1-v_2-\frac{\partial w}{\partial y}\left(\frac{h_1}{2}+\frac{h_2}{2}+t\right)\right]^2-qw \qquad (3.13)$$

The minimum potential energy theorem and variational approach are used to perform the deformation and stress analysis of the laminated glass unit. The minimum potential energy states that "for protective structural systems, all kinematically acceptable deformations make the total potential energy of those corresponding to the equilibrium state excessive. If the extreme is minimum, the equilibrium state is stable."

The total potential energy function is written using in-plane and lateral displacement terms such as w, u1, v1, u2, and v2. The Euler Equation given in Langhaar's (1962) study is applied to the problem. While five nonlinear differential equations are obtained for undelaminated regions of plate, five nonlinear differential equations are obtained for the delaminated regions of unit at the end of the mathematical formulation and given as follows:

Euler Equation,

$$\frac{\partial F}{\partial u_i}-\frac{\partial}{\partial\theta}\left(\frac{\partial F}{\partial ui_\theta}\right)-\frac{\partial}{\partial y}\left(\frac{\partial F}{\partial ui_y}\right)+\frac{\partial^2}{\partial\theta^2}\left(\frac{\partial F}{\partial ui_{\theta\theta}}\right)+\frac{\partial^2}{\partial\theta\partial y}\left(\frac{\partial F}{\partial ui_{\theta y}}\right)+\frac{\partial^2}{\partial y^2}\left(\frac{\partial F}{\partial ui_{yy}}\right)=0 \qquad (3.14)$$

where,

u_i = indicates u_1, v_1, u_2, v_2, and w,

$u_{i,x}$ = the first derivation of u_i according to x,

$u_{i,y}$ = the first derivation of u_i according to y,

$u_{i,xx}$ = the second derivation of u_i according to y,

$u_{i,yy}$ = the second derivation of u_i according to y,

$u_{i,xy}$ = the second order cross derivation of u_i,

The behaviour of laminated regions is governed using the five non-linear equations. The equations are obtained by Vallabhan, Magdi and Das (1990) with respect to in-plane and lateral displacements, are presented as;

$$\left[\left(D1+D2\right)\nabla^4-\frac{G_I}{t}\left(\frac{h_1}{2}+\frac{h_2}{2}+t\right)^2\nabla^2\right]w=q$$

$$+\frac{Eh_1}{1-\mu^2}\left[(e_{1x}+\mu e_{1y})\frac{\partial^2 w}{\partial x^2}+(e_{1y}+\mu e_{1x})\frac{\partial^2 w}{\partial y^2}+(1-\mu)e_{1xy}\frac{\partial^2 w}{\partial x\partial y}\right]$$

$$+\frac{Eh_2}{1-\mu^2}\left[(e_{2x}+\mu e_{2y})\frac{\partial^2 w}{\partial x^2}+(e_{2y}+\mu e_{2x})\frac{\partial^2 w}{\partial y^2}+(1-\mu)e_{2xy}\frac{\partial^2 w}{\partial x\partial y}\right]$$

$$-\frac{G_I}{t}\left(\frac{h_1}{2}+\frac{h_2}{2}+t\right)\left(\frac{\partial u_1}{\partial x}-\frac{\partial u_2}{\partial x}+\frac{\partial v_1}{\partial y}-\frac{\partial v_2}{\partial y}\right) \qquad (3.15)$$

$$\left[\frac{\partial^2}{\partial x^2}+\frac{1-\mu}{2}\frac{\partial^2}{\partial y^2}-\frac{G_I(1-\mu)}{2Gh_1t}\right]u_1=-\left[\frac{1+\mu}{2}\frac{\partial^2}{\partial x\partial y}\right]v_1-\left[\frac{G_I(1-\mu)}{2Gh_1t}\right]u_2-$$

$$\frac{\partial w}{\partial x}\left[\frac{\partial^2 w}{\partial x^2}+\frac{1-\mu}{2}\frac{\partial^2 w}{\partial y^2}\right]-\frac{1+\mu}{2}\frac{\partial^2 w}{\partial x\partial y}\frac{\partial w}{\partial y}-\frac{G_I(1-\mu)}{2Gh_1t}\left(\frac{h_1}{2}+\frac{h_2}{2}+t\right)\frac{\partial w}{\partial x} \qquad (3.16)$$

$$\left[\frac{\partial^2}{\partial y^2}+\frac{1-\mu}{2}\frac{\partial^2}{\partial x^2}-\frac{G_I(1-\mu)}{2Gh_1t}\right]v_1=-\left[\frac{1+\mu}{2}\frac{\partial^2}{\partial x\partial y}\right]u_1-\left[\frac{G_I(1-\mu)}{2Gh_1t}\right]v_2-$$

$$\frac{\partial w}{\partial y}\left[\frac{\partial^2 w}{\partial y^2}+\frac{1-\mu}{2}\frac{\partial^2 w}{\partial x^2}\right]-\frac{1+\mu}{2}\frac{\partial^2 w}{\partial x\partial y}\frac{\partial w}{\partial x}-\frac{G_I(1-\mu)}{2Gh_1t}\left(\frac{h_1}{2}+\frac{h_2}{2}+t\right)\frac{\partial w}{\partial y} \qquad (3.17)$$

$$\left[\frac{\partial^2}{\partial x^2}+\frac{1-\mu}{2}\frac{\partial^2}{\partial y^2}-\frac{G_I(1-\mu)}{2Gh_2t}\right]u_2=-\left[\frac{1+\mu}{2}\frac{\partial^2}{\partial x\partial y}\right]v_2-\left[\frac{G_I(1-\mu)}{2Gh_2t}\right]u_1-$$

$$\frac{\partial w}{\partial x}\left[\frac{\partial^2 w}{\partial x^2}+\frac{1-\mu}{2}\frac{\partial^2 w}{\partial y^2}\right]-\frac{1+\mu}{2}\frac{\partial^2 w}{\partial x\partial y}\frac{\partial w}{\partial y}+\frac{G_I(1-\mu)}{2Gh_2t}\left(\frac{h_1}{2}+\frac{h_2}{2}+t\right)\frac{\partial w}{\partial x}$$

(3.18)

$$\left[\frac{\partial^2}{\partial y^2}+\frac{1-\mu}{2}\frac{\partial^2}{\partial x^2}-\frac{G_I(1-\mu)}{2Gh_2t}\right]v_2=-\left[\frac{1+\mu}{2}\frac{\partial^2}{\partial x\partial y}\right]u_2+\left[\frac{G_I(1-\mu)}{2Gh_2t}\right]v_1-$$

$$\frac{\partial w}{\partial y}\left[\frac{\partial^2 w}{\partial y^2}+\frac{1-\mu}{2}\frac{\partial^2 w}{\partial x^2}\right]-\frac{1+\mu}{2}\frac{\partial^2 w}{\partial x\partial y}\frac{\partial w}{\partial x}+\frac{G_I(1-\mu)}{2Gh_2 t}\left(\frac{h_1}{2}+\frac{h_2}{2}+t\right)\frac{\partial w}{\partial y} \tag{3.19}$$

To analyze behaviour of delaminated regions of glass plate, Euler equation is applied to the total potential energy equation written by neglecting shear strain energy terms. The equations govern behaviour of delaminated regions of plate are given below.

$$[(D_1+D_2)\nabla^4]w=q+\frac{Eh1}{1-\mu^2}\left[(e_{1x}+\mu e_{1y})\frac{\partial^2 w}{\partial x^2}+(e_{1y}+\mu e_{1x})\frac{\partial^2 w}{\partial y^2}+(1-\mu)e_{1xy}\frac{\partial^2 w}{\partial x\partial y}\right]$$

$$+\frac{Eh_2}{1-\mu^2}\left[(e_{2x}+\mu e_{2y})\frac{\partial^2 w}{\partial x^2}+(e_{2y}+\mu e_{2x})\frac{\partial^2 w}{\partial y^2}+(1-\mu)e_{2xy}\frac{\partial^2 w}{\partial x\partial y}\right] \tag{3.20}$$

$$\left[\frac{\partial^2}{\partial x^2}+\frac{1-\mu}{2}\frac{\partial^2}{\partial y^2}\right]u_1=-\left[\frac{1+\mu}{2}\frac{\partial^2}{\partial x\partial y}\right]v_1-\frac{\partial w}{\partial x}\left[\frac{\partial^2 w}{\partial x^2}+\frac{1-\mu}{2}\frac{\partial^2 w}{\partial y^2}\right]-\frac{1+\mu}{2}\frac{\partial^2 w}{\partial x\partial y}\frac{\partial w}{\partial y} \tag{3.21}$$

$$\left[\frac{\partial^2}{\partial y^2}+\frac{1-\mu}{2}\frac{\partial^2}{\partial x^2}\right]v_1=-\left[\frac{1+\mu}{2}\frac{\partial^2}{\partial x\partial y}\right]u_1-\frac{\partial w}{\partial y}\left[\frac{\partial^2 w}{\partial y^2}+\frac{1-\mu}{2}\frac{\partial^2 w}{\partial x^2}\right]-\frac{1+\mu}{2}\frac{\partial^2 w}{\partial x\partial y}\frac{\partial w}{\partial x} \tag{3.22}$$

$$\left[\frac{\partial^2}{\partial x^2}+\frac{1-\mu}{2}\frac{\partial^2}{\partial y^2}\right]u_2=-\left[\frac{1+\mu}{2}\frac{\partial^2}{\partial x\partial y}\right]v_2-\frac{\partial w}{\partial x}\left[\frac{\partial^2 w}{\partial x^2}+\frac{1-\mu}{2}\frac{\partial^2 w}{\partial y^2}\right]-\frac{1+\mu}{2}\frac{\partial^2 w}{\partial x\partial y}\frac{\partial w}{\partial y} \tag{3.23}$$

$$\left[\frac{\partial^2}{\partial y^2}+\frac{1-\mu}{2}\frac{\partial^2}{\partial x^2}\right]v_2=-\left[\frac{1+\mu}{2}\frac{\partial^2}{\partial x\partial y}\right]u_2-\frac{\partial w}{\partial y}\left[\frac{\partial^2 w}{\partial y^2}+\frac{1-\mu}{2}\frac{\partial^2 w}{\partial x^2}\right]-\frac{1+\mu}{2}\frac{\partial^2 w}{\partial x\partial y}\frac{\partial w}{\partial x} \tag{3.24}$$

where,

$D_1 = Eh_1 / 12\,(1-\mu^2)$ = the flexural rigidity of the top glass unit, (3.25)

$D_2 = Eh_2 / 12\,(1-\mu^2)$ = the flexural rigidity of the bottom glass unit, (3.26)

μ = the Poisson's ratio of the unit,

q = the distributed lateral pressure per unit area,

G_I = the interlayer shear modulus,

Young's modulus (E) of the glass is connected with the shear modulus (G) of the glass as;

$$G=\frac{E}{2(1+\mu)} \tag{3.27}$$

In equations (3.15) and (3.20),

$$\nabla^4 = \frac{\partial^4}{\partial x^4} + 2\frac{\partial^4}{\partial x^2 \partial y^2} + \frac{\partial^4}{\partial y^4} \tag{3.28}$$

$$\nabla^2 = \frac{\partial^2}{\partial x^2} + \frac{\partial^2}{\partial y^2} \tag{3.29}$$

The classical finite difference method presented in the next section is used to solve the equations obtained above.

To take advantage of symmetry one quarter of glass plate is analyzed in the study. Axes are taken as shown in Figure 3.1. The boundary conditions obtained for fixed supported rectangular unit subjected to uniform pressure are as;

<u>At x = 0:</u>

$u_1 = 0,$

$e_{1xy} = 0,$

$u_2 = 0,$

$e_{2xy} = 0,$

$$\frac{\partial w}{\partial x} = 0,$$

$$\frac{\partial}{\partial x}\left(\frac{\partial^2 w}{\partial x^2} + \mu\frac{\partial^2 w}{\partial y^2}\right) + \frac{\partial}{\partial y}\left[2(1-\mu)\frac{\partial^2 w}{\partial x \partial y}\right] = 0$$

<u>At x = a</u>

$e_{1x} + \mu e_{1y} = 0,$

$e_{1xy} = 0,$

$e_{2x} + \mu e_{2y} = 0,$

$e_{2xy} = 0,$

$w = 0,$

$$\frac{\partial w}{\partial x} = 0$$

At y = 0 :

$v_1 = 0,$

$e_{1xy} = 0,$

$v_2 = 0,$

$e_{2xy} = 0,$

$$\frac{\partial w}{\partial y} = 0.$$

$$\frac{\partial}{\partial y}\left(\frac{\partial^2 w}{\partial y^2} + \mu\frac{\partial^2 w}{\partial x^2}\right) + \frac{\partial}{\partial x}\left[2(1-\mu)\frac{\partial^2 w}{\partial x \partial y}\right] = 0$$

At y = b

$e_{1y} + \mu e_{1x} = 0,$

$e_{1xy} = 0,$

$e_{2y} + \mu e_{2x} = 0,$

$e_{2xy} = 0,$

$\omega = 0,$

$$\frac{\partial w}{\partial y} = 0.$$

3.2. Finite Difference Forms of Field Equations and Boundary Conditions and the Iterative Solution Technique

Considering the symmetry, a quarter plate is focused. Five equations which governs the behavior of laminated glass plate obtained. While the differential equations of in plane displacements are linear, that of lateral displacement, w, is nonlinear. Due to its non-linearity, an iterative numerical technique should be used for the solution.

Equations are transformed into algebraic equations and written in matrix form using finite difference method (FDM) which is one of the most applied numerical methods. Nonlinear terms of the equations are put into right side and equations are obtained as matrix systems. The coefficient matrix of lateral displacement is symmetric banded, while it is full coefficient for in plane deflections. On the other hand, since storing full matrices requires huge memory, the modified strongly implicit procedure suggested by Zedan and Schneider (1981) is used for in-plane deflections in this study. This reduces computational cost and storage capacity.

In the finite difference method, central finite difference technique is used to convert the continuous functions u1, v1, u2, v2 and w to separate values at every point of the finite difference network. Using the finite difference method, equations 3.15 to 3.19 for non-delaminated regions and 3.20 to 3.24 for delaminated regions are arranged so that the left-hand sides are linear and converted into a series of linear algebraic equations.

The left side of the algebraic equations are stored as a matrix [A] and the right hand side vector contains all the nonlinear terms and applied pressure in the field equation.

The equations are written as follows:

$$[A]\{w\}=\{q + \{f_1 (w, u_1, v_1, u_2, v_2\} \quad (3.30)$$

where,

$\{w\}$ = the lateral displacement vector,

q = applied pressure magnitude.

The coefficients of the matrix [A] and the corresponding right-hand side equation for the grid points in the area as well as those at the boundaries are given below. The presented iterative procedure is also used to reach the final solution.

The finite difference mesh size is chosen as $n_x \times n_y$ for the lateral displacement, where n_x and n_y are the numbers of subdivisions in the x and y directions. The lateral displacement value is zero at simply supported edges and it is not included in the finite difference network to reduce the total number of equations.

According to Magdi's (1990) research, the finite difference form of the lateral deflection field equation for a point in the undelaminated region of laminated glass plate is;

For i =3,4, …. n_x –2; j=3,4, ….. n_y –2

$$Cw_{(i,j)} + Bw_{(i+1,j)} + Bw_{(i-1,j)} + Hw_{(i+2,\,j)} + Hw_{(i-2,\,j)} + Jw_{(i,\,j+1)} + Jw_{(i,\,j-1)} + Gw_{(i,\,j+2)} + Gw_{(i,\,j-2)} + Fw_{(i+1,j+1)} + Fw_{(i+1,j-1)} + Fw_{(i-1,\,j+1)} + Fw_{(i-j\,,\,j-1)} = \{RSH\}_{(i,j)} \tag{3.31}$$

where,

$$\{RSH\}_{(i,j)} = \{q + \frac{Eh_1}{2(1-\mu^2)}\left[\left(e_{1x} + e_{1y}\right)\frac{\partial^2 w}{\partial x^2} + \left(e_{1y} + e_{1x}\right)\frac{\partial^2 w}{\partial y^2} + (1-\mu)e_{1xy}\frac{\partial^2 w}{\partial x \partial y}\right]$$

$$+ \frac{Eh_2}{2(1-\mu^2)}\left[\left(e_{2x} + e_{2y}\right)\frac{\partial^2 w}{\partial x^2} + \left(e_{2y} + e_{2x}\right)\frac{\partial^2 w}{\partial y^2} + (1-\mu)e_{2xy}\frac{\partial^2 w}{\partial x \partial y}\right]$$

$$- \frac{G_I}{t}\left(\frac{h_1}{2} + \frac{h_2}{2} + t\right)\left(\frac{\partial u_1}{\partial x} - \frac{\partial u_2}{\partial x} + \frac{\partial v_1}{\partial y} - \frac{\partial v_2}{\partial y}\right)\Bigg\}(i,\,j) \tag{3.32}$$

$$C = \left(D_1 + D_2\right)\left(\frac{6}{h_x^4} + \frac{6}{h_y^4} + \frac{8}{h_x^2 h_y^2}\right) + \frac{G_I}{t}\left(\frac{h_1}{2} + \frac{h_2}{2} + t\right)^2\left(\frac{2}{h_x^2} + \frac{2}{h_y^2}\right) \tag{3.33}$$

$$B = \left(D_1 + D_2\right)\left(\frac{-4}{h_x^4} + \frac{-4}{h_x^2 h_y^2}\right) + \frac{G_I}{t}\left(\frac{h_1}{2} + \frac{h_2}{2} + t\right)^2\left(\frac{-1}{h_x^2}\right) \tag{3.34}$$

$$H = \left(D_1 + D_2\right)\frac{1}{h_x^4} \tag{3.35}$$

$$F = \left(D_1 + D_2\right)\frac{2}{h_x^2 h_y^2} \tag{3.36}$$

$$J = \left(D_1 + D_2\right)\left(\frac{-4}{h_y^4} + \frac{-4}{h_x^2 h_y^2}\right) + \frac{G_I}{t}\left(\frac{h_1}{2} + \frac{h_2}{2} + t\right)^2\left(\frac{-1}{h_y^2}\right) \tag{3.37}$$

$$G = (D_1 + D_2)\frac{1}{h_y^4} \tag{3.38}$$

Equation (3.31) is also valid for the solution of delaminated region of unit but since the total potential energy of the delaminated region is different than that of the undelaminated region, the elements of the elements of right hand side vector and the coefficient matrix need to be modified in the delaminated region of unit as given below:

$$\{RHS\}_{(i,j)} = \{ q + \frac{Eh_1}{2(1-\mu^2)}\left[(e_{1x} + e_{1y})\frac{\partial^2 w}{\partial x^2} + (e_{1y} + e_{1x})\frac{\partial^2 w}{\partial y^2} + (1-\mu)e_{1xy}\frac{\partial^2 w}{\partial x \partial y}\right]$$

$$\mp \frac{Eh_2}{2(1-\mu^2)}(e_{2x} + e_{2y})\frac{\partial^2 w}{\partial x^2} + (e_{2y} + e_{2x})\frac{\partial^2 w}{\partial y^2} + (1-\mu)e_{2xy}\frac{\partial^2 w}{\partial x \partial y}\}(i, j) \tag{3.39}$$

$$C = (D_1 + D_2)\left(\frac{6}{h_x^4} + \frac{6}{h_y^4} + \frac{8}{h_x^2 h_y^2}\right) \tag{3.40}$$

$$B = (D_1 + D_2)\left(\frac{-4}{h_x^4} + \frac{-4}{h_x^2 h_y^2}\right) \tag{3.41}$$

$$H = (D_1 + D_2)\frac{1}{h_x^4} \tag{3.42}$$

$$F = (D_1 + D_2)\frac{2}{h_x^2 h_y^2} \tag{3.43}$$

$$J = (D_1 + D_2)\left(\frac{-4}{h_y^4} + \frac{-4}{h_x^2 h_y^2}\right) \tag{3.44}$$

$$G = (D_1 + D_2)\frac{1}{h_y^4} \tag{3.45}$$

Equation 3.31 should be modified at plate boundaries to account for boundary conditions. The following equations are obtained,

For i=1; j=1

$$\frac{C}{4}w_{(i,j)}+\frac{B}{2}w_{(i+1,j)}+\frac{H}{2}w_{(i+2,j)}+\frac{J}{2}w_{(i,j+1)}+\frac{G}{2}w_{(i,j+2)}+F_{w_{(i-1,j-1)}}=\frac{1}{4}\{RHS\}_{(i,j)} \quad (3.46)$$

For i=1; j=2

$$\frac{C+G}{2}w_{(i,j)}+B_{w_{(i+1,j)}}+H_{w_{(i+2,j)}}+\frac{J}{2}w_{(i,j+1)}+\frac{J}{2}w_{(i,j-1)}+\frac{G}{2}w_{(i,j+2)}+F_{w_{(i+1,j+1)}}$$

$$+F_{w_{(i+1,j-1)}}=\frac{1}{2}\{RHS\}_{(i,j)} \quad (3.47)$$

For i=1; j=3, n_y-1

$$\frac{C}{2}w_{(i,j)}+B_{w_{(i+1,j)}}+H_{w_{(i+2,j)}}+\frac{J}{2}w_{(i,j+1)}+\frac{J}{2}w_{(i,j-1)}+\frac{G}{2}w_{(i,j+2)}+\frac{G}{2}w_{(i,j-2)}$$

$$+F_{w_{(i+1,j+1)}}+F_{w_{(i+1,j-1)}}=\frac{1}{2}\{RHS\}_{(i,j)} \quad (3.48)$$

For i=1; j=n_y

$$(C-G)_{w_{(i,j)}}+B_{w_{(i+1,j)}}+H_{w_{(i+2,j)}}+\frac{J}{2}w_{(i,j-1)}+G_{w_{(i,j-2)}}+F_{w_{(i+1,j-1)}}=\frac{1}{2}\{RHS\}_{(i,j)} \quad (3.49)$$

For i=2; j=1

$$\frac{C+H}{2}w_{(i,j)}+\frac{B}{2}w_{(i+1,j)}+\frac{B}{2}w_{(i-1,j)}+\frac{H}{2}w_{(i+2,j)}+F_{w_{(i+1,j+1)}}+F_{w_{(i-1,j+1)}}+G_{w_{(i,j+2)}}$$

$$=\frac{1}{2}\{RHS\}_{(i,j)} \quad (3.50)$$

For i=2; j=2

$$(C+H+G)_{w_{(i,j)}}+B_{w_{(i+1,j)}}+B_{w_{(i-1,j)}}+H_{w_{(i+2,j)}}+J_{w_{(i,j+1)}}+J_{w_{(i,j-1)}}\ G_{w_{(i,j+2)}}$$

$$+F_{w_{(i+1,j+1)}}+F_{w_{(i+1,j+1)}}+F_{w_{(i+1,j-1)}}+F_{w_{(i-1,j-1)}}=\{RHS\}_{(i,j)} \quad (3.51)$$

For i=2; j=3,4, …. n_y-1

$$(C+H)_{w_{(i,j)}}+B_{w_{(i+1,j)}}+B_{w_{(i-1,j)}}+H_{w_{(i+2,j)}}+J_{w_{(i,j+1)}}+J_{w_{(i,j-1)}}+G_{w_{(i,j+2)}}$$

$$+G_{w_{(i,j-2)}}+F_{w_{(i+1,j+1)}}+F_{w_{(i+1,j-1)}}+F_{w_{(i-1,j+1)}}+F_{w_{(i-1,j-1)}}=\{RHS\}_{(i,j)} \quad (3.52)$$

For i=2, j=n_y

$$(C-H+G)w_{(i,j)}+B w_{(i+1,j)}+B w_{(i-1,j)}+H w_{(i+2,j)}+J w_{(i,j-1)}+F w_{(i-1,j-1)}$$

$$+F w_{(i+1,j-1)}+G w_{(i,j-2)}=\{RHS\}_{(i,j)} \quad (3.53)$$

For i=3,4, … n_x –1; j=n_y

$$\frac{C}{2}w_{(i,j)}+\frac{B}{2}w_{(i+1,j)}+\frac{B}{2}w_{(i-1,j)}+\frac{H}{2}w_{(i-2,j)}+\frac{H}{2}w_{(i-2,j)}+J w_{(i-2,j)}+F w_{(i+1,j+1)}$$

$$+F w_{(i-1,j+1)}+G w_{(i,j+2)}=\frac{1}{2}\{RHS\}_{(i,j)} \quad (3.54)$$

For i=3,4,….n_x –1; j=n_y

$$(C-G)w_{(i,j)}+B w_{(i+1,j)}+B w_{(i-1,j)}+H w_{(i+2,j)}+H w_{(i-2,j-1)}+F w_{(i-1,j-1)}+F w_{(i+1,j-1)}$$

$$+J w_{(i,j-1)}+G w_{(i,j-2)}=\{RHS\}_{(i,j)} \quad (3.55)$$

For i=n_x; j=1

$$\frac{C-H}{2}w_{(i,j)}+\frac{B}{2}w_{(i-1,j)}+\frac{H}{2}w_{(i-1,j+1)}+F w_{(i-1,j+1)}+J w_{(i,j+1)}+G w_{(i,j+2)}=\frac{1}{2}\{RHS\}_{(i,j)}$$

(3.56)

For i=n_x; j=2

$$(C-H+G)w_{(i,j)}+B w_{(i-1,j)}+H w_{(i-2,j)}+F w_{(i-j,j-1)}+F w_{(i-1,j+1)}+J w_{(i,j+1)}$$

$$+J w_{(i,j+1)}+G w_{(i,j+2)}=\{RHS\}_{(i,j)} \quad (3.57)$$

For i=n_x; j=3,4, … n_y –1

$$(C-H)w_{(i,j)}+B w_{(i-1,j)}+H w_{(i-2,j)}+J w_{(i,j-1)}+J w_{(i,j+1)}+F w_{(i-1,j-1)}+F w_{(i-1,j+1)}$$

$$+G w_{(i,j+2)}+G w_{(i,j-2)}=\{RHS\}_{(i,j)} \quad (3.58)$$

For i=n_x; j=n_y

$$(C-H-G)w_{(i,j)}+B w_{(i-1,j)}+H w_{(i-2,j)}+J w_{(i,j-1)}+F w_{(i-1,j-1)}+G w_{(i,j-2)}=\{RHS\}_{(i,j)} \quad (3.59)$$

For in-plane deflections, Modified Strongly Implicit Method developed by Zedan and Schneider (1981), used to have the in-plane deflections u_1, v_1, u_2, v_2. With respect to boundary conditions, these equations are modified. This method provides less calculation time and less storage. According to the study of Aşık (1998), coefficients for undelaminated region of unit are as,

$$Apu(i,j)\, u_1(i,j) = Awu(i,j)\, u_1(i-1,j) + Aeu(i,j)\, u_1(i+1,j) + Asu(i,j)\, u_1(i,j-1)$$
$$+ Anu(i,j)\, u_1(i,j+1) - Fu_1(i,j) \qquad (3.60)$$

$$Apu(i,j)\, u_2(i,j) = Awu(i,j)\, u_2(i-1,j) + Aeu(i,j)\, u_2(i+1,j) + Asu(i,j)\, u_2(i,j-1)$$
$$+ Anu(i,j)\, u_2(i,j+1) - Fu_2(i,j) \qquad (3.61)$$

$$Apv(i,j)\, v_1(i,j) = Awv(i,j)\, v_1(i-1,j) + Aev(i,j)\, v_1(i+1,j) + Asv(i,j)\, v_1(i,j-1)$$
$$+ Anv(i,j)\, v_1(i,j+1) - Fv_1(i,j) \qquad (3.62)$$

$$Apv(i,j)\, v_2(i,j) = Awv(i,j)\, v_2(i-1,j) + Aev(i,j)\, v_2(i+1,j) + Asv(i,j)\, v_2(i,j-1)$$
$$+ Anv(i,j)\, v_2(i,j+1) - Fv_2(i,j) \qquad (3.63)$$

In the above equations the coeffcients of delaminated glass unit are given in extended form as follows:

$$Apu(i,j) = \frac{2}{hx^2} + \frac{(1-\mu)}{hy^2} + G_I$$

$$Awu(i,j) = Aeu(i,j) = \frac{1}{hx^2}$$

$$Asu(i,j) = Anu(i,j) = \frac{(1-\mu)}{2hy^2}$$

$$Apv(i,j) = \frac{2}{hy^2} + \frac{(1-\mu)}{hx^2} + G_I$$

$$Awv(i,j) = Aev(i,j) = \frac{(1-\mu)}{2hx^2}$$

$$Asv(i,j) = Anv(i,j) = \frac{1}{hy^2}$$

Equations 3.60-3.63 can be applied for the delaminated region of unit by modifying the coefficient matrix and right hand side vector. The coefficients of delaminated region in

extended form are obtained as follows:

$$Apu(i,j) = \frac{2}{hx^2} + \frac{(1-\mu)}{hy^2}$$

$$Awu(i,j) = Aeu(i,j) = \frac{1}{hx^2}$$

$$Asu(i,j) = Anu(i,j) = \frac{(1-\mu)}{2hy^2}$$

$$Apv(i,j) = \frac{2}{hy^2} + \frac{(1-\mu)}{hx^2}$$

$$Awv(i,j) = Aev(i,j) = \frac{(1-\mu)}{2hx^2}$$

$$Asv(i,j) = Anv(i,j) = \frac{1}{hy^2}$$

After obtain the equations in matrix form the iterative solution method, which the steps are given below, is applied.

1. w is assumed,
2. RHS of equation (3.30) is calculated,
3. From equation (3.30), w(i,j) is obtained,
4. $w(i,j) = \alpha\, w(i,j) + (1-\alpha)\, w_o(i,j)$,
5. if $\frac{\sum_{i,j} |w(i,j) - wo(i,j)|}{(num * w_{max})} \le l$ then stop the iteration,
6. $Fu_1(i,j)$ is calculated and u_1 is obtained from equation (3.60),
7. $Fu_2(i,j)$ is calculated and u_2 is obtained from equation (3.61),
8. $Fv_1(i,j)$ is calculated and v_1 is obtained from equation (3.62),
9. $Fv_2(i,j)$ is calculated and v_2 is obtained from equation (3.63),
10. go to step 2.

Where α = the variable under relaxation parameter.

In order to overcome difficulties in convergence, this parameter is used for w. It is calculated with the corresponding interpolation of the lateral deflection $w_o(i,j)$ that is calculated in the previous section and the non-dimensional maximum deflection $2*w(1,1)/(h_1+h_2)$ as a result of numerical testing. Lateral deflection (w) is interpolated by using $\alpha\left(\frac{\omega_{max}}{h}\right)$ and in-plane displacements are extrapolated by using $\beta = 1.4$.

4. RESULTS

In this research, certain loads are applied to laminated glass plate with delamination at certain points, laminated glass plate unit without delamination, layered glass and monolithic glass. The numerical solution of developed mathematical model that describes behaviour of different glass types is presented, the obtained partial differential equations are discretized using the finite difference method and the resulting matrix systems are solved through a software developed with the Fortran programming language. The graphs of the axial displacements, lateral displacements and stress are drawn using the Excel program.

Simply supported laminated glass plate units are tested in this research has 1 m in length and 1 m width. Laminated glass is combining of two glass layers and each of them has a thickness of 5 mm and the thickness of the interlayer is 0.76 mm. The total thickness of the unit is 10.76 mm. The Poisson's ratio and Young's modulus of glass are taken to be 0.22 and 70 GPa, respectively. Poisson's ratio and shear modulus of the intermediate layer are taken as 0.29 and 1000 kPa, respectively. Mechanical and geometrical properties of laminated plate are given in Table 4.1.

In this research; three different delaminated glass plate specimens, laminated glass, layered glass which combines two independent glass layers and monolithic glass which contains a single sheet of glass are examined by considering both fixed and simply supported situations. Representation of laminated, layered and monolithic units are given in Figure 4.1 while the locations of delamination in the delaminated specimens are given in Figure 4.2.

Table 4.1. Physical properties of laminated glass plate unit.

	Dimensions(mm)			**Poisson's Ratio**	**Modulus**	
	Thickness	**Length**	**Width**		**E**	**G**
Glass 1	5	1000	1000	0.25	72 GPa	28.8 Gpa
PVB	0,76	1000	1000	0.29	2900 kPa	1000 kPa
Glass 2	5	1000	1000	0.25	72 GPa	28.8 GPa

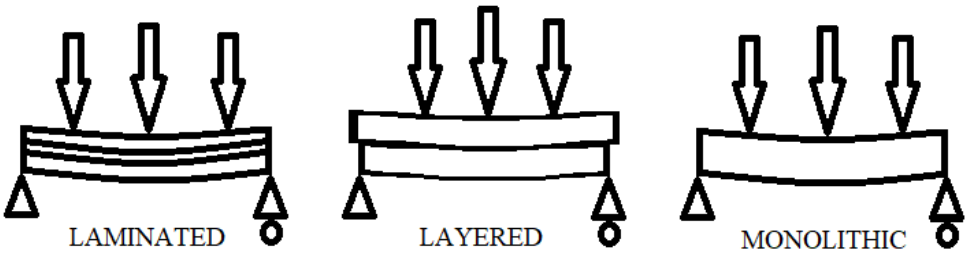

Figure 4.1. Laminated, Layered and Monolithic systems.

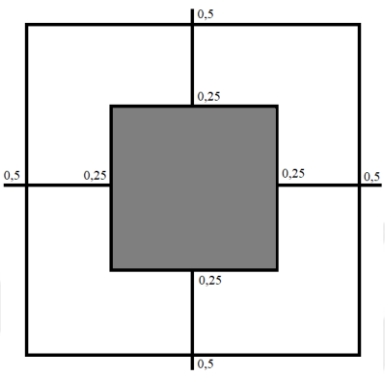

a) Specimen 1 (delamination between 0-0.25 m)

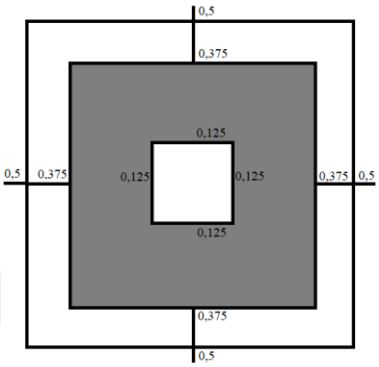

b) Specimen 2 (delamination between 0.125-0.375 m)

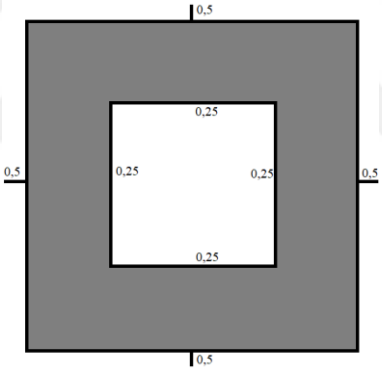

c) Specimen 3 (delamination between 0.25-0.5 m)

Figure 4.2. The location of delamination for experimental specimens.

4.1. Verification of Model

The objective of this chapter is comparing the obtained displacement values by the improved mathematical model with results of finite element model. The assumptions used in the current mathematical model are validated using a simulation done by using ABAQUS software (version 6.14) for laminated unit and Specimen 1. Results of finite element model are checked with the results from the improved model for laminated glass plate subjected to lateral pressure.

Present model is constructed to scrutinize behavior of delaminated and laminated glass plate which combines two glass layers and an intermediate layer. Delaminated glass plate is subjected to initial delamination. In the first step the results of laminated unit are confirmed using finite element package program. The laminated glass unit considered in this research has nominal size of the 1x1 m. Each of the glass plate has the same nominal thickness is $h_1=h_2=0.005$ m. Poisson's ratio and modulus of elasticity of the glass plates are assumed as $\nu=0.25$ and E=72 GPa, respectively. Shear modulus of elasticity and nominal thickness of the PVB are accepted as 1287 kPa and 0.00076 m, respectively. The 3-D finite element model is created and solved via ABAQUS software (version 6.14). The plate is subjected to uniformly distributed pressure. Since the unit may undergo large deflection, analysis are conducted considering ''geometric nonlinearity'' option. To get more efficient and correct solution conducting less iteration and to get a faster convergence, meshes are created using Twenty node quadratic brick elements (C3D20R). Using the advantage of symmetry a quarter laminated glass plate is modeled. The boundaries of unit are modelled symmetric at the center and fixed at the edges of unit as shown in Figure 4.3.

Horizontal and vertical degrees of freedom of all the nodes of the plate unit are set to be zero. The representation of load and boundary conditions of unit can be seen in Figure 4.3. Each unit in the laminated glass plate is divided into nearly 10000 elements. To bond the layers of laminated glass unit tie constraint option is used. In the delaminated regions of plate unit the constraints are not created and layers were not bounded each other to be able to analyze effect of delamination

Figures 4.4 and 4.5 show the representation of constraints for laminated and delaminated glass unit. Delaminations are arranged at the center of plate between 0 and 0.25 m. Results of mathematical and finite element model are taking place in Table 4.2 and Figure 4.6 for laminated unit while the comparison of results for delaminated glass units are given in figure 4.7. Maximum difference between the results is about 7.2% at most for laminated glass unit while it is 7.9 % for delaminated glass plate. An appearance of contours of lateral displacements obtained from ABAQUS is seen in Figures 4.8 and 4.9. At the center of unit, lateral deflection takes its maximum value.

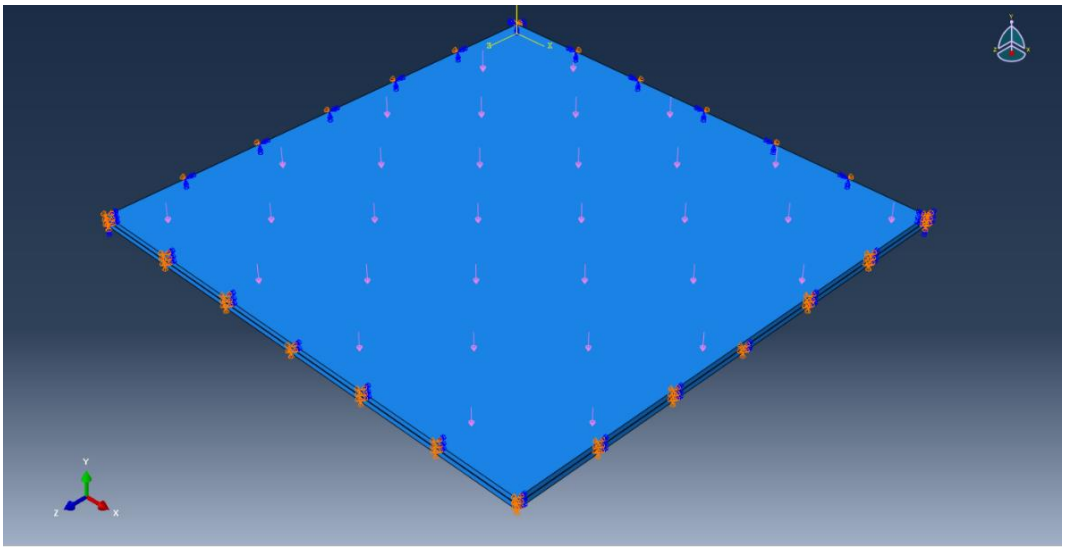

Figure 4.3. Boundary conditions of unit

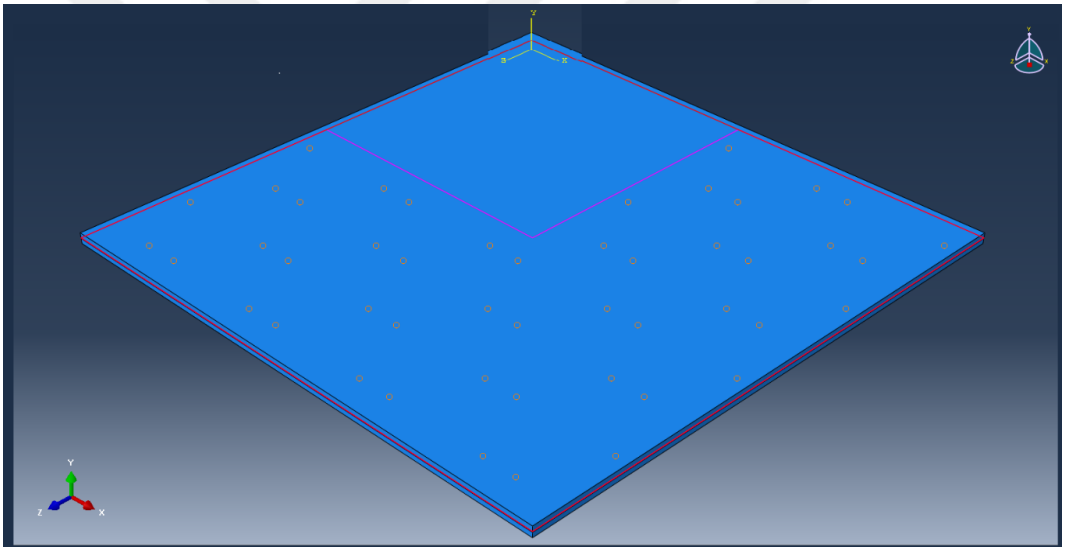

Figure 4.4. Constraints of delaminated glass unit.

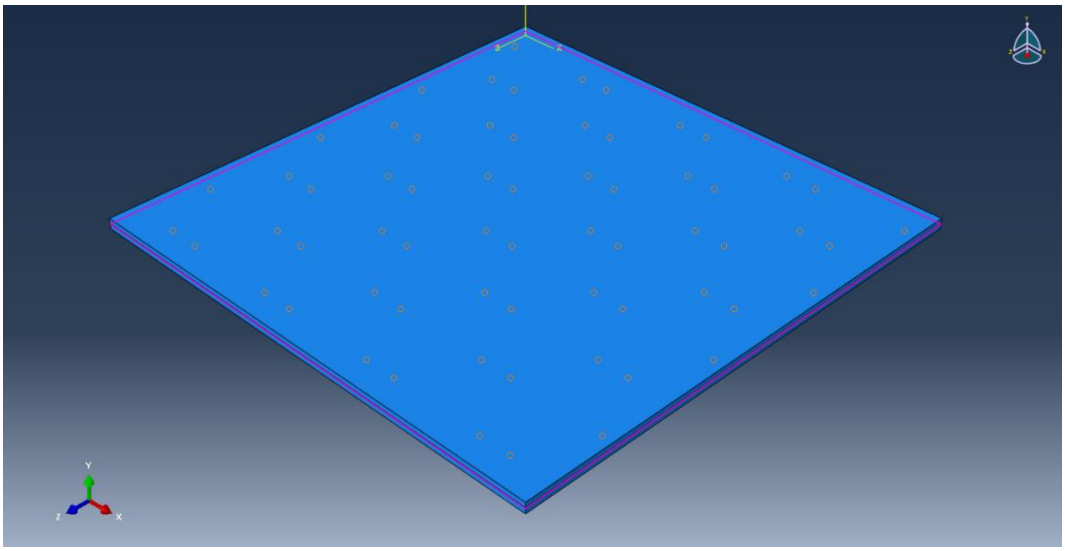

Figure 4.4. Constraints of laminated glass unit.

Table 4.2. Comparison of the results for the fixed supported laminated glass plate.

Load (kPa)	Finite Element Model (mm)	Mathematical Model (mm)	Error (%)
0.5	0.258	0.278	7.260
1	0.514	0.554	7.214
1.5	0.768	0.827	7.148
2	1.018	1.095	7.063
2.5	1.263	1.358	6.986
3	1.503	1.614	6.855
3.5	1.737	1.862	6.714
4	1.964	2.103	6.592
4.5	2.185	2.335	6.442
5	2.389	2.560	6.676

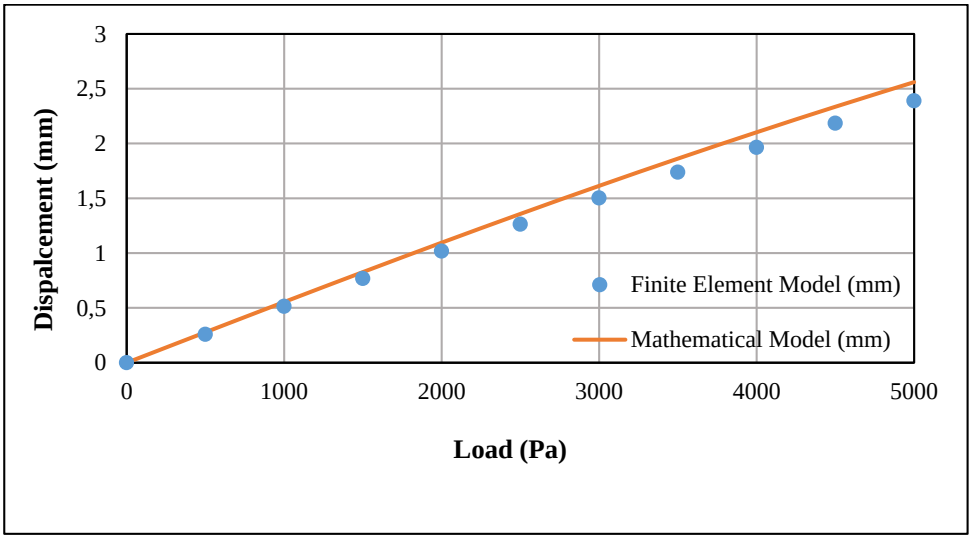

Figure 4.6. Comparison of the central deflection values for laminated glass plate.

Table 4.3. Deflection values of delaminated glass plate.

Load (kPa)	Finite Element Model (mm)	Mathematical Model (mm)	Error (%)
0.5	0.240	0.260	7.853
1	0.479	0.519	7.693
1.5	0.717	0.775	7.489
2	0.953	1.028	7.254
2.5	1.187	1.276	6.989
3	1.418	1.519	6.661
3.5	1.645	1.757	6.356
4	1.869	1.988	5.970
4.5	2.088	2.212	5.605
5	2.302	2.430	5.255

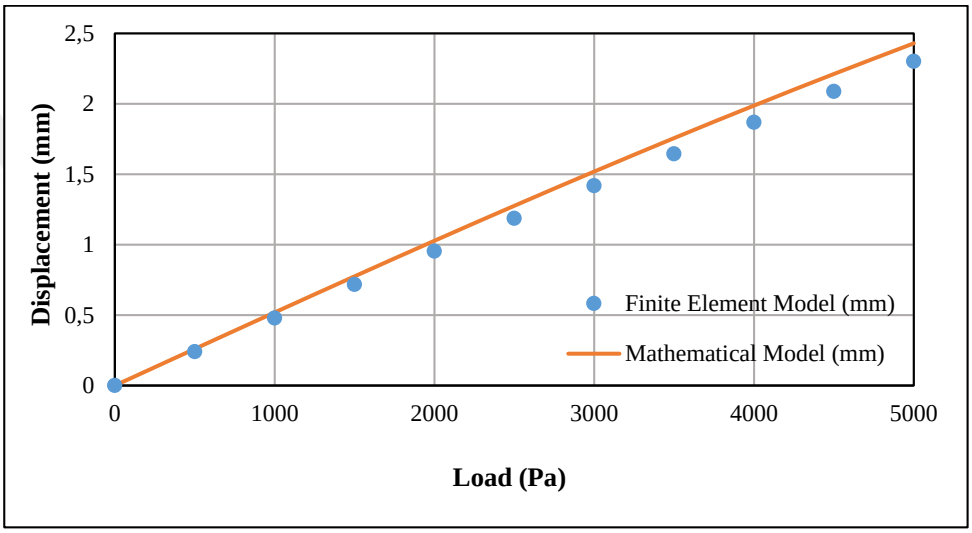

Figure 4.7. Comparison of deflection values for delaminated glass plate.

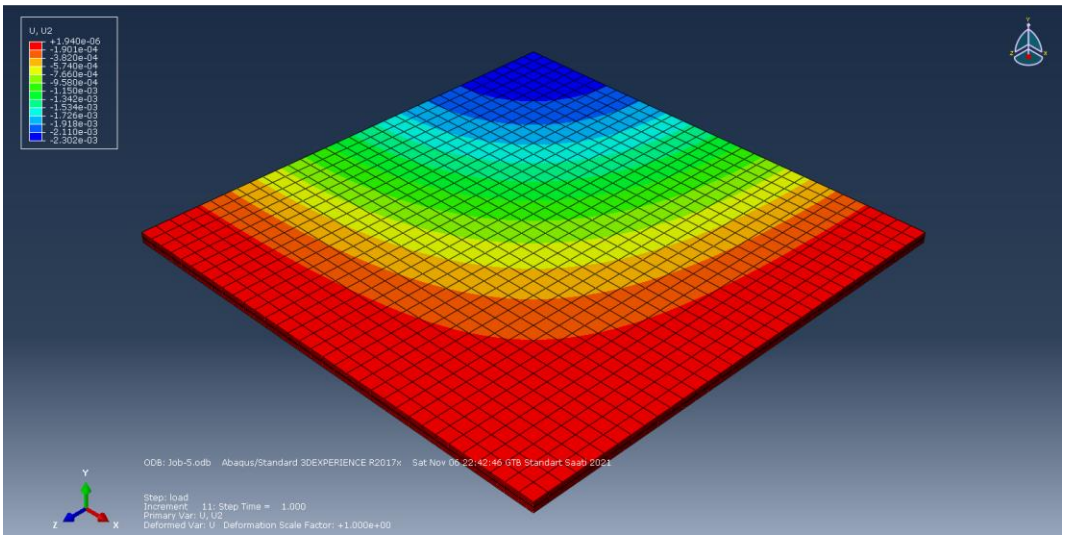

Figure 4.8. A view of contours of lateral deflection values of delaminated glass unit.

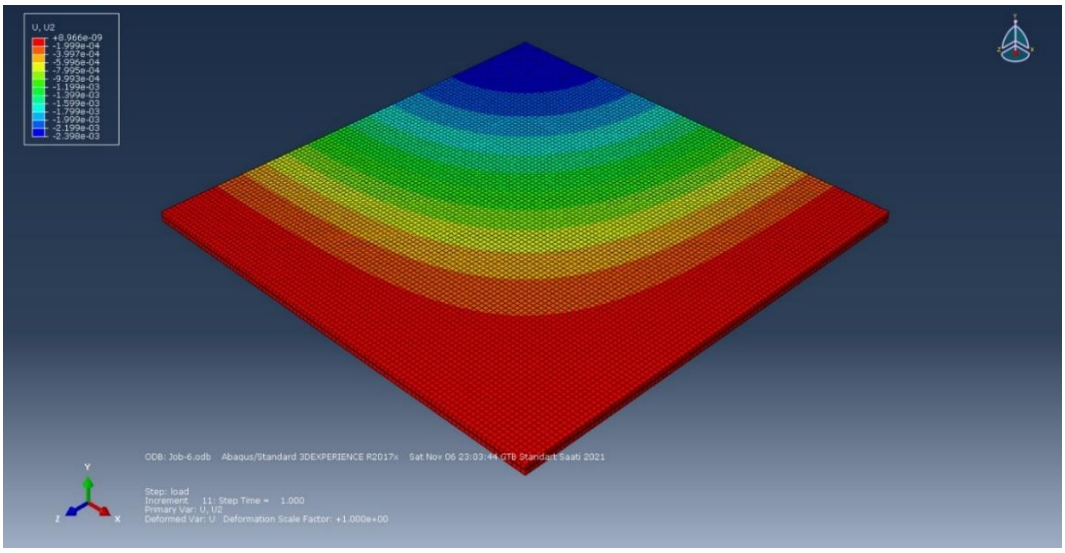

Figure 4.9. A view of contours of lateral deflection values of laminated glass unit.

4.2. Numerical Results of Fixed Supported Laminated Glass Plate Under to Uniform Distributed Load

Numerical analysis is performed for the physical properties given in Table 4.1. A crosscheck of the linear and nonlinear approach to suppose the behavior of the compressed laminated glass sheet is shown in Figures 4.10 and 4.11. In Figure 4.10, linear and non-linear solution results are drawn as normalized deflection against load. The nonlinearity level is the ratio of the deviation in the center of the plate to the thickness of the individual glass plates. It can be seen in Figure 4.10 that this ratio (non-linearity level) is around 0.88 for a P=10 kPa load. Consequently, it can be interpreted that, the level of nonlinearity is nearly 0.88 for applied 10 kPa pressure. The central displacement obtained from the linear approximation is nearly 1.24 of times greater than the displacement obtained with the nonlinear approximation at P=10 kPa load. It is also observed from the figure that while the results of linear and nonlinear approach are very close to each other till 3.5 kPa load value , after this value the difference between the results begins to widen. Figure 4.11 is plotted to observe the linear and non-linear stress values. Similar to displacement values, the stress values for linear behavior are higher than the stress values of nonlinear behavior although the difference between the results is smaller with respect to displacement. In contrary to deflection values separation between the results starts for higher load values.

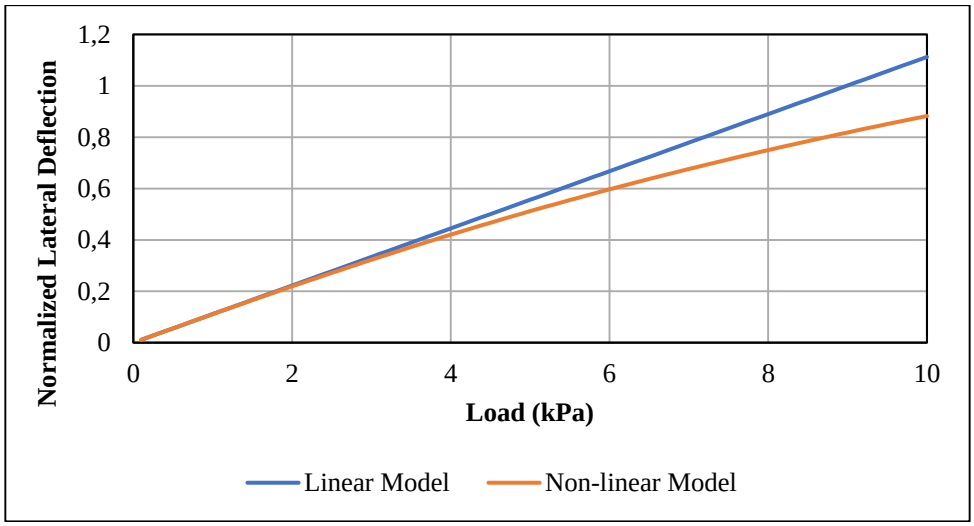

Figure 4.10. Normalized maximum deflection ($\frac{w_{max}}{h}$) versus load for fixed supported laminated glass plate.

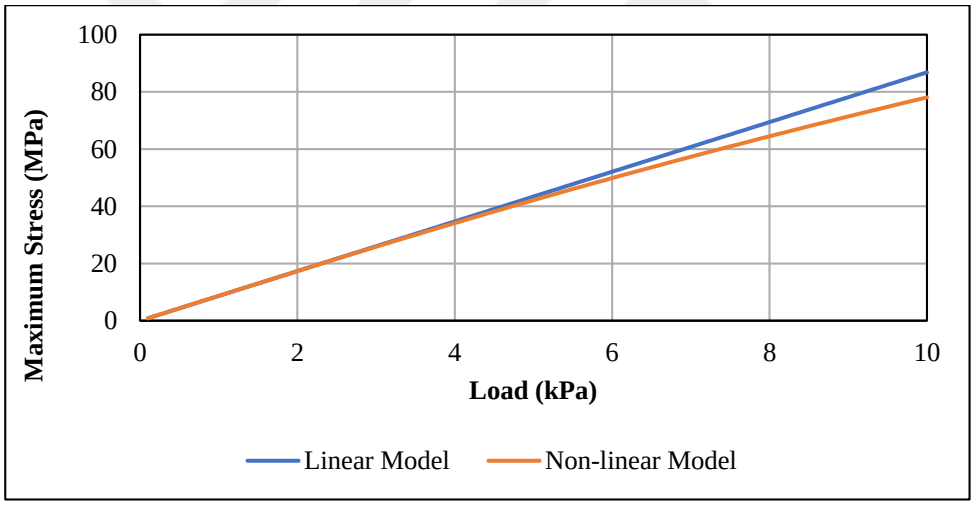

Figure 4.11. Stress versus load for fixed supported laminated glass plate.

Figures 4.12 and 4.13 show the normalized deflection and stress versus load graphs obtained using linear and nonlinear model for Specimen 2. It is observed from the Figure 4.12 that the level of nonlinearity for delaminated specimen is 0.867 for P=10 kPa pressure value and its smaller than that of laminated specimen. The result of linear solution is nearly 1.34 times higher than the result of nonlinear solution. If we compare with respect to that of laminated glass the difference between the results of linear and nonlinear approaches we observe that differences are greater for delaminated unit for both stress and normalized deflections.

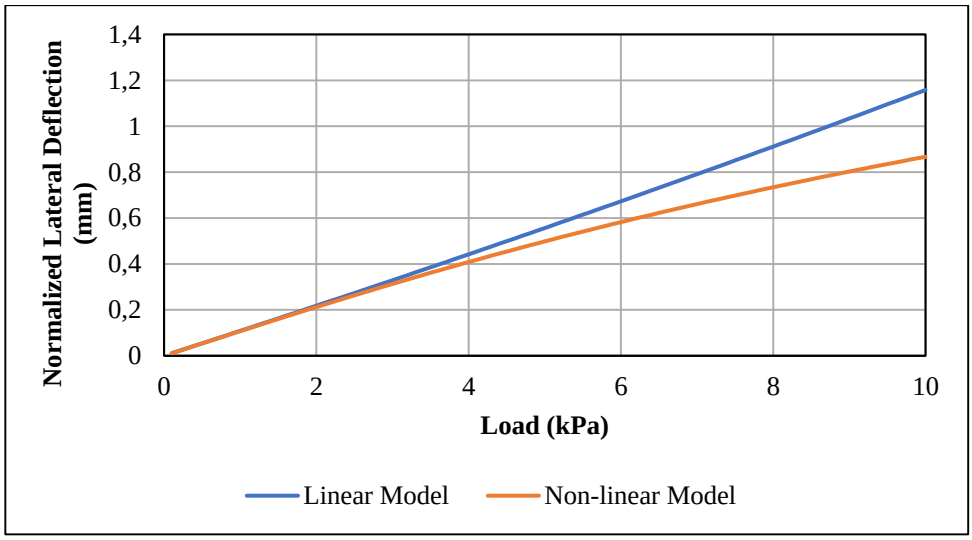

Figure 4.12. Normalized maximum deflection ($\frac{w_{max}}{h}$) versus load for fixed supported delaminated glass plate. (Specimen 2).

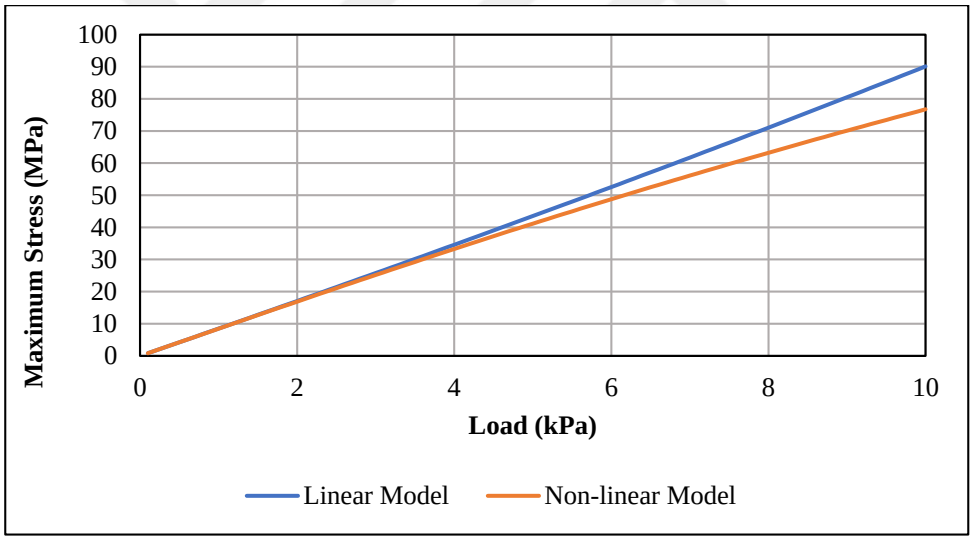

Figure 4.13. Stress versus load for fixed supported delaminated glass plate. (Specimen 2).

The modified model, in the current study, has also capable of predicting the behaviour of laminated, layered and monolithic glass plates. Figures 4.14 and 4.15 are plotted for the comparison of the behaviour of delaminated glass plates with laminated, layered and monolithic plates. In the figures below, it is presumed that origin pass through the center of the glass. Figures 4.14 and 4.15 are plots of deflection and maximum stress against load, respectively.

It is observed from Figure 4.14 that displacement values of laminated and delaminated glass units are limited by layered and monolithic units. Displacements of Specimen 3 which has delamination at the boundary of unit are very close to those of layered unit. It's safe to say delamination has an increasing and decreasing effects on displacement values according to location of the delamination region. Delamination causes an increase in displacement and stress if it at the boundary of unit. Figure 4.15 shows that while the stress values of Specimen 3 take the highest values, stress values of Specimen 2 and Specimen 1 are delimited by values of laminated and monolithic specimens.

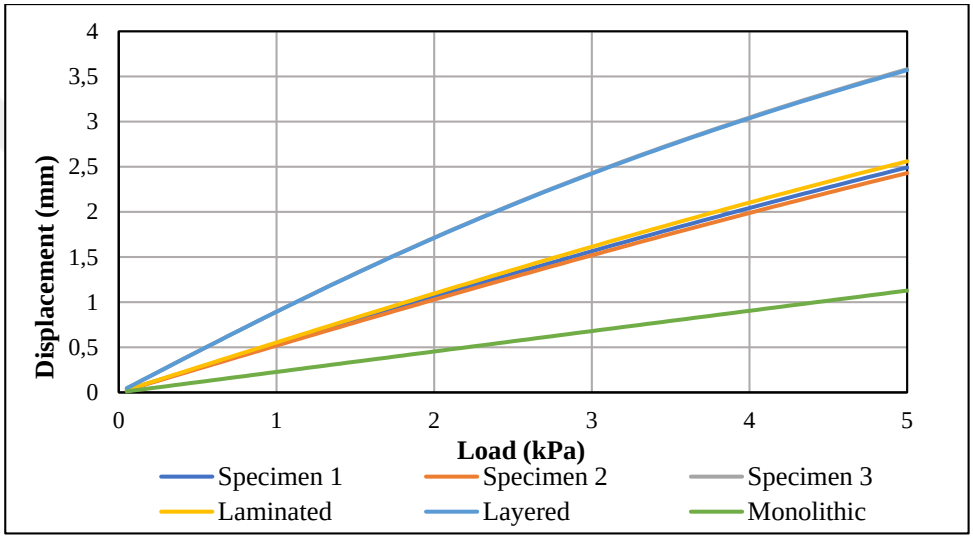

Figure 4.14. Maximum deflection versus load.

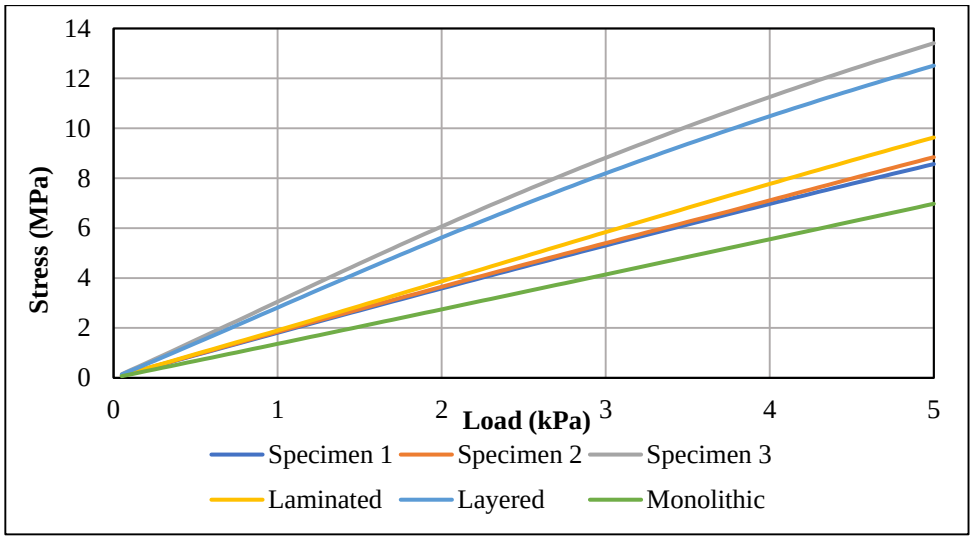

Figure 4.15. Maximum stress versus load.

Figures 4.16 and 4.17 show the axial deflections in x direction along the diagonal of unit (u1 and u2) for top and bottom glass sheets, respectively. Figure 4.16 shows that while the axial displacement values of other units change their sign along the diagonal, axial displacements of laminated glass units are negative along the diagonal. In Figure 4.17, the axial deflections of bottom glass unit take both positive and negative values for Specimen 3 and layered unit. For Specimen 1, Specimen 2 and laminated unit they are positive along the diagonal. The axial displacements of the top unit are lower than those of the bottom unit for the mentioned units.

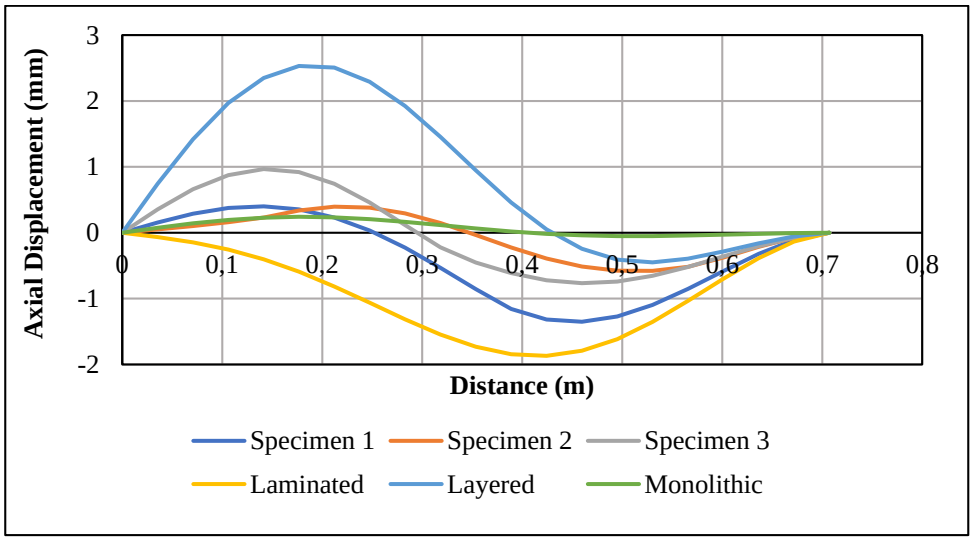

Figure 4.16. Top glass unit's axial displacement in x direction along the diagonal.

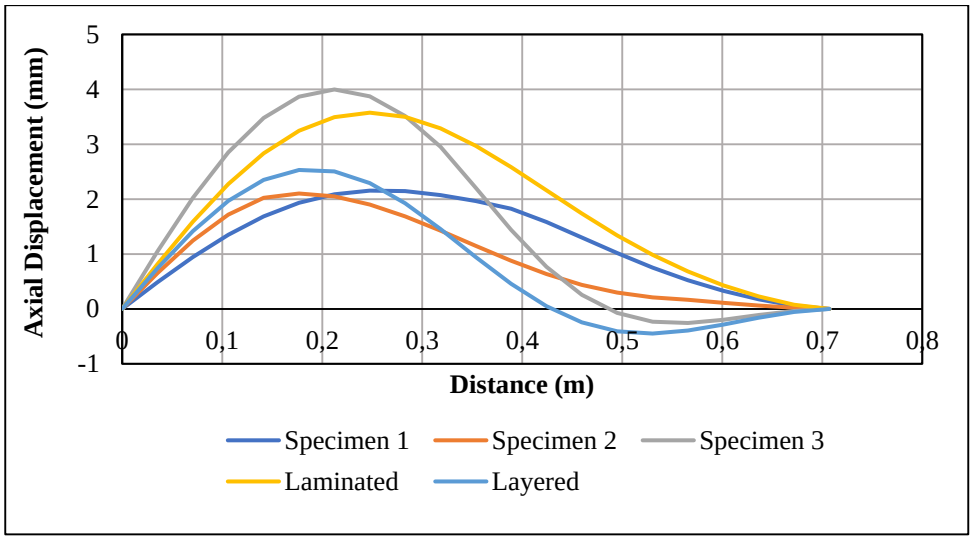

Figure 4.17. Bottom glass unit's axial displacement in x direction along the diagonal.

Figures 4.18 and 4.19 are plotted to symbolize axial displacements directed along y direction (v1 and v2) through the diagonal for the top and bottom units. Displacements in y direction (v1 and v2) are zero at the center and at the corner of the quarter plate. They are also zero at a node within the domain. Specimen 3 and layered unit take maximum value close to center of the unit. In contrary, the other units take maximum value close to the corner of the plate unit. Similar to u1 values, v1 values of laminated glass are negative along the diagonal. Bottom glass axial displacements (v2) of laminated glass unit are positive along the diagonal. Bottom glass axial deflection (v2) of Specimen 3 and layered unit take positive and negative values along the diagonal.

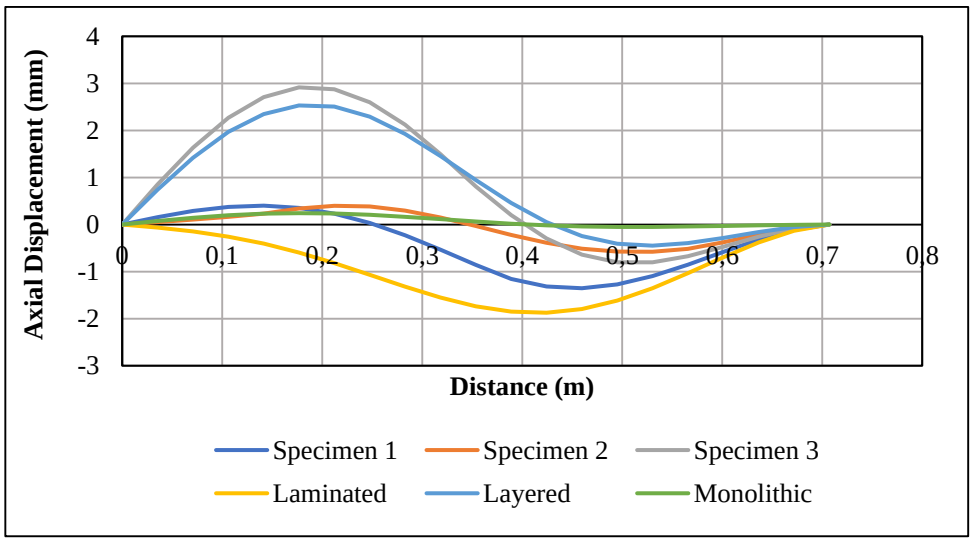

Figure 4.18. Top glass unit's axial displacement in y direction along the diagonal.

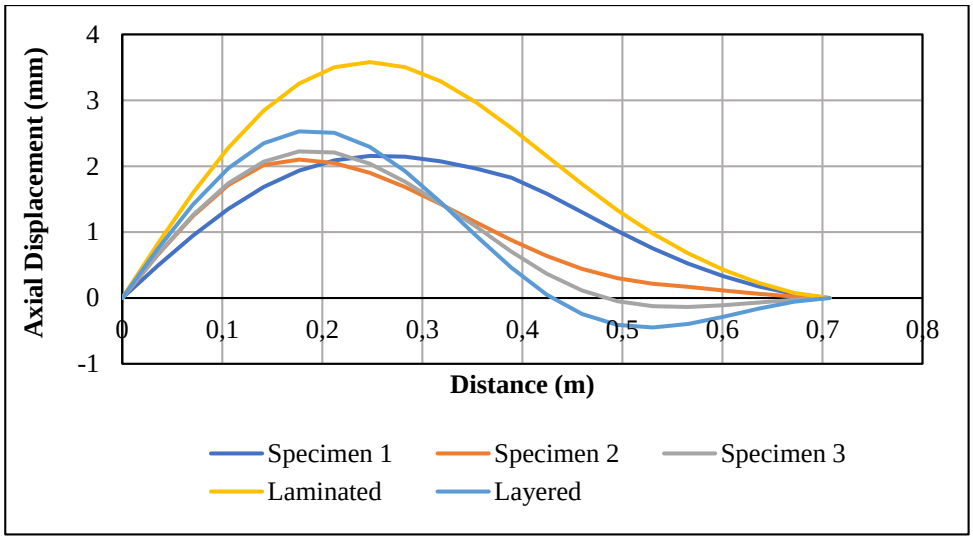

Figure 4.19. Bottom glass unit's axial displacement in y direction along the diagonal.

Change of lateral displacements of glass units along the diagonal are given in figure 4.20. Maximum value of lateral displacements are taking place at the center of the unit while their minimum value are taking place at the corner as zero. As can be seen from figure displacement lines of layered unit and Specimen 3 are nearly coincident and they are greater than the other units. Displacement lines of monolithic unit are smaller than the other units. Displacement values of Specimen 1 and Specimen 2 are limited by the lines of monolithic and laminated glass units.

Figures 4.21 and 4.22 show the lateral displacements of the glass plates at the centerline in x and y direction. At the center of the plate, lateral displacements take their maximum value. For cases of Specimen 1, Specimen 2 and laminated unit the lateral displacements are very close to each other. The maximum displacements are observed in the layered glass unit; the minimum displacements are observed in the monolithic glass unit.

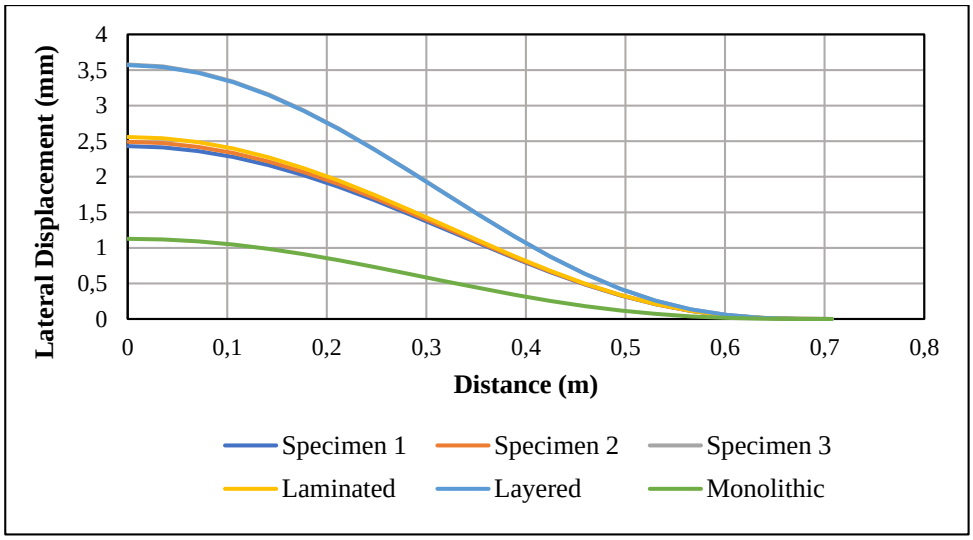

Figure 4.20. Lateral displacement of the unit along the diagonal.

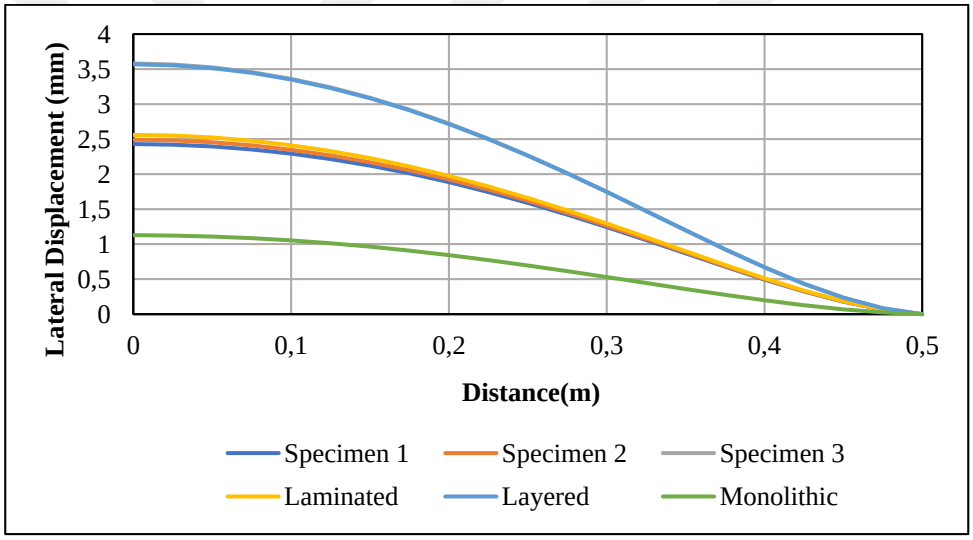

Figure 4.21. Lateral displacement of the unit along x direction.

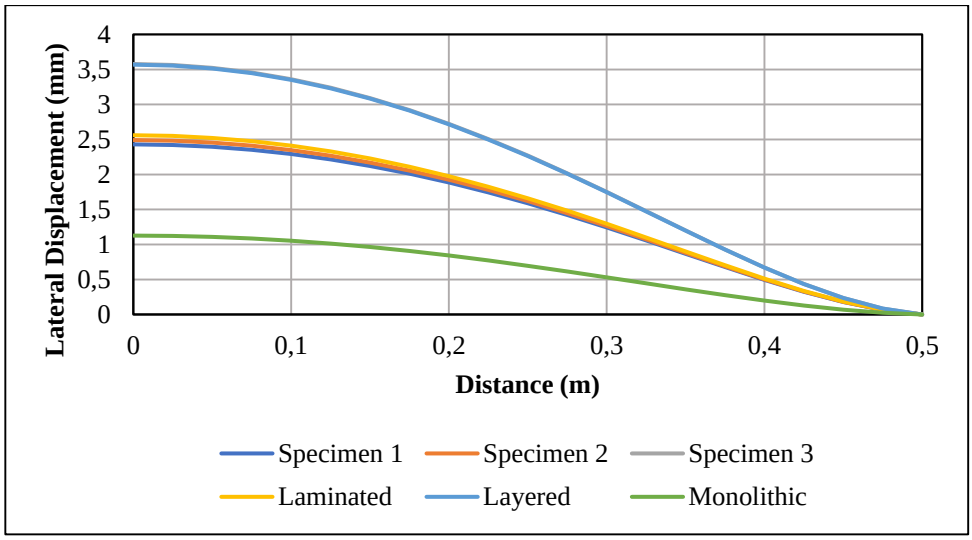

Figure 4.22. Lateral displacement of the unit along y direction.

Spread of bottom surface maximum and minimum principal stresses at the centerline along x direction for applied P=5 kPa pressure have been given in Figures 4.23 and 4.24, respectively. At the center, maximum principal stresses take maximum value as tensile stress while they are compressive close to the boundary of unit. Specimen 3 has the maximum stress value. In the delaminated regions, stresses of layered unit and Specimen 3 get closer to each other. Similar to maximum principal stress curves, minimum principal stresses are tensile at the center and compressive close to the boundary of unit.

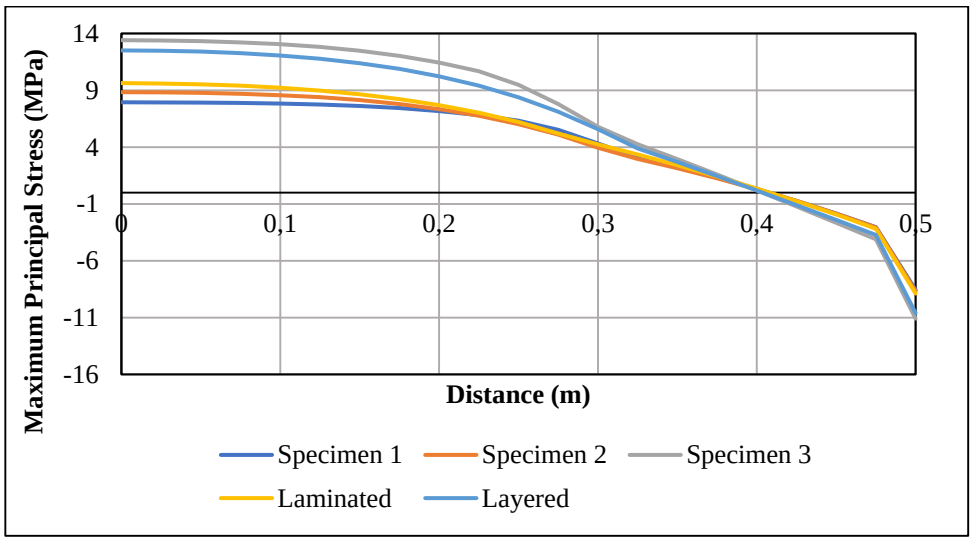

Figure 4.23. Maximum stresses on the bottom surface of the glass along the center line at y=0.

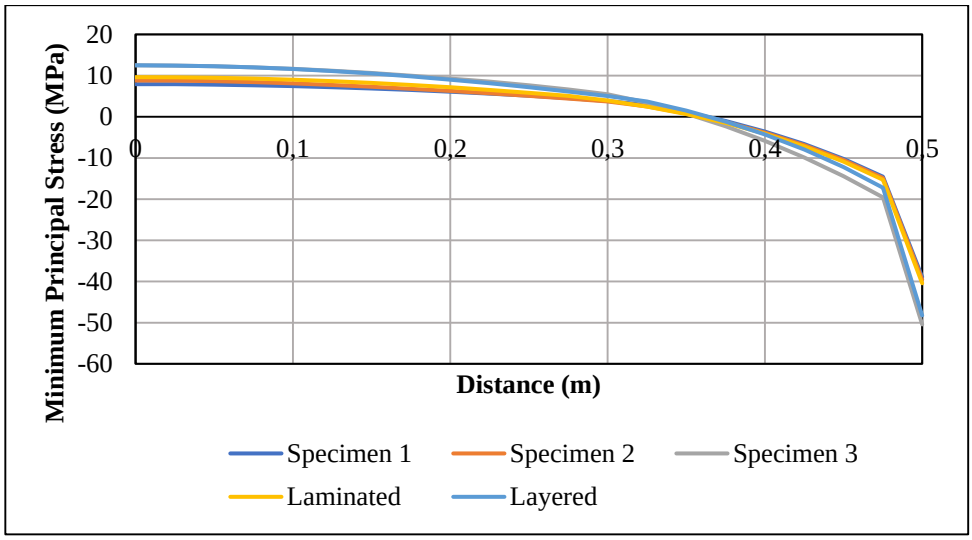

Figure 4.24. Minimum stresses on the bottom surface of the glass along the center line at y=0.

Distribution of top surface maximum and minimum principal stresses at the centerline along x direction for applied P=5 kPa pressure have been given in Figures 4.25 and 4.26, respectively. The principal stresses on the top surface of the unit are tension at the unit boundary and compression at the center. Unlike the maximum stresses on the bottom surface, the maximum stresses on the top surface have maximum values at the boundary of the plate unit.

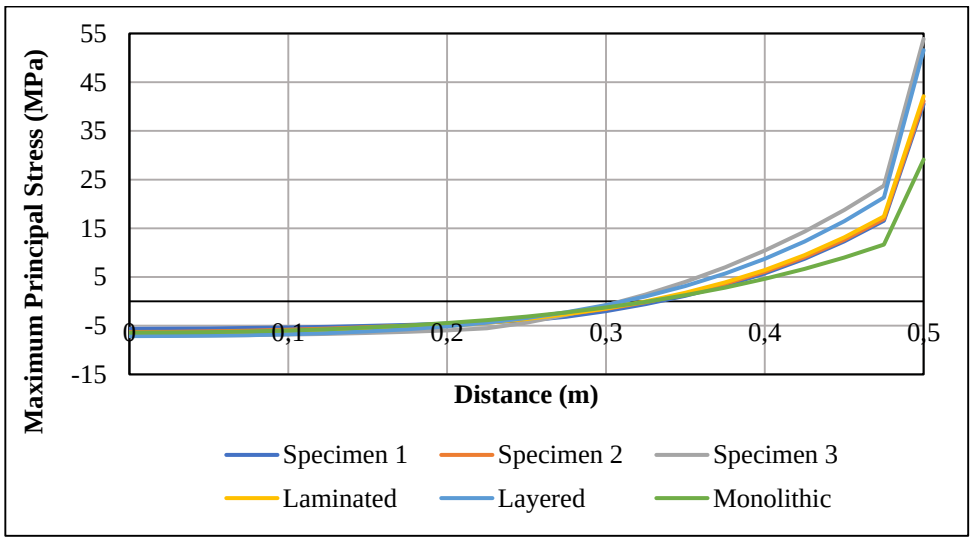

Figure 4.25. Maximum stresses on the top surface of the glass along the center line at y=0.

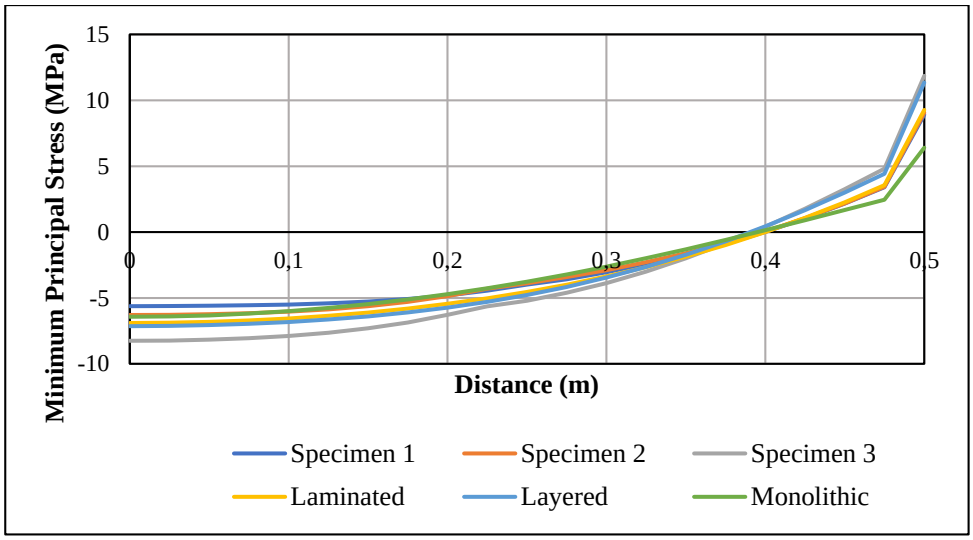

Figure 4.26. Minimum stresses on the top surface of the glass along the center line at y=0.

Figures 4.27 and 4.28 are plotted to represent the maximum and minimum principal stresses on the top surface of along the centerline of the plate unit at x=0 for applied 5 kPa pressure. Maximum stress on the top surface of the plate is maximum at the unit boundary as tensile stress. As seen in Figure 4.27, the maximum stresses at the top surface of the glass are compressive between the center and 0,32 m along the centerline at x=0. In Figure 4.28, the minimum stresses at the top surface of the plate are compressive between center and nearly 0.4 m along the centerline at x=0. At the unit boundary, they take maximum value as tensile stress.

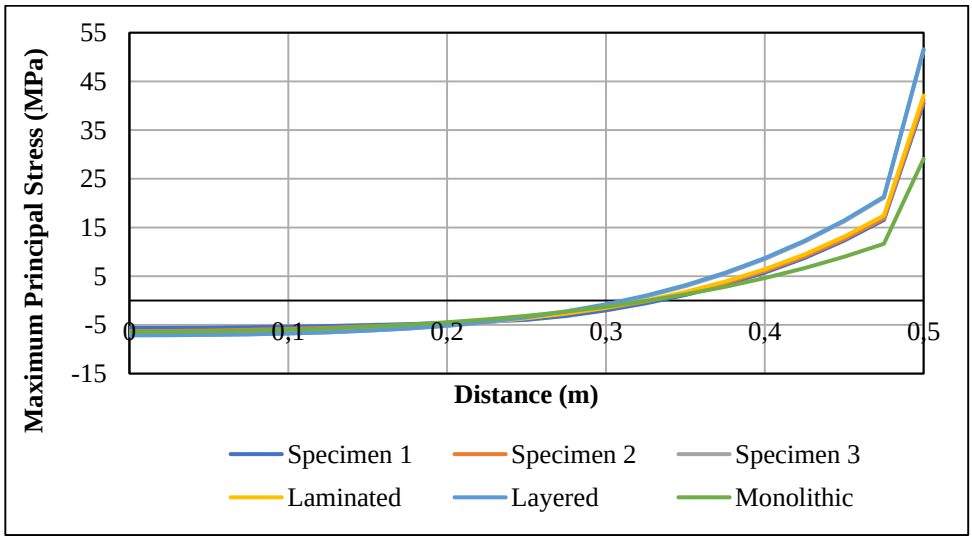

Figure 4.27. Maximum stresses on the top surface of the glass along the center line at x=0.

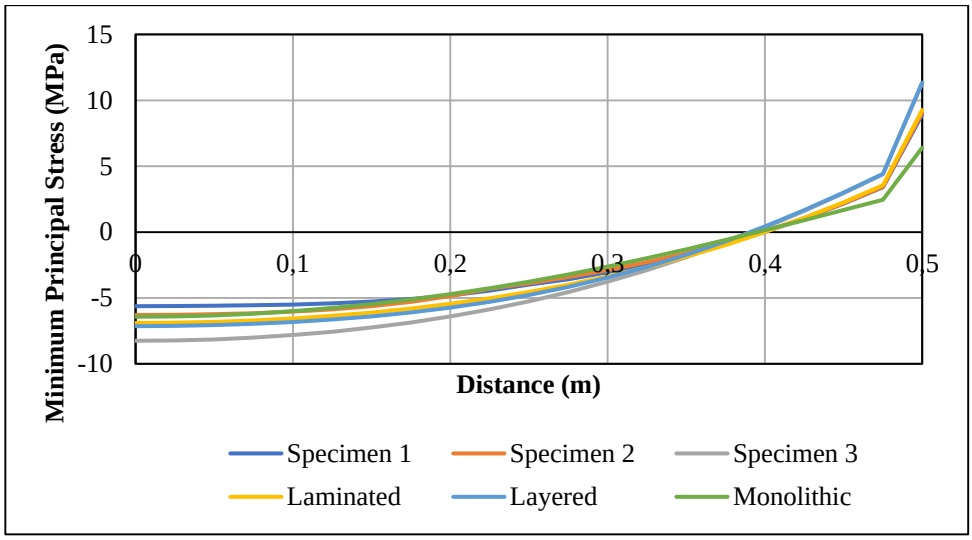

Figure 4.28. Minimum stresses on the top surface of the glass along the center line at x=0.

Distribution of bottom surface maximum and minimum principal stresses for applied P=5 kPa pressure at the centerline along y direction have been given in Figures 4.29 and 4.30, respectively. The maximum and minimum principal stresses on the bottom surface of the glass units are tension to a certain point and compression at the unit boundary. Unlike the maximum stresses on the top surface, the maximum stresses on the top surface have their maximum values at the boundary of the plate unit as tensile stress. Minimum principal stresses on the top surface are compression near the center and they are tension near the boundary of plate. The situation is opposite for bottom glass surface while they are tension at the center and neighborhood, they are compression in the neighborhood of unit boundary.

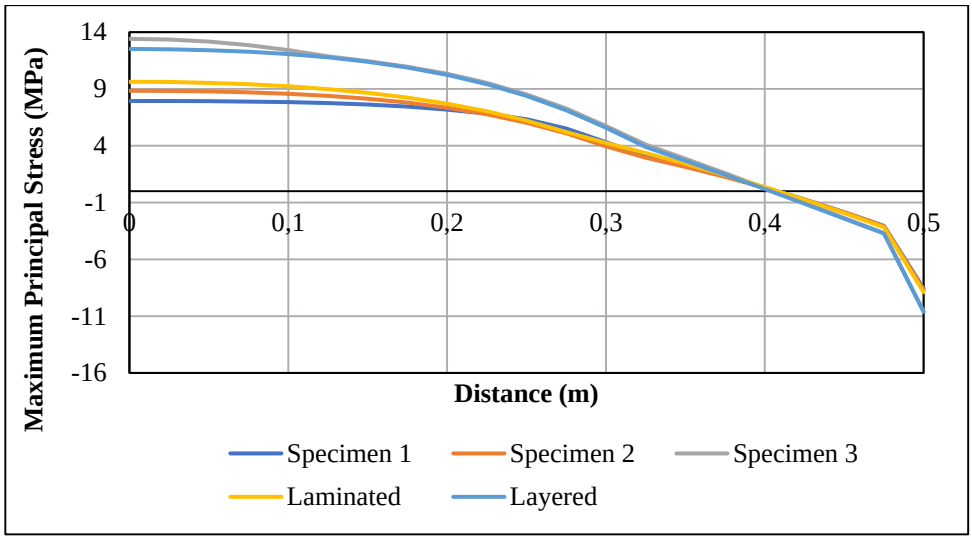

Figure 4.29. Maximum stresses on the bottom surface of the glass along the center line at x=0.

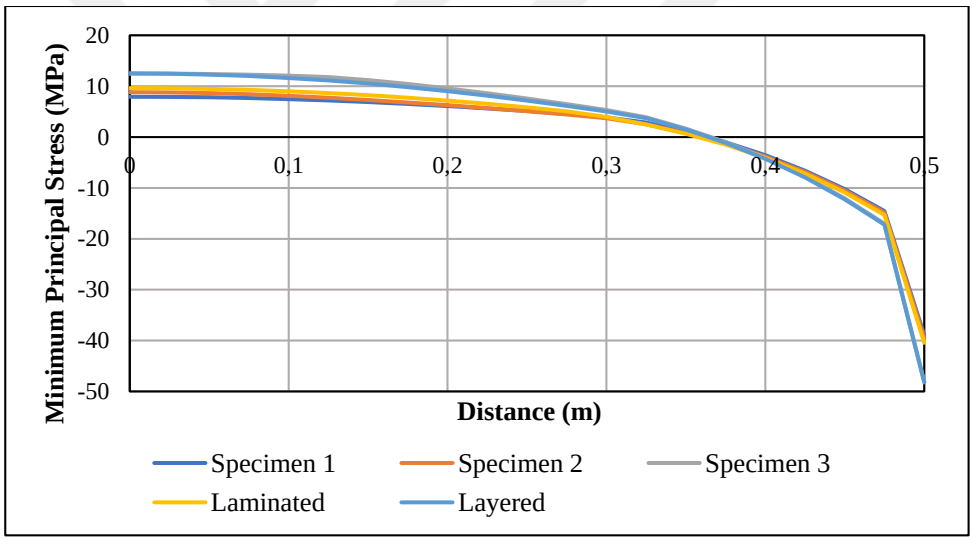

Figure 4.30. Minimum stresses on the bottom surface of the glass along the center line at x=0.

Figures 4.31-4.34 symbolize the maximum and minimum principal stresses along the diagonal of the plate unit at the top and bottom surfaces for applied P=5 kPa pressure, respectively. In Figure 4.31, the maximum principal stress of the top surface takes the greatest value as compression at the center and they are zero at the corner of unit. Double curvature which is proof of nonlinear behavior is observable in the figure. Figure 4.32 shows how the top surface minimum principal stress changes through the diagonal. It resets as it approaches the unit limit, up to this point the minimum stresses are observed as tension.

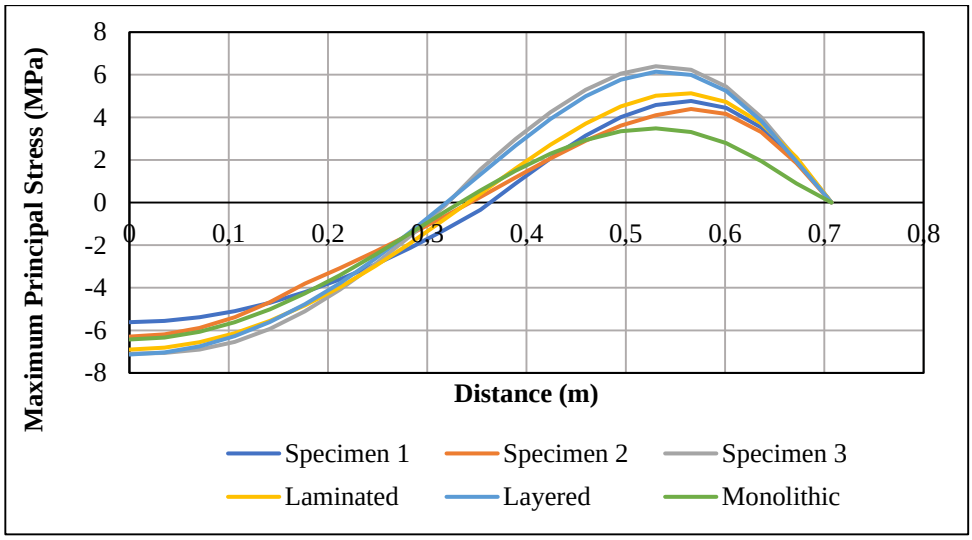

Figure 4.31. Maximum stresses on the top surface of the glass along the diagonal.

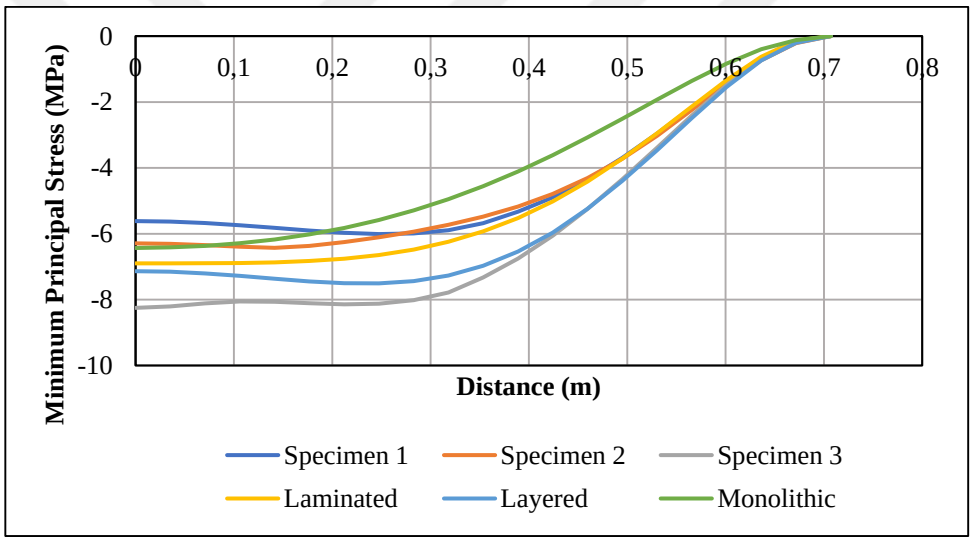

Figure 4.32. Minimum stresses on the top surface of the glass along the diagonal.

While the 5 kPa pressure is acting on the plate surfaces, the maximum stress of the bottom surface is tension along the diagonals shown in Figure 4.33. It is seen that at the center of the plate the maximum stresses on the bottom surface of the unit is maximum. The minimum stress lines for the same load value on the bottom surface of the unit along the diagonal are shown in Figure 4.34. We observe that beyond a certain point (nearly 0.4 meter), stresses stop being tensile stress and they behave as compressive stress. They are maximum at the boundary of the plate.

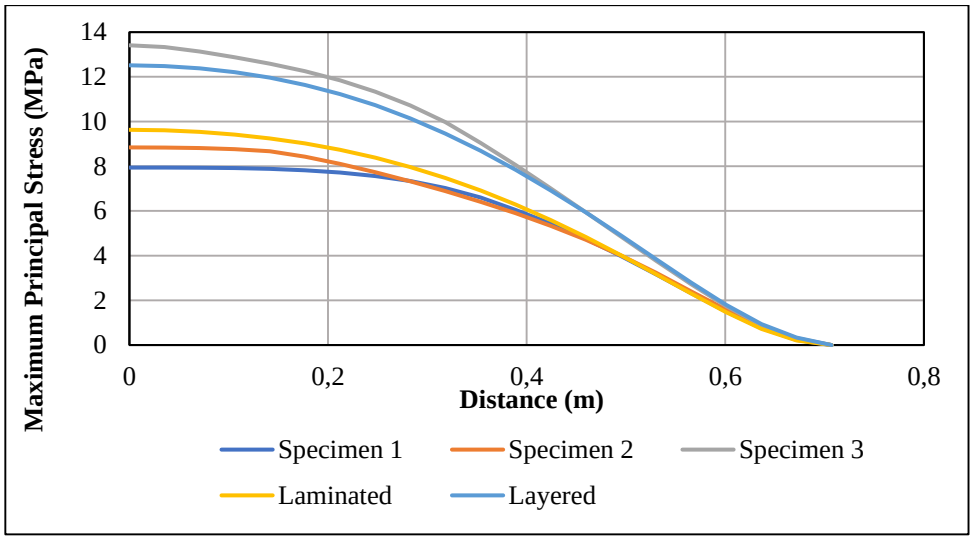

Figure 4.33. Maximum stresses on the bottom surface of the glass along the diagonal.

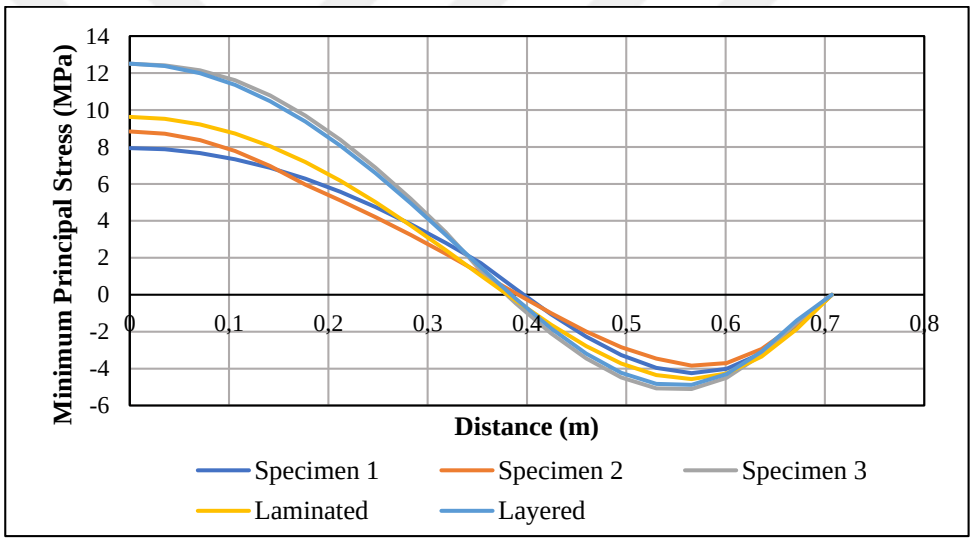

Figure 4.34. Minimum stresses on the bottom surface of the glass along the diagonal.

Figures 4.35 and 4.36 indicate maximum stress versus load curves on the surfaces of top layer of laminated glass unit. Maximum principal stresses on the top surface of the glass unit are compression while they are tension on the bottom surface of corresponding unit due to the applied pressure. In Figure 4.35, the limits of the behavior change for increasing load values. For load values less than 2.5 kPa, the lower limit of the behavior is observed as behavior of monolithic glass, while it is observed as the behavior of specimen 1 after this load value. As observable in the figures, stress values of layered unit and Specimen 3 are quite close to each other but those of layered unit are slightly higher.

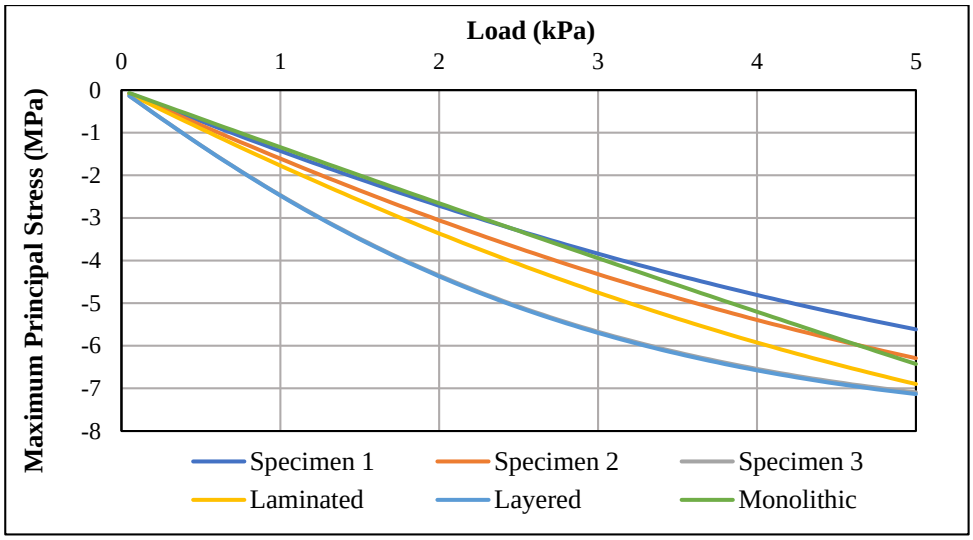

Figure 4.35. Maximum stresses on the top surface of the glass unit.

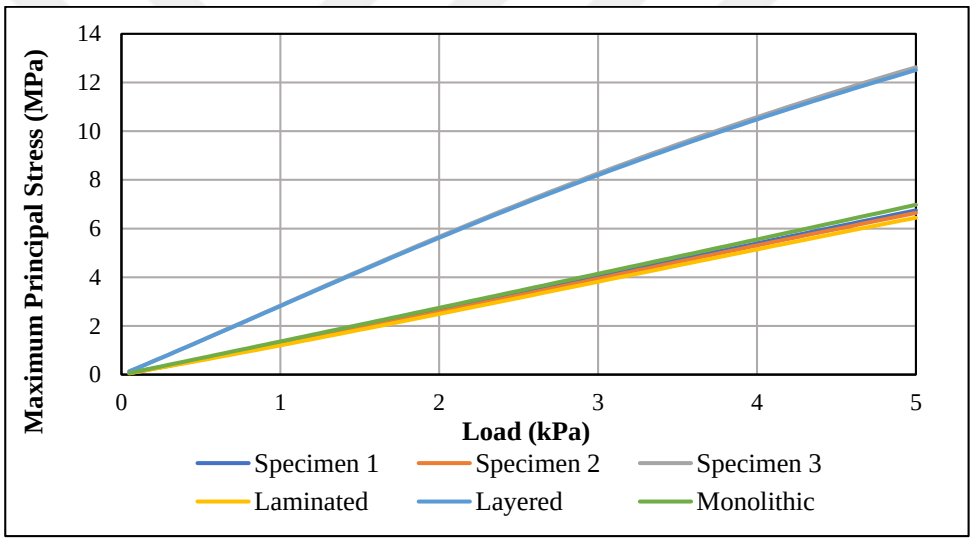

Figure 4.36. Maximum stresses on the bottom surface of the top glass unit.

Figures 4.37-4.38 are plotted to symbolize the maximum principal stresses against different load values for the surfaces of bottom glass unit. The maximum principal stresses on the top surface of the bottom glass unit are compression. The maximum principal stresses at the bottom surface of bottom layer are tension. While the maximum stress level on the top surface is observed in the layered unit, the maximum stress on the bottom surface is observed in the Specimen 3 glass unit. On the top surface maximum principal stress values of delaminated specimens are limited by stress values of layered and laminated unit. In contrary on the bottom surface the upper limit is the behavior of Specimen 3.

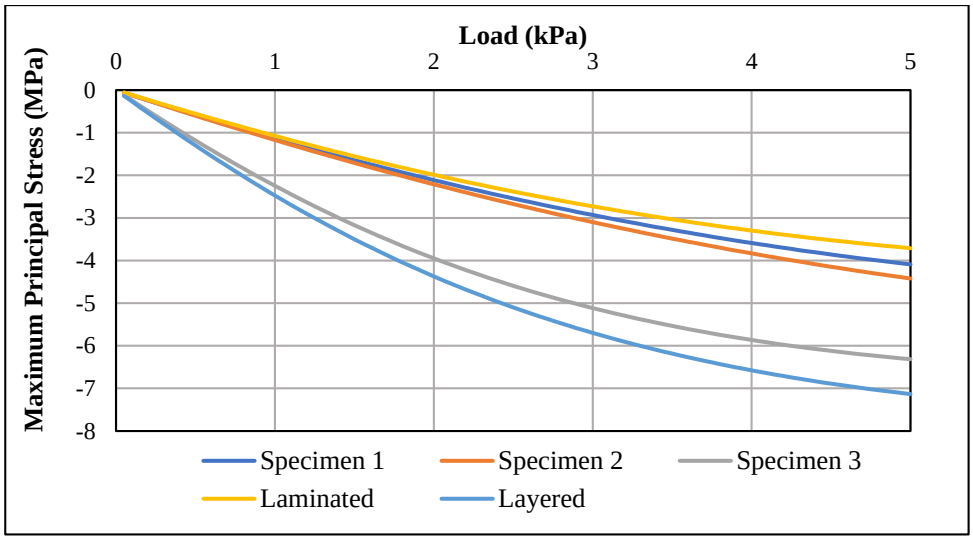

Figure 4.37. Maximum stresses on the top surface of the bottom glass unit.

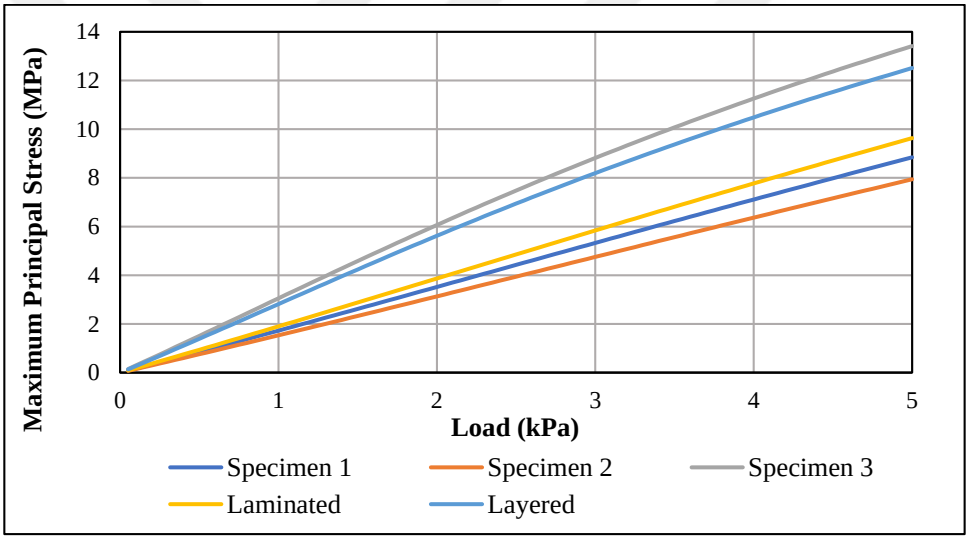

Figure 4.38. Maximum stresses on the bottom surface of the glass unit.

In order to define the behavioral limits of laminated glass units, theoretical stress analyzes of laminated and monolithic glass units are performed. The strength factor is defined as the ratio of the maximum principal stress of the monolithic glass unit to the maximum principal stress of the laminated glass unit. If the PVB interlayer is strong enough to transfer the entire shear between the glass units, the strength factor is 1.0, which means that the radial compressive strength is similar for laminated and monolithic glass units.

The stresses and displacements of the monolithic and laminated glass units are compared to arrive at the strength factor value of the laminated glass unit. For the laminated

unit, the strength factor value is calculated by the following formula;

$$\text{Strength Factor} = \frac{\text{Maximum Principal Stress in Monolithic Glass Unit}}{\text{Maximum Principal Stress in Laminated Glass Unit}}$$

Membrane stresses occur as radial pressures increase due to large deformations in addition to bending stresses. As a result, the strength factor changes. In Figure 4.39, the strength factor value for the fixed supported laminated glass plate unit varies between 0.45-0.8. As the load increases, the strength factor value increases slightly. While approximate values are observed in other laminated glass units, the lowest strength factor value is seen in Specimen 3.

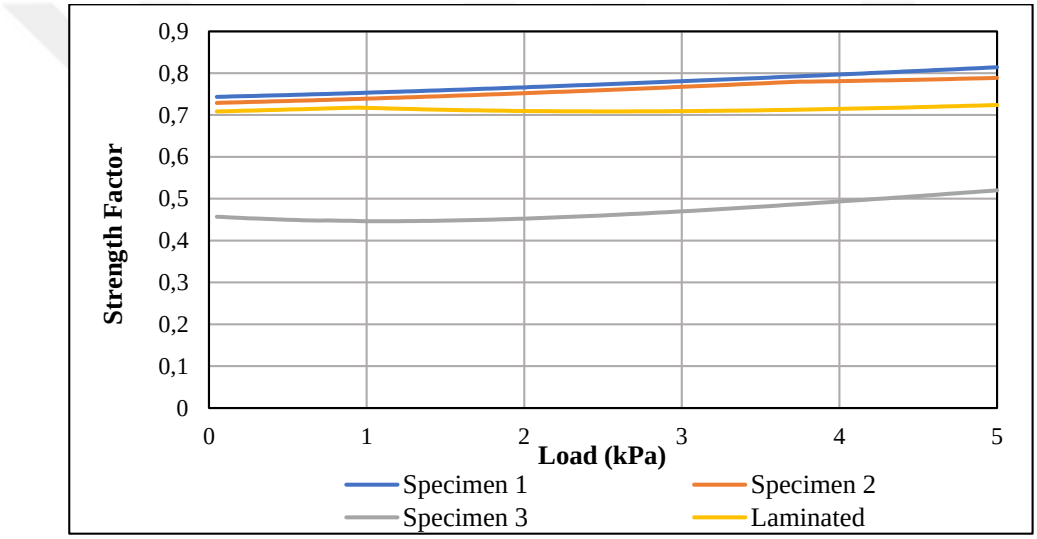

Figure 4.39. Strength factor for the fixed supported laminated plate.

For fixed supported laminated glass plate, contours of the maximum and minimum principal stress values on the top and bottom glass units for applied 5 kPa pressure are shown in Figures 4.40-4.55.

Maximum principal stress contours for the top and bottom glass surfaces of Specimen 1 are presented in Figure 4.40 and 4.41, respectively. On the top surface of the unit maximum principal stresses are tension and they are at the boundaries of the quarter plate. The maximum principal stress on the bottom surface of the unit are tension and located at the center of the unit.

Minimum principal stress contours are given in Figure 4.42 for the top of the unit

(Specimen 1) and in Figure 4.43 for the bottom unit. The minimum principal stress on both of the surfaces are at the boundaries of the quarter plate. Minimum principal stresses take maximum value as compression on bottom surface and tension on top surface. The maximum stresses develop at the boundary of unit on both of the surfaces.

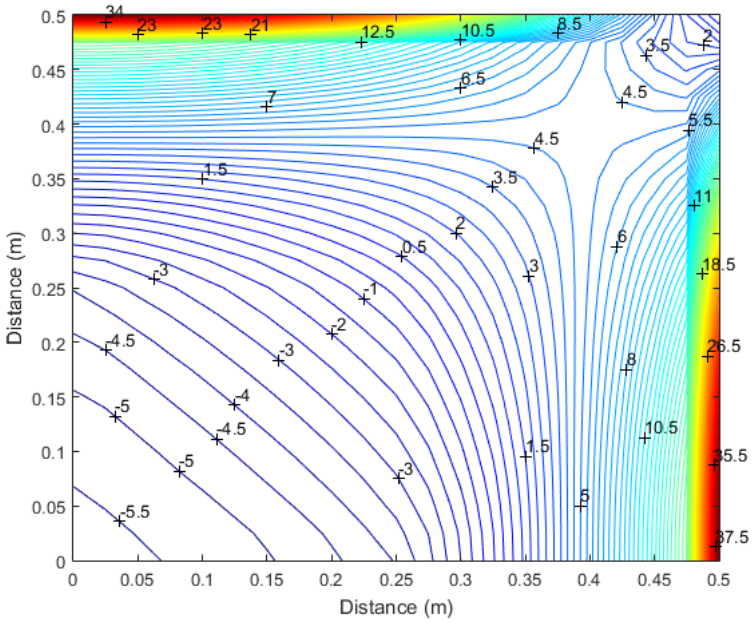

Figure 4.40. Contours of maximum principal stress on the top surface of Specimen 1.

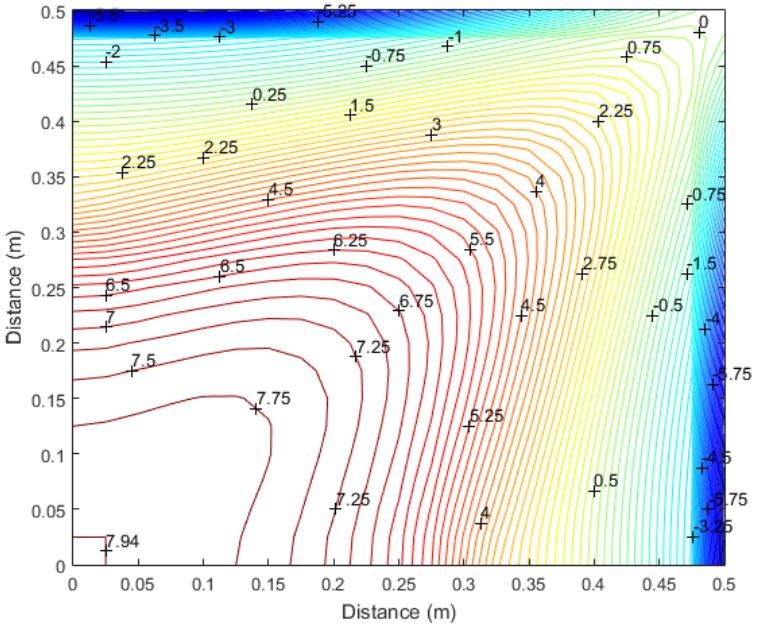

Figure 4.41. Contours of maximum principal stress on the bottom surface of Specimen 1.

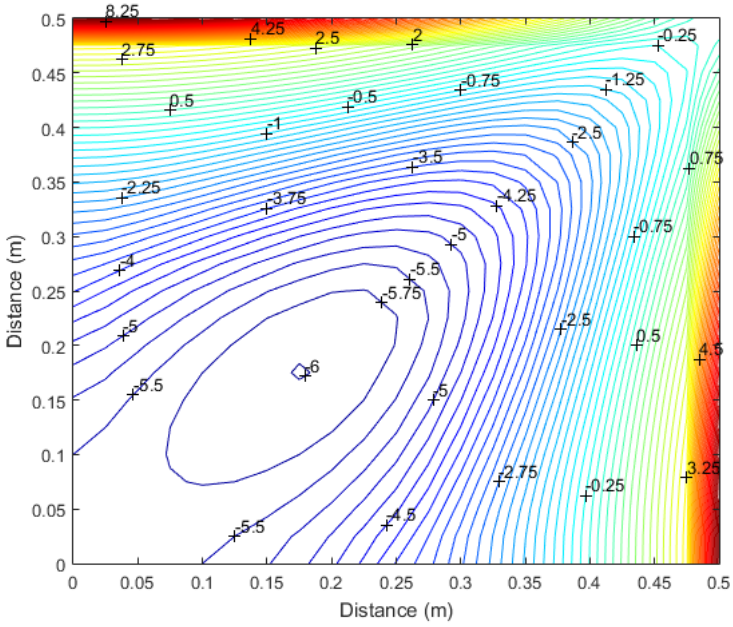

Figure 4.42. Contours of minimum principal stress on the top surface of Specimen 1.

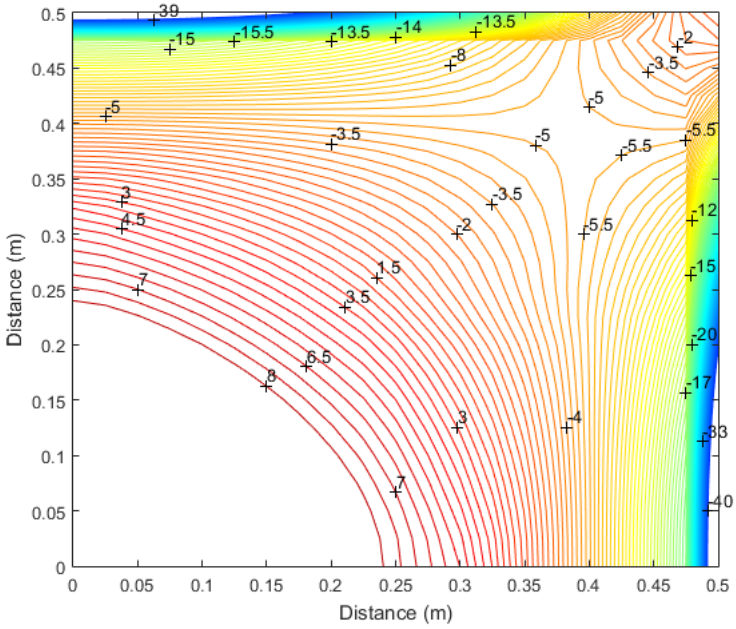

Figure 4.43. Contours of minimum principal stress on the bottom surface of Specimen 1.

Maximum principal stress contours of Specimen 2 are given in Figure 4.44 for the top surface and in Figure 4.45 for the bottom surface of the unit. The maximum principal stress at the top surface is at the boundaries of the quarter plate. The maximum principal stress on the bottom surface of the glass is located in the center of the unit. It has been observed that

there is a region where stresses are zero in the top and bottom plates. Maximum principal stresses are tensile on the top surface at the boundaries of unit and compressive on the bottom surface. In the center the situation is opposite.

The minimum principal stress contours of Specimen 2 are shown in Figures 4.45 and 4.46 for the top and bottom surface of the unit. The minimum principal stress on the bottom surface of the glass and the top surface of the glass are at the boundaries of the quarter plate.

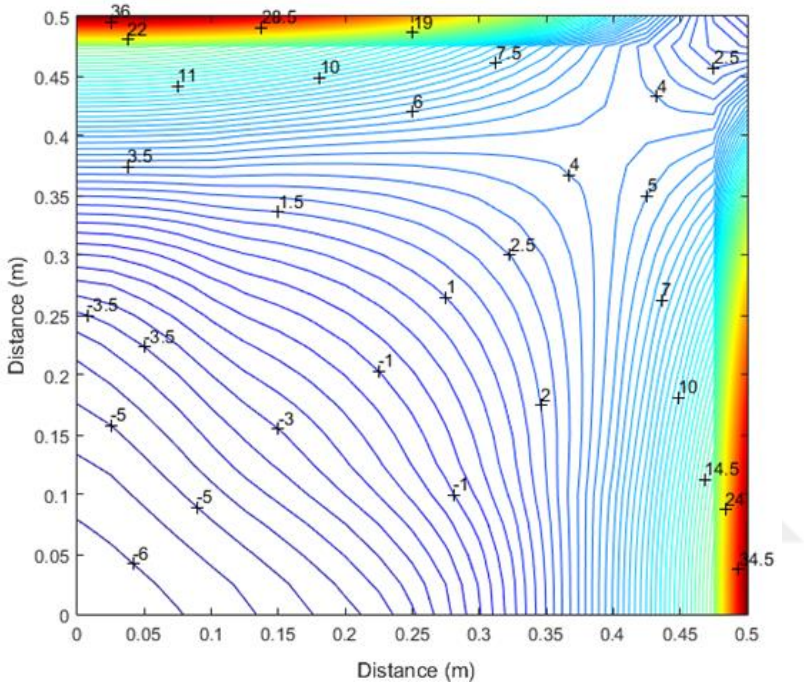

Figure 4.44. Contours of maximum principal stress on the top surface of Specimen 2.

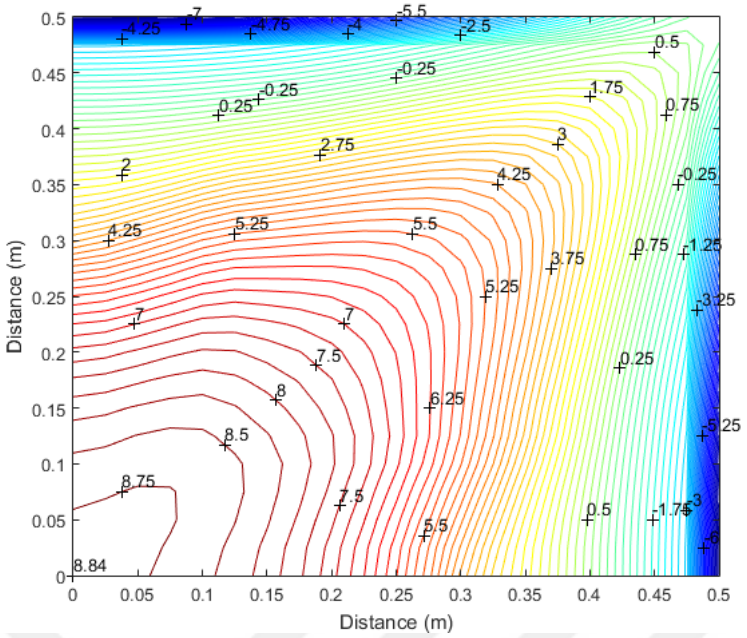

Figure 4.45. Contours of maximum principal stress on the bottom surface of Specimen 2.

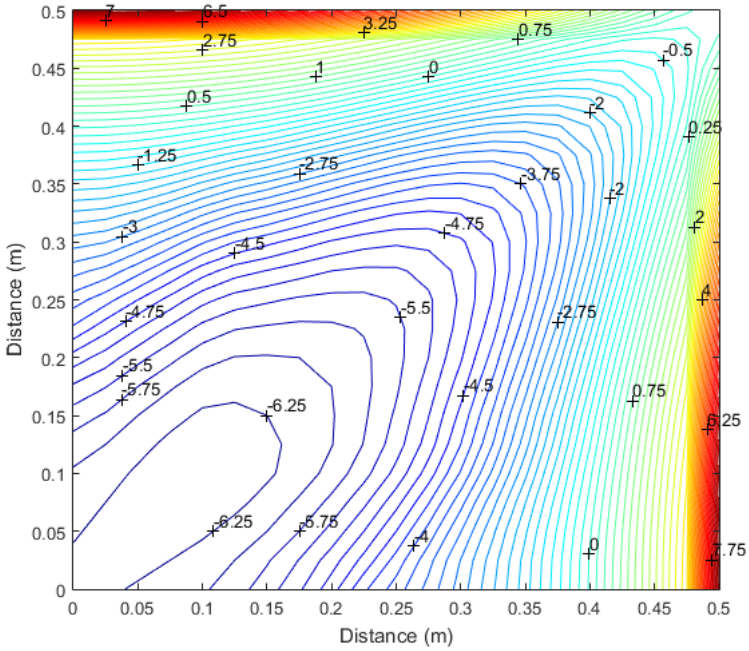

Figure 4.46. Contours of minimum principal stress on the top surface of Specimen 2.

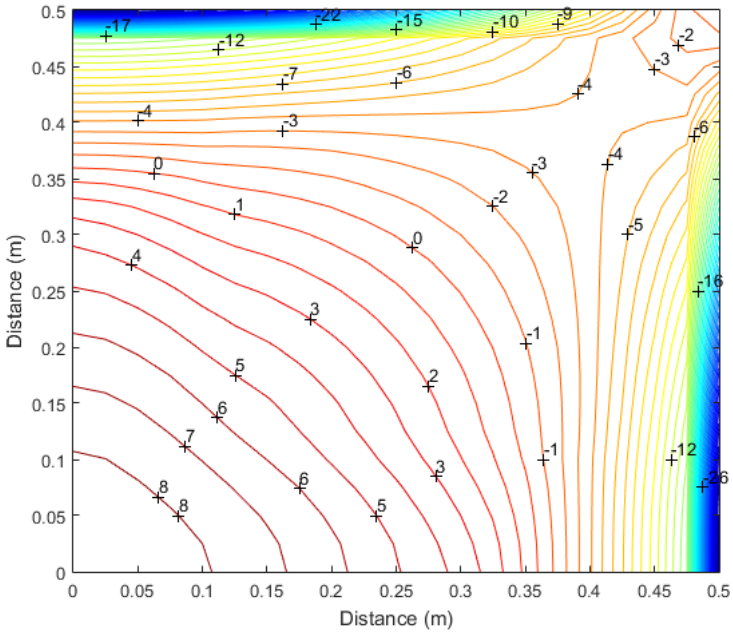

Figure 4.47. Contours of minimum principal stress on the bottom surface of Specimen 2.

Maximum principal stress contours are given in Figure 4.48 for top of the Specimen 3 and in Figure 4.49 for the bottom of the unit. The maximum principal stress at the top surface take maximum value at the boundaries of the quarter plate as tensile stress while they are compressive stress at the center of the whole plate. The maximum principal stress on the bottom surface of the glass is located in the center of the whole unit.

The minimum principal stress contours are given in Figure 4.50 for the top of the unit which has delamination at the boundary of unit (Specimen 3) and in Figure 4.51 for the bottom of the unit. The minimum principal stress on the bottom surface of the glass and the top surface of the glass are at the boundaries of the quarter plate.

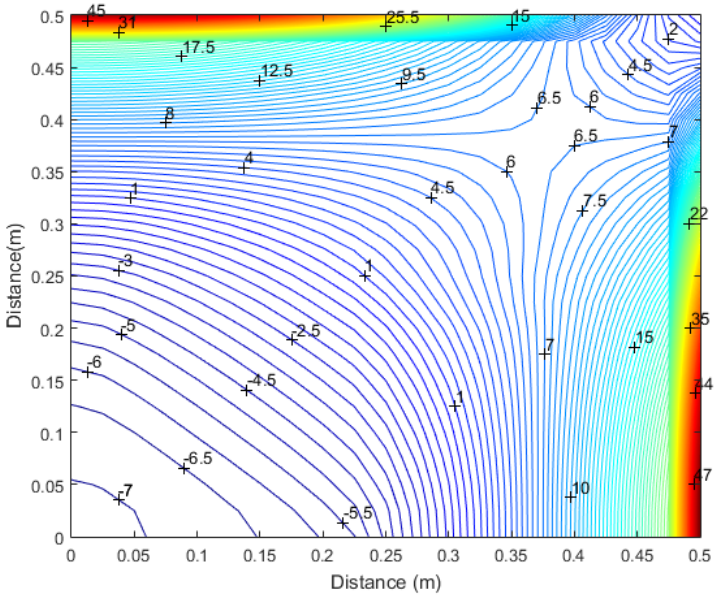

Figure 4.48. Contours of maximum principal stress on the top surface of Specimen 3.

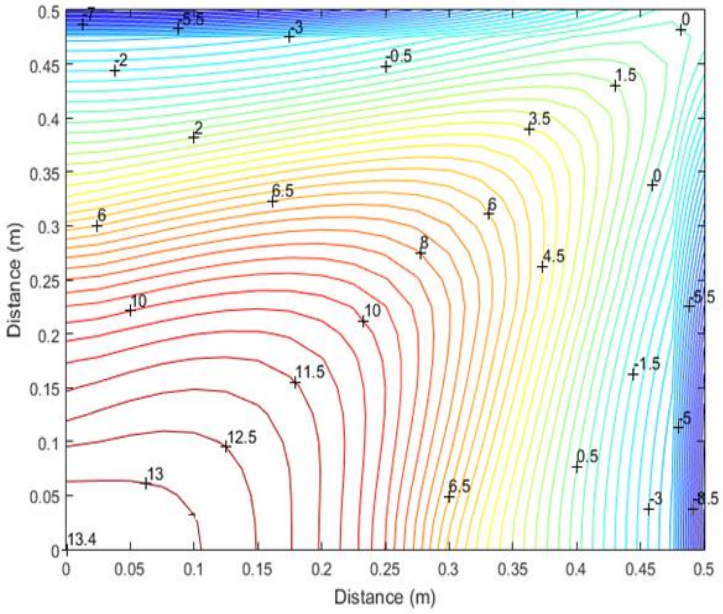

Figure 4.49. Contours of maximum principal stress on the bottom surface of Specimen 3

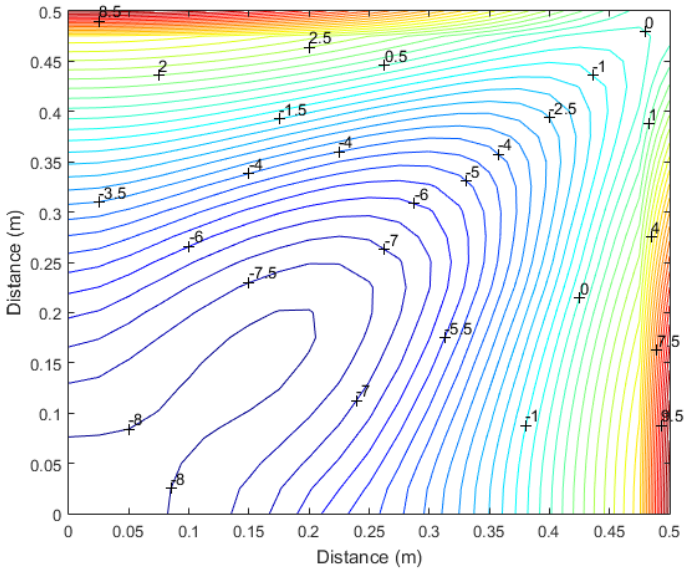

Figure 4.50. Contours of minimum principal stress on the top surface of Specimen 3.

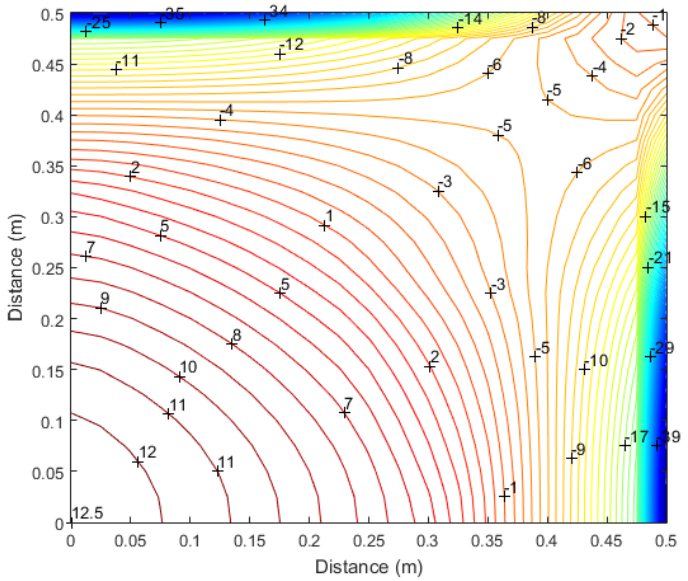

Figure 4.51. Contours of minimum principal stress on the bottom surface of Specimen 3.

Maximum principal stress contours are given in figure 4.52 for the top of the laminated glass unit and in Figure 4.53 for the bottom of the unit. The maximum principal stress at the top surface is at the boundaries of the quarter plate. The maximum principal stress on the bottom surface of the laminated unit is located in the center of the unit. Similar to the delaminated units, zero stress region is observable for laminated glass unit.

The minimum principal stress contours are given in Figure 4.54 for the top of the laminated unit and Figure 4.55 for the bottom unit. The minimum principal stress on the bottom and top surface of laminated unit are at the boundaries of the quarter plate.

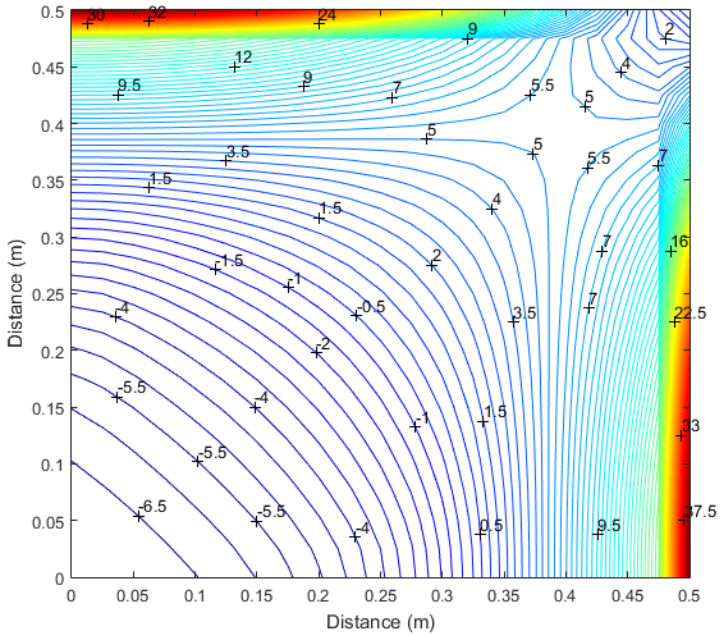

Figure 4.52. Contours of maximum principal stress on the top surface of laminated glass unit.

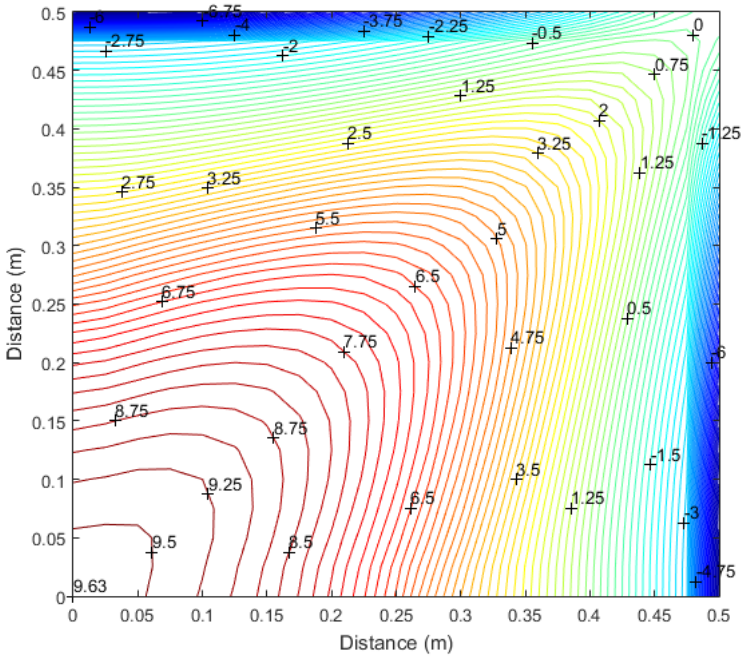

Figure 4.53. Contours of maximum principal stress on the bottom surface of laminated glass unit.

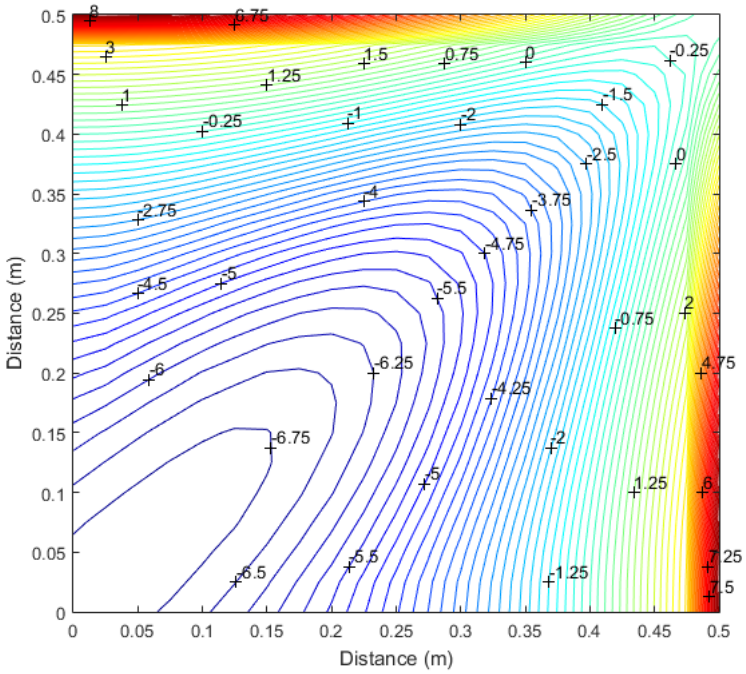

Figure 4.54. Contours of minimum principal stress on the top surface of laminated glass unit.

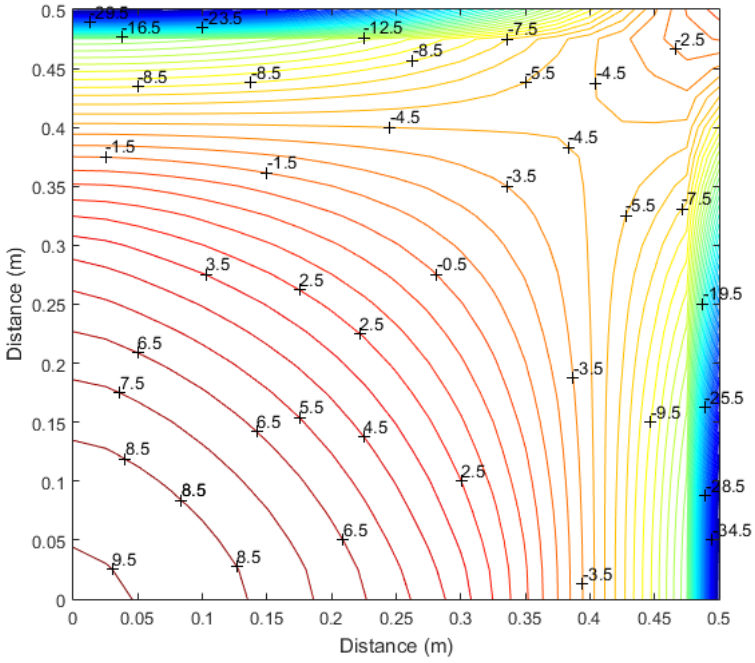

Figure 4.55. Contours of minimum principal stress on the bottom surface of laminated glass unit.

Contour plots of lateral displacement distribution of glass plates subjected to 5 kPa pressure e are given for a quarter laminated glass plate unit to have an accurate observation. Lateral deflection contours are plotted in figures 4.57-4.59. The maximum lateral displacement is at the center of the unit. Below figures show that displacements are maximum for Specimen 3 which has delamination at the boundary of unit while they are minimum for Specimen 1 which has central delamination.

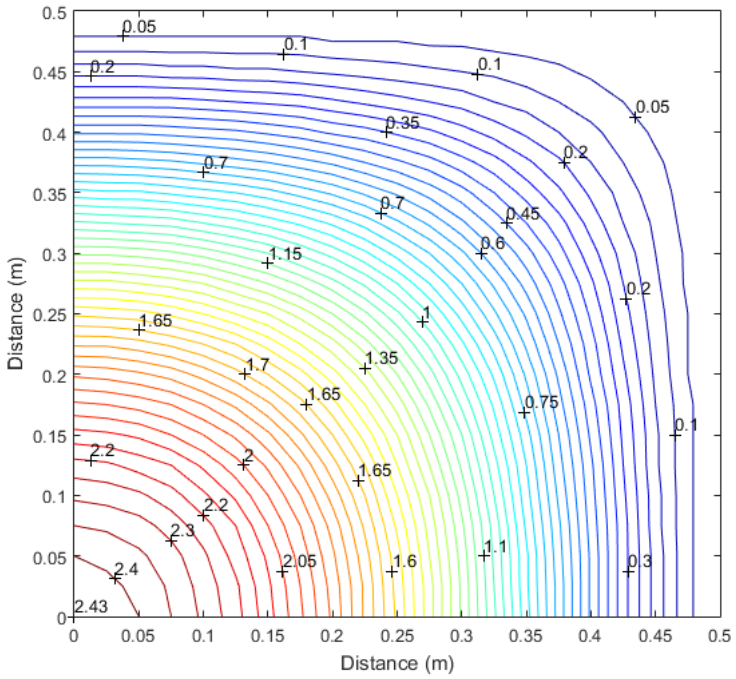

Figure 4.56. Contours of lateral displacement of Specimen 1.

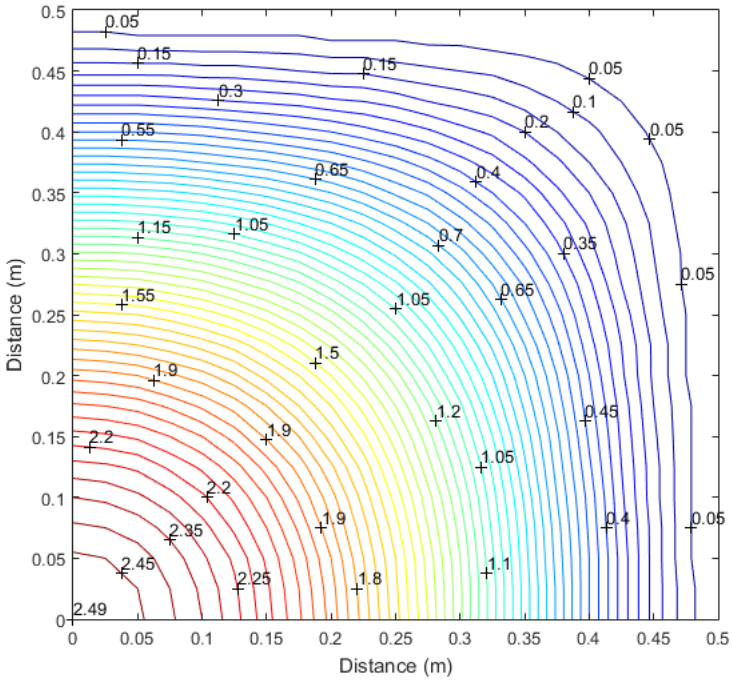

Figure 4.57. Contours of lateral displacement of Specimen 2.

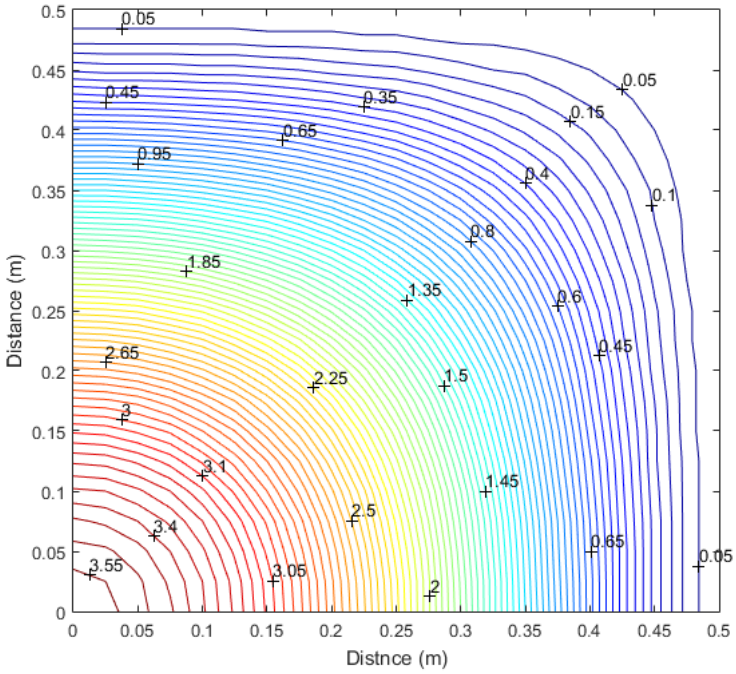

Figure 4.58. Contours of lateral displacement of Specimen 3.

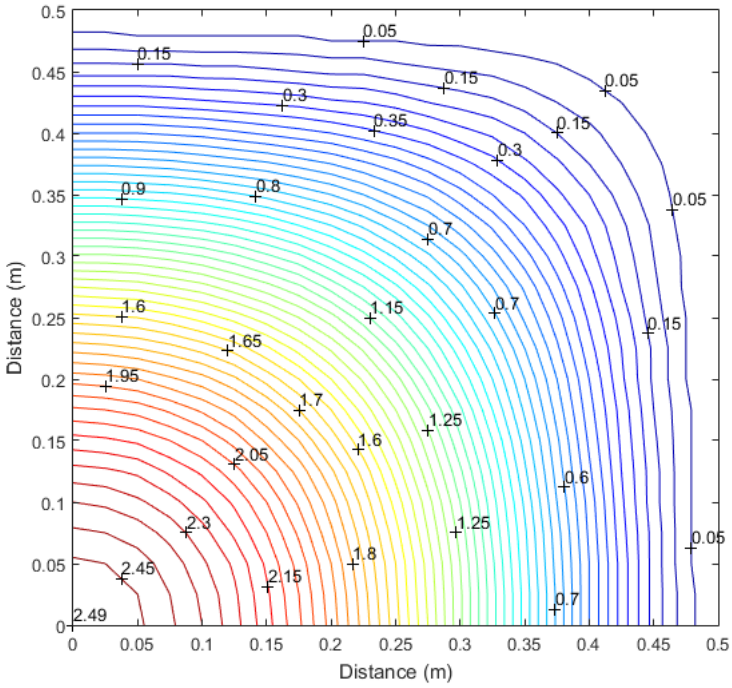

Figure 4.59. Contours of lateral displacement laminated glass unit.

4.3. Numerical Results of Simply Supported Laminated Glass Plate Under Uniform Distributed Load

To examine the influence of boundary conditions to the mechanical behavior of laminated glass plate the current model is rearranged for fixed supported . Tested fixed supported laminated glass plate has 1 m in length and 1 m width. It contains two glass layer and each of them has a thickness of 5 mm and the thickness of the interlayer is 0.76 mm. The total thickness of the unit is 10.76 mm. The Poisson's ratio and Young's modulus of glass are taken to be 0.22 and 70 GPa, respectively. Poisson's ratio and shear modulus of the intermediate layer are taken as 0.29 and 1000 kPa, respectively.

The obtained governing equations can be applied for the solution of simply supported unit. For simply supported unit subjected to uniform pressure, the boundary conditions are as follows:

At x = 0:

$u_1 = 0,$

$e_{1xy} = 0,$

$u_2 = 0,$

$e_{2xy} = 0,$

$$\frac{\partial w}{\partial x} = 0,$$

$$\frac{\partial}{\partial x}\left(\frac{\partial^2 w}{\partial x^2} + \mu\frac{\partial^2 w}{\partial y^2}\right) + \frac{\partial}{\partial y}\left[2(1-\mu)\frac{\partial^2 w}{\partial x \partial y}\right] = 0$$

At x = a

$e_{1x} + \mu e_{1y} = 0,$

$e_{1xy} = 0,$

$e_{2x} + \mu e_{2y} = 0,$

$e_{2xy} = 0,$

$w = 0,$

$$\frac{\partial^2 w}{\partial x^2} = 0$$

At y = 0 :

$v_1 = 0,$

$e_{1xy} = 0,$

$v_2 = 0,$

$e_{2xy} = 0,$

$$\frac{\partial w}{\partial y} = 0.$$

$$\frac{\partial}{\partial y}\left(\frac{\partial^2 w}{\partial y^2} + \mu\frac{\partial^2 w}{\partial x^2}\right) + \frac{\partial}{\partial x}\left[2(1-\mu)\frac{\partial^2 w}{\partial x \partial y}\right] = 0$$

At y = b

$e_{1y} + \mu e_{1x} = 0,$

$e_{1xy} = 0,$

$e_{2y} + \mu e_{2x} = 0,$

$e_{2xy} = 0,$

$\omega = 0,$

$$\frac{\partial^2 w}{\partial y^2} = 0$$

Figures 4.60 and 4.61 compares results of linear and nonlinear approach to guess the behavior of the simply supported glass plate. Normalized deflection against load distribution obtained as result of linear and nonlinear approximations are given in Figure 4.60. When the nonlinearity level of the maximum deflection to the thickness of a single glass plate is greater than 0.9, nonlinear solution must be considered. Figure 4.60 shows that this ratio (nonlinearity level) is around 0.9 for a P=4 kPa load. The central deflection from the linear approximation is nearly 1.3 times the deflection from the nonlinear approximation at a load of P=10 kPa.

Figure 4.61 symbolizes stress against load distribution obtained using linear and nonlinear approximation methods. Unlike the deflection values, the stress values obtained by the linear approximation method are lower than those of obtained via nonlinear approximation method. While this situation continued until P=7 kPa load, linear behavior started to be higher than nonlinear behavior after this load value.

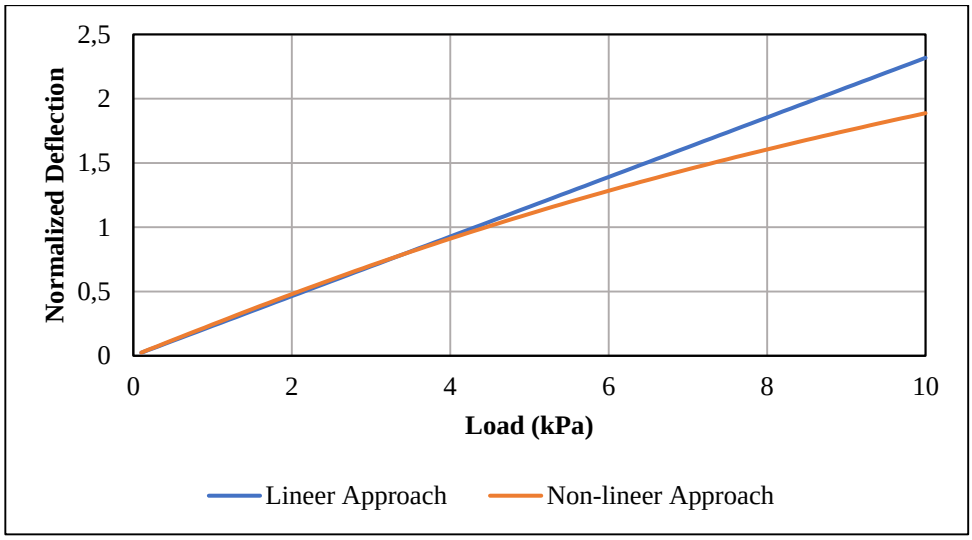

Figure 4.60. Normalized maximum deflection ($\frac{w_{max}}{h}$) against load for simply supported laminated glass plate.

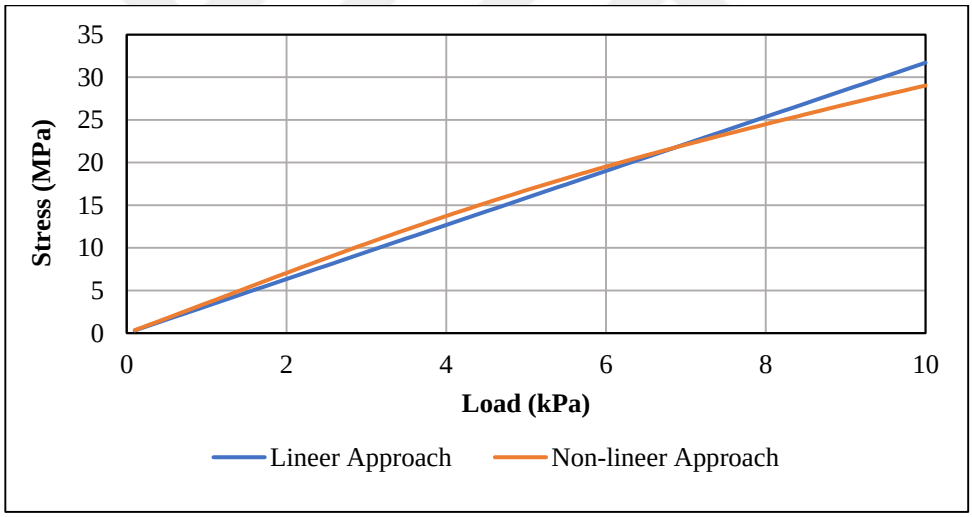

Figure 4.61. Stress against load for simply supported laminated glass plate.

Figures 4.62 and 4.63 show a comparison of the results obtained via linear and nonlinear approach to suppose the behavior of simply supported delaminated glass plate (Specimen 2). The nonlinear approximation method should be considered when the ratio of the maximum deviation to the thickness of a glass plate is greater than 0.6. Figure 4.62 shows that this ratio (non-linearity level) is around 0.6 for a P=3 kPa load. The central deflection from linear approximation is nearly 1.2 times the deflection from nonlinear approximation at P=10 kPa load. Figure 4.63 shows information about stress versus load for

linear and nonlinear behavior. The stress values for the linear response are higher than the stress values obtained for the nonlinear response. This situation started after P=4 kPa load.

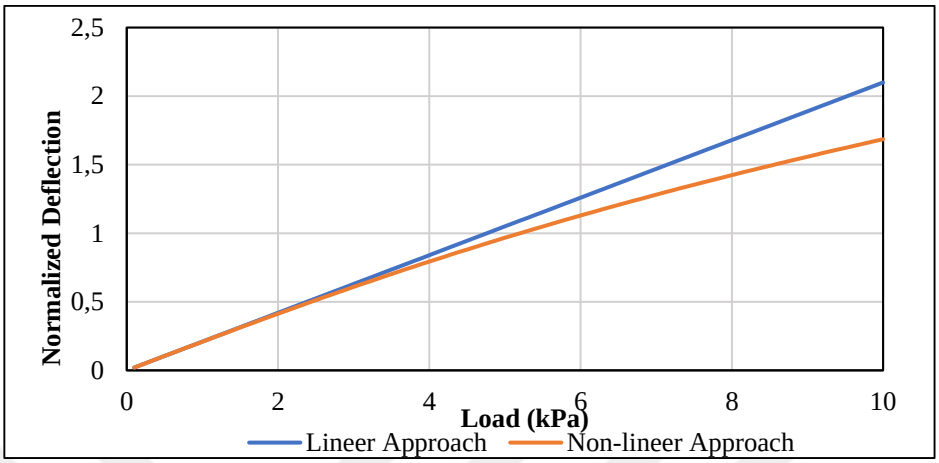

Figure 4.62 Normalized maximum deflection ($\frac{w_{max}}{h}$) versus load for simply supported delaminated glass plate (Specimen 2).

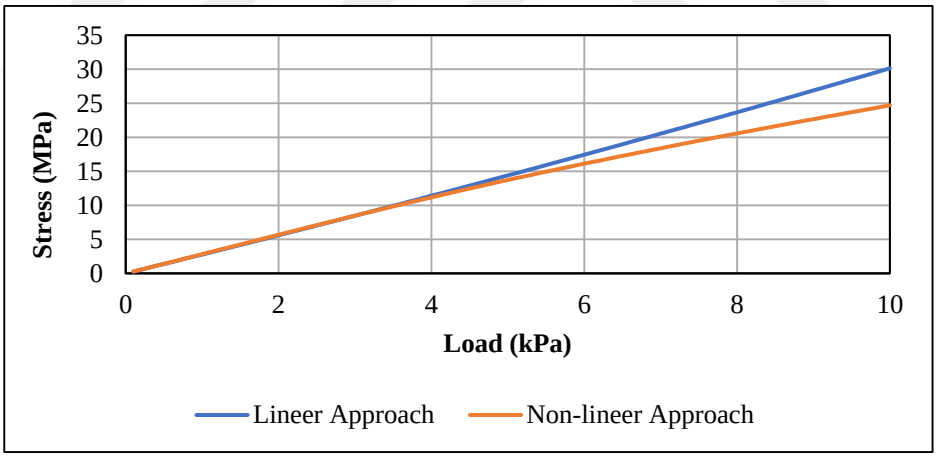

Figure 4.63. Stress versus load for simply supported delaminated glass plate (Specimen 2).

Figures 4.64 and 4.65 shows comparison of the response of delaminated glass units with the behavior of monolithic, layered and laminated glass plates. In Figure 4.64, the maximum displacement is observed in layered glass, while the minimum displacement is observed in monolithic glass. According to Figure 4.65, maximum stress is observed in Specimen 3 while minimum stress is observed in monolithic glass.

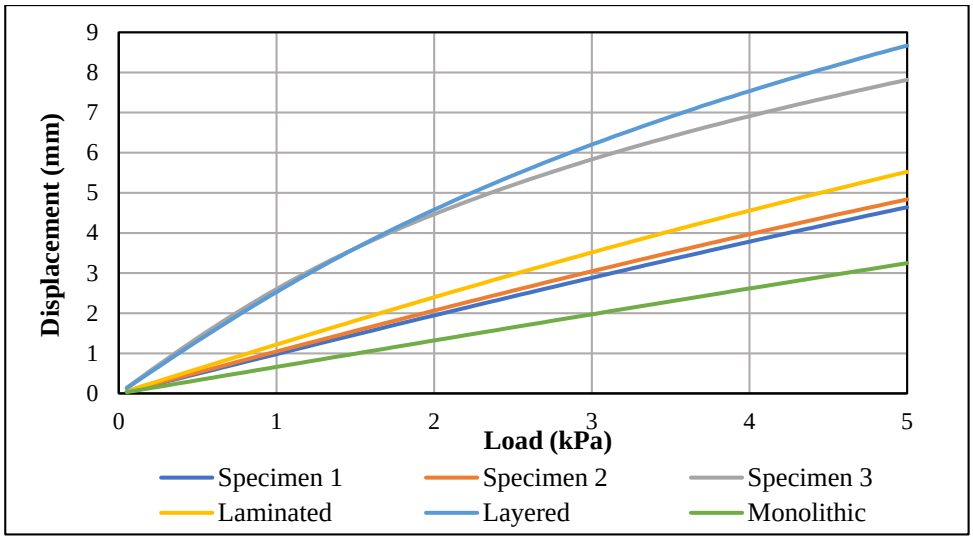

Figure 4.64. Comparison of maximum displacements.

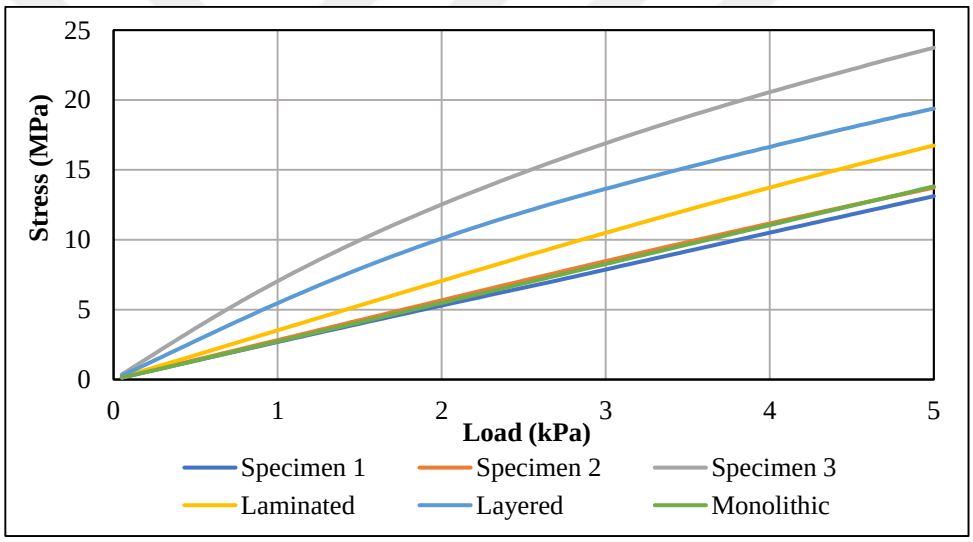

Figure 4.65. Comparison of maximum stresses.

Figures 4.66 and 4.67 are circumferential displacements (u1 and u2) along the diagonal for the top and bottom glass units, respectively. At the beginning of the quarter plate, the circumferential displacements are zero, as we expected. After a certain point the behavior of the unit changes for layered glass. At the boundary of the quarter plate unit, the circumferential displacements take their maximum values. After the maximum values, a tend towards negative values is observed. In addition, minimum displacements were observed in monolithic glass compared to other glasses. Maximum displacements were observed in the layered glass.

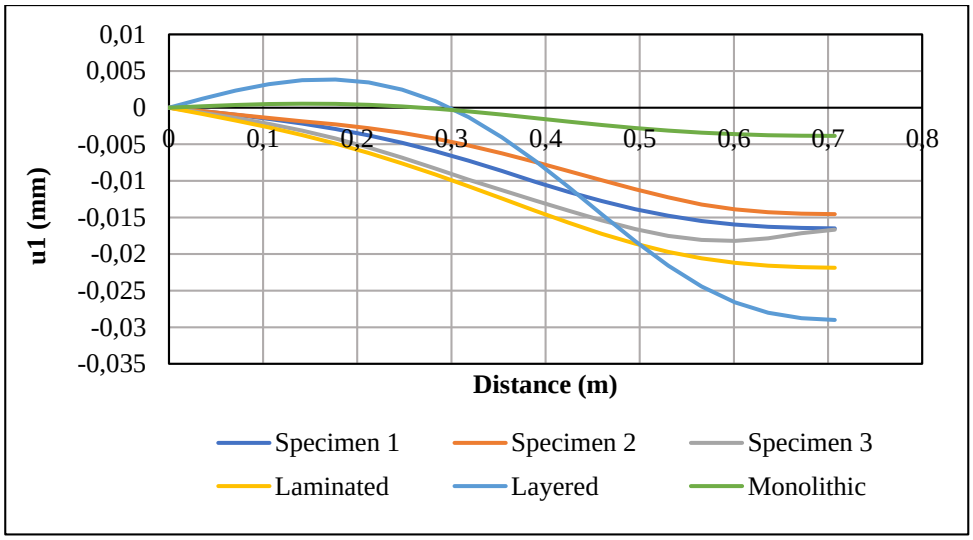

Figure 4.66. Circumferential displacement in x direction of the top glass unit along the diagonal.

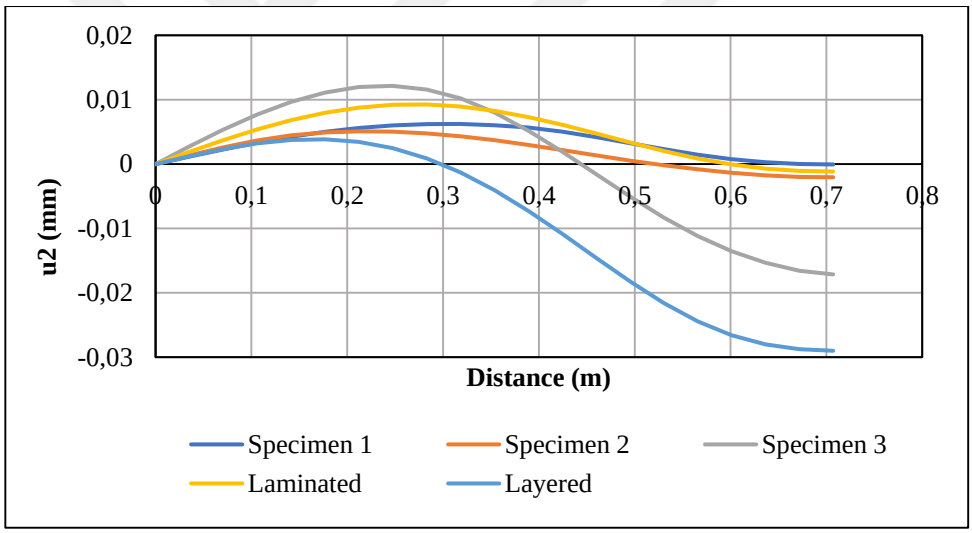

Figure 4.67. Circumferential displacement in x direction of the bottom glass unit along the diagonal.

Figures 4.68 and 4.69 symbolize the axial displacements (v1 and v2) along the diagonal for the top and bottom glass units. The axial displacements (v1 and v2) are zero at the beginning of the quarter unit, as we expected. For the layered glass unit and Specimen 3; the behavior of the units changes at a point in the domain.. Minimum displacements were observed in monolithic glass compared to other glasses.

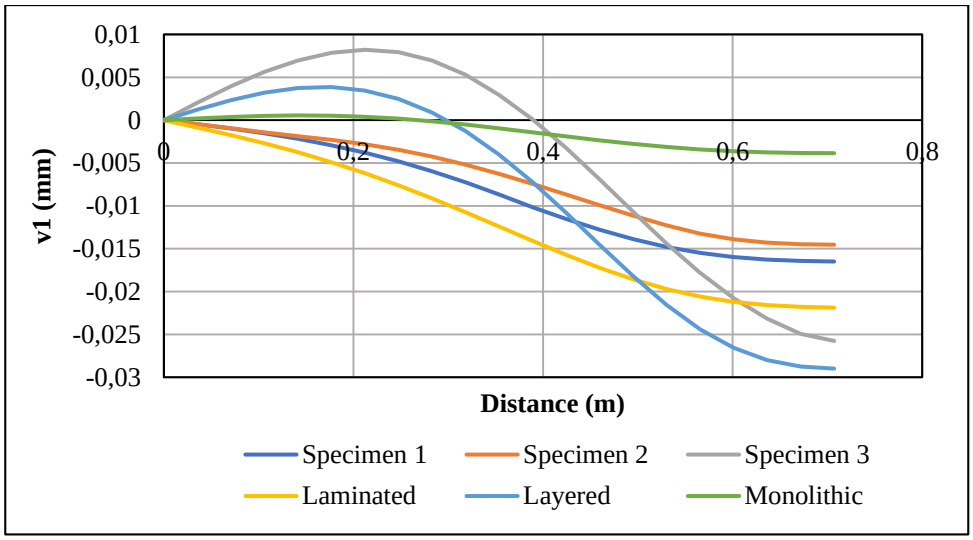

Figure 4.68. Axial displacement in y direction of the top glass unit along the diagonal.

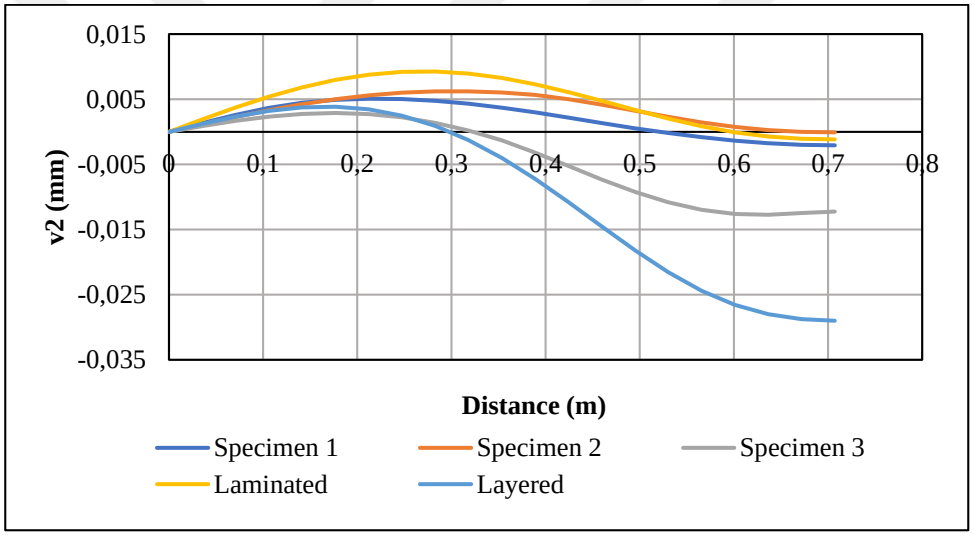

Figure 4.69. Axial displacement in y direction of the bottom glass unit along the diagonal.

Figures 4.70-4.72 show the lateral displacements of the laminated glass plate at the centerline in x, y direction and along the diagonal of the unit, respectively. Lateral displacements are maximum at the center while they are zero at the boundary. Lateral displacements along the center line took the same values in the x and y directions due to geometric properties of unit. As different from the fixed supported effect of delamination is more observable in simply supported unit and in simply supported unit lateral deflection values of delaminated units are bounded by those of layered and monolithic units.

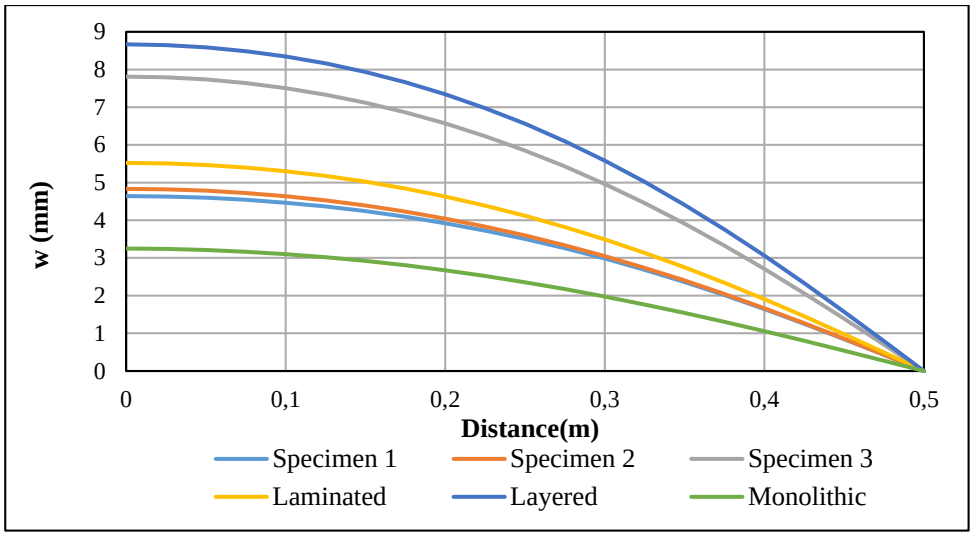

Figure 4.70. Lateral displacement of the unit at the center along the center line at y=0.

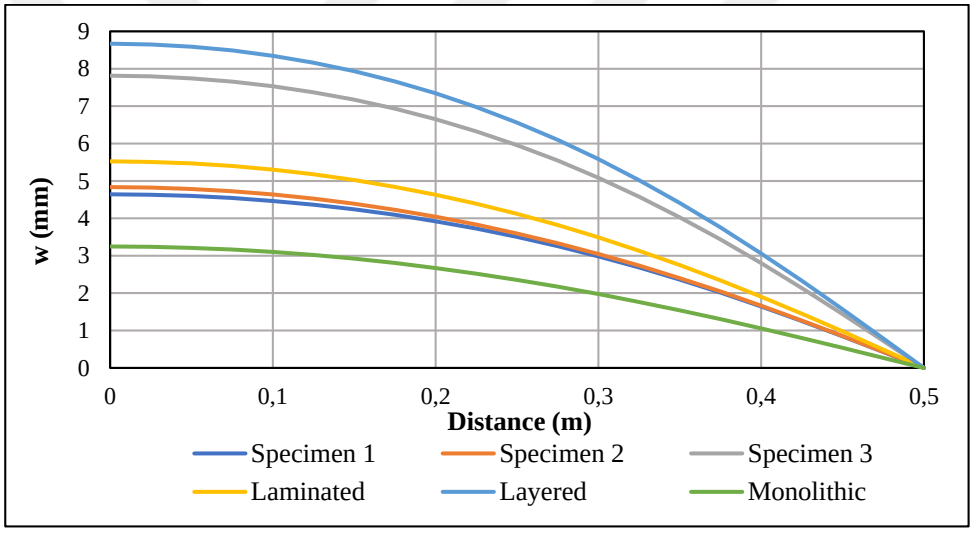

Figure 4.71. Lateral displacement of the unit at the center along the center line at x=0.

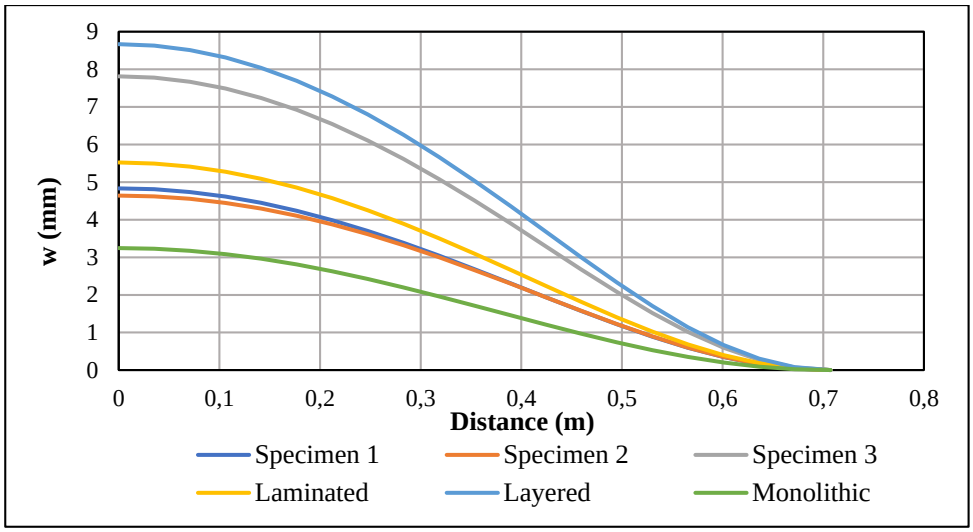

Figure 4.72. Lateral displacement of the unit along the diagonal of unit.

Principal stress distributions on the surfaces of units at the centerline along x direction for applied P=5 kPa pressure have been given in Figures 4.73 and 4.74, respectively. Along the center line maximum principal stresses at the top surface of the glass are compression while they are tension on the bottom surface of unit. They do not change sign along the center line and have their maximum value at beginning point of the quarter unit.

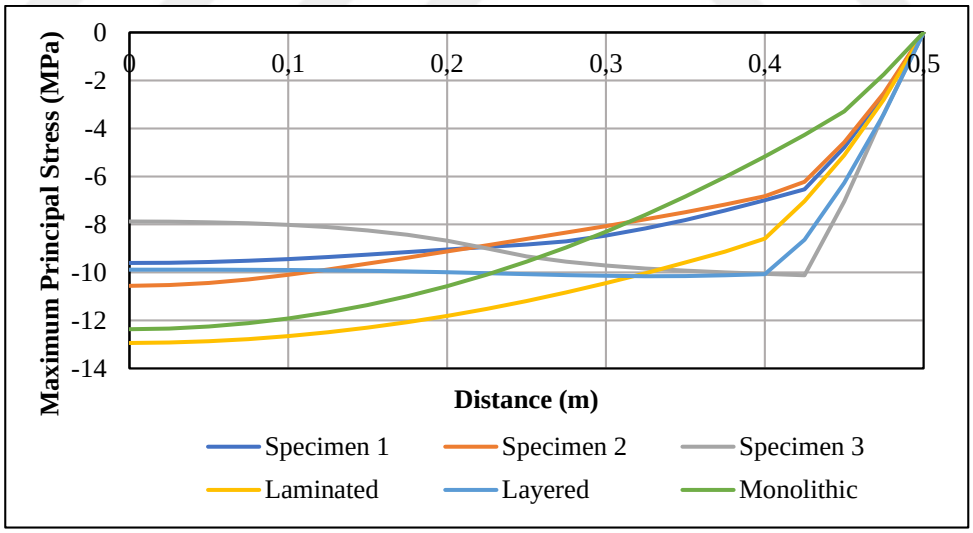

Figure 4.73. Maximum stresses on the top surface of the glass along the center line at y=0.

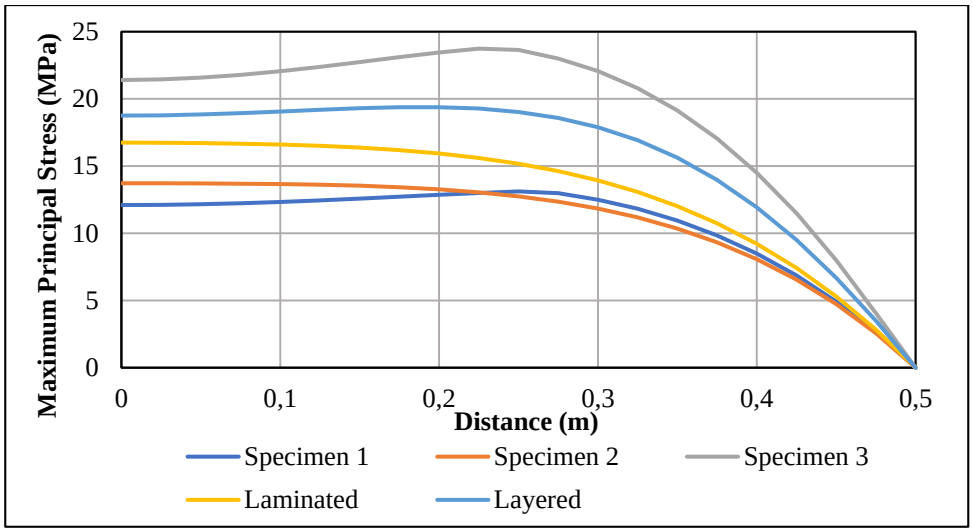

Figure 4.74. Maximum stresses on the bottom surface of the glass along the center line at y=0.

Minimum principal stress curves at the centerline along x direction for applied P=5 kPa pressure have been given in Figures 4.75 and 4.76. The minimum principal stresses at the top surface of the glass unit are compression while they are tension on the surface of unit. In Figure 4.76, there tends to be compression towards the end of the line.

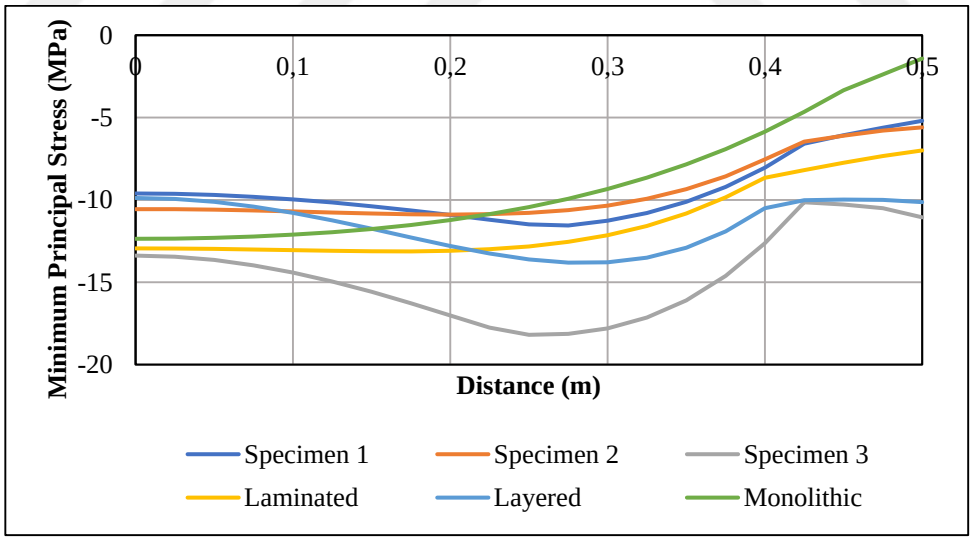

Figure 4.75. Minimum stresses on the top surface of the glass along the center line at y=0.

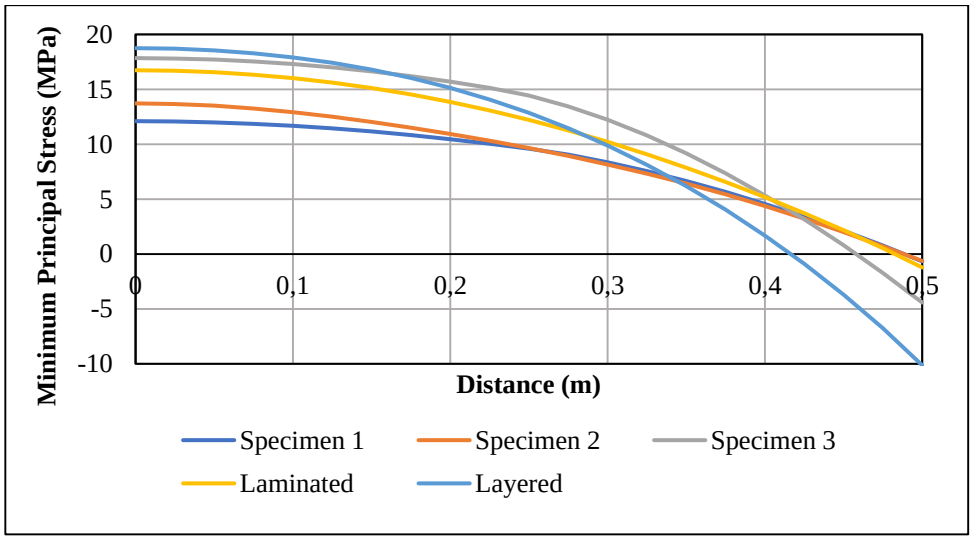

Figure 4.76. Minimum stresses on the bottom surface of the glass along the center line at y=0.

Figures 4.77 and 4.78 are plotted to symbolize the maximum principal stresses on the top and bottom surfaces of the plate unit along the centerline at x=0 for applied P=5 kPa pressure. Maximum principal stresses at the top surface of the glass are compression through the centerline while they are tension on bottom glass surface. They do not change sign through the center line and maximum value as compression at the beginning of quarter unit.

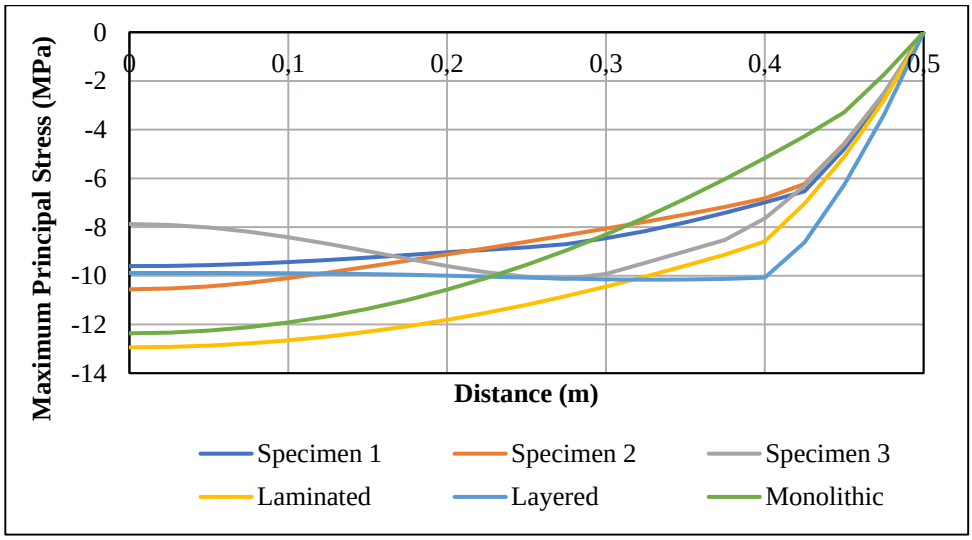

Figure 4.77. Maximum stresses on the top surface of the glass along the center line at x=0.

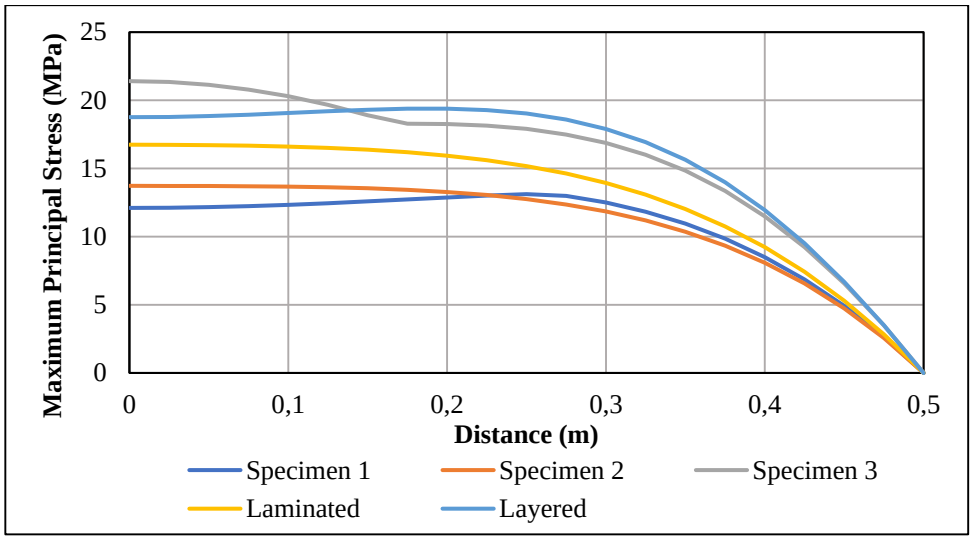

Figure 4.78. Maximum stresses on the bottom surface of the glass along the center line at x=0.

minimum principal stress curves for applied P=5 kPa pressure at the centerline along y direction have been given in Figures 4.72 and 4.73. The minimum principal stresses at the top surface of the glass unit are compression through the center line. The minimum principal stresses at the bottom surface of the glass unit are tension. There tends to be compression towards the end of the line.

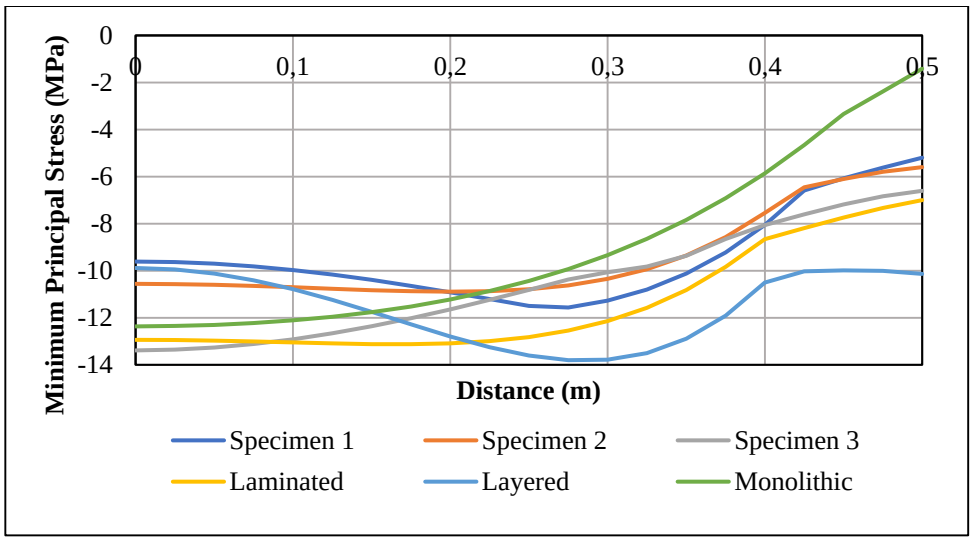

Figure 4.79. Minimum stresses on the top surface of the glass along the center line at x=0.

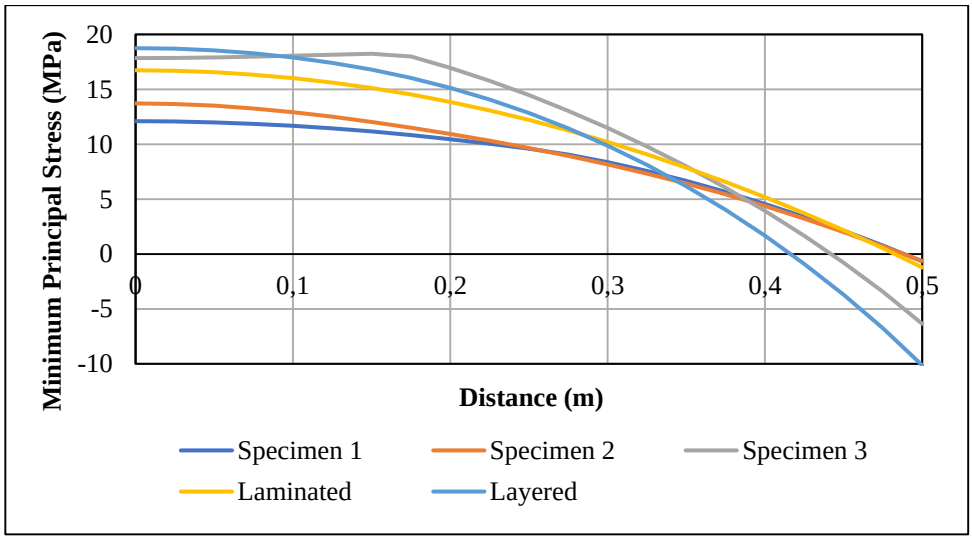

Figure 4.80. Minimum stresses on the bottom surface of the glass along the center line at x=0.

Figures 4.81-4.84 symbolize the maximum and minimum principal stresses curves through plate diagonal on the top and bottom surfaces for applied P=5 kPa pressure, respectively.

Figures 4.81 and 4.82 are plotted to symbolize the maximum principal stress curves at the top and bottom surface of the glass unit through the diagonal. The maximum principal stresses on the top surface of the glass are compressive in the first half of the diagonal while they turn into tension after a certain point on the diagonal. The maximum principal stresses at the bottom surface of the glass are the compressive along the diagonal to the end of the line. They do not change sign. As different than fixed supported plate stresses at the edge of plate are different than zero for simply supported unit. Stresses of simply supported unit are greater than those of fixed supported units.

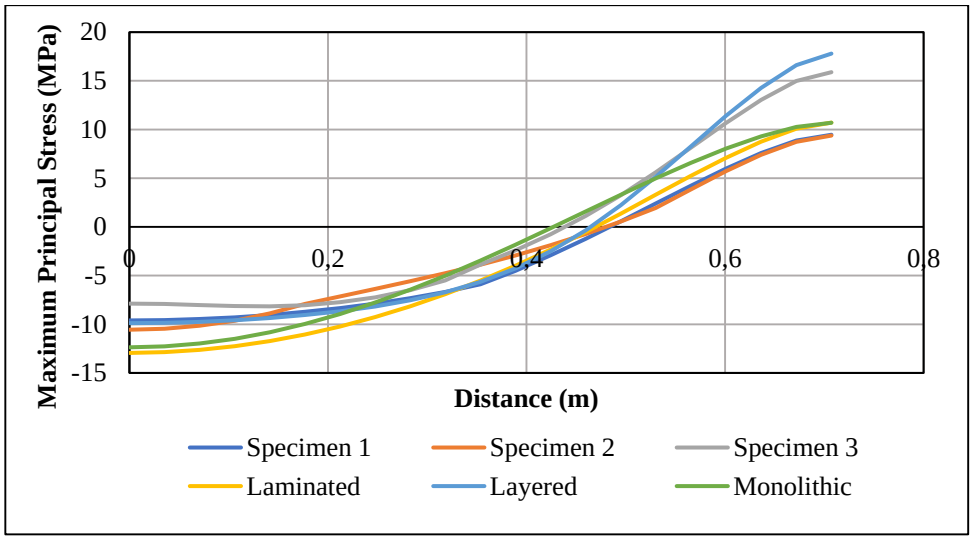

Figure 4.81. Maximum stresses on the top surface of the glass along the diagonal.

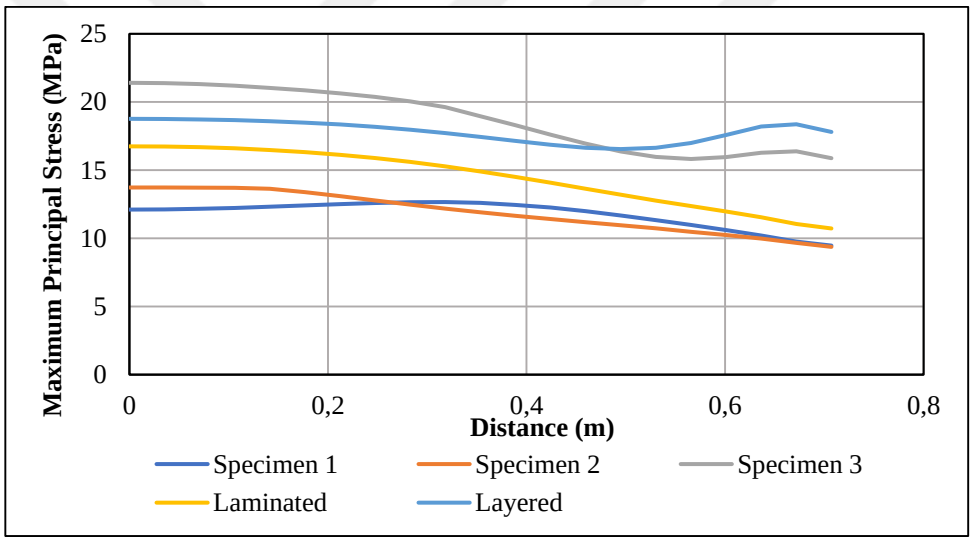

Figure 4.82. Maximum stresses on the bottom surface of the glass along the diagonal.

As seen in Figure 4.83, the minimum stress of the bottom surface is compression along the diagonal for applied P=5 kPa pressure value. It is seen that the maximum stresses on the top surface of the unit take maximum value at the 0.45. meter of the plate. The minimum stress lines for the same load value on the bottom surface of the unit along the diagonal are shown in Figure 4.84. Maximum value of the minimum stresses on the bottom surface of the unit is at the boundary of the plate as tension up to nearly 0,5. meter, after this point turns into compression.

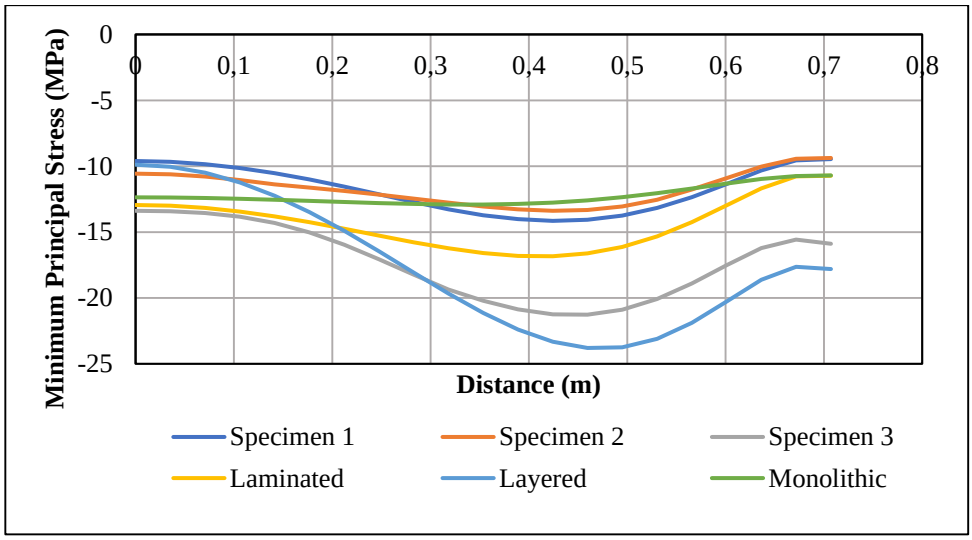

Figure 4.83. Minimum stresses on the top surface of the glass along the diagonal.

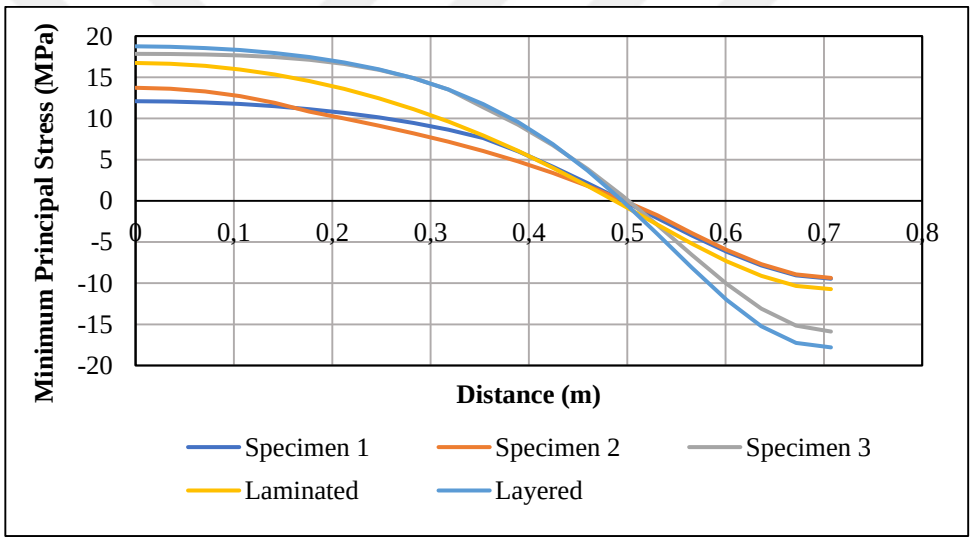

Figure 4.84. Minimum stresses on the bottom surface of the glass along the diagonal.

Figures 4.85 and 4.86 indicate maximum stress versus load curves, each corresponding to a different glass types for the surfaces of the top unit of the laminated glass unit. Maximum principal stresses on the top surface of the top glass unit are compression while they are tension on the bottom surface of corresponding unit due to the applied pressure. In Figure 4.85, the limits of the behavior change for increasing load values. For load values less than 2.8 kPa, the lower limit of the behavior is observed as behavior of specimen 1, while it is observed as the behavior of specimen 3 after this load value. As observable in the Figure 4.86, stress values of layered unit and Specimen 3 are close to each other but those of Specimen 3 unit are higher.

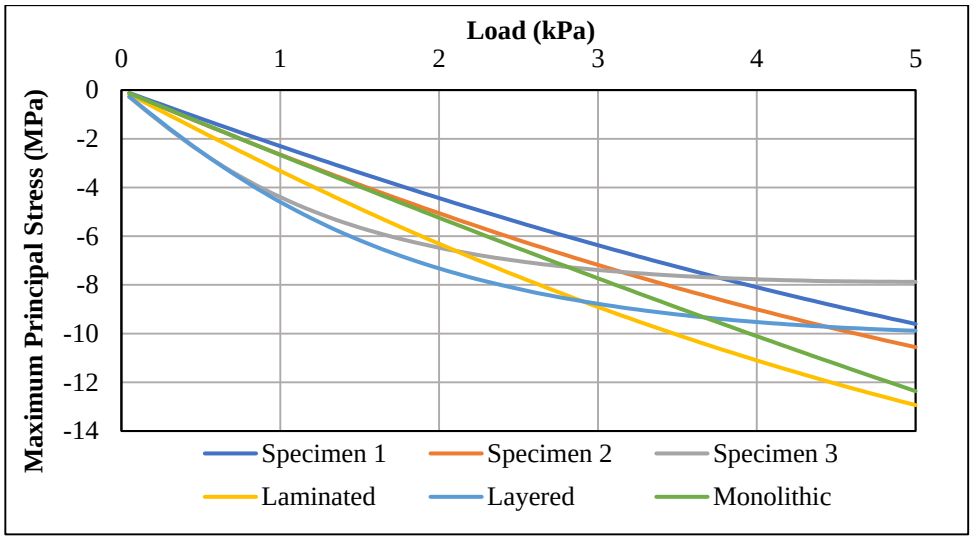

Figure 4.85. Maximum principal stresses on the top surface of the glass.

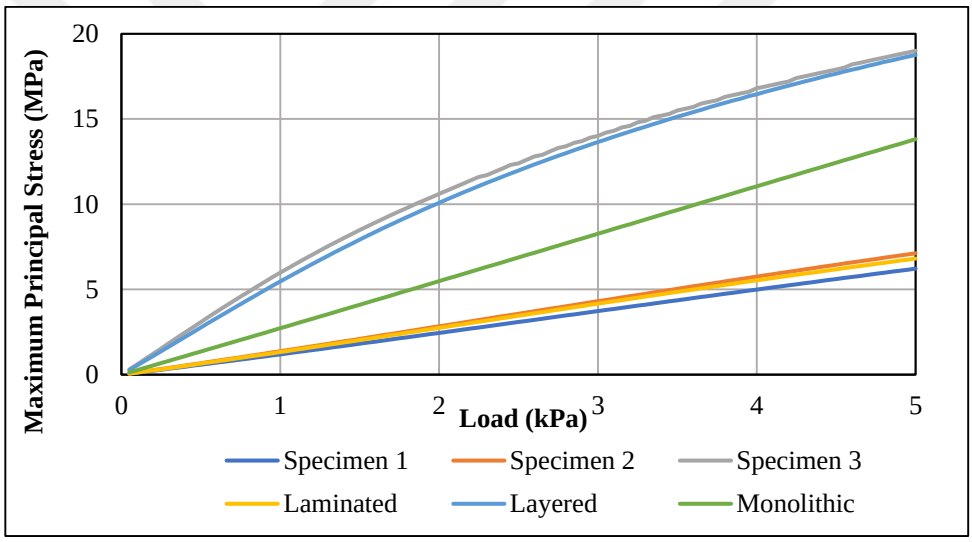

Figure 4.86. Maximum principal stresses on the bottom surface of the top glass.

Figures 4.87-4.88 show the maximum principal stresses against different load values for the top and bottom surface of the bottom glass unit. The maximum principal stresses on the top surface of the bottom glass are compression. Unlike other glass units, more compression was observed in the layered glass unit. The maximum principal stresses on the bottom surface of the top glass are tension. They do not change sign. The maximum stress was observed in Specimen 3.

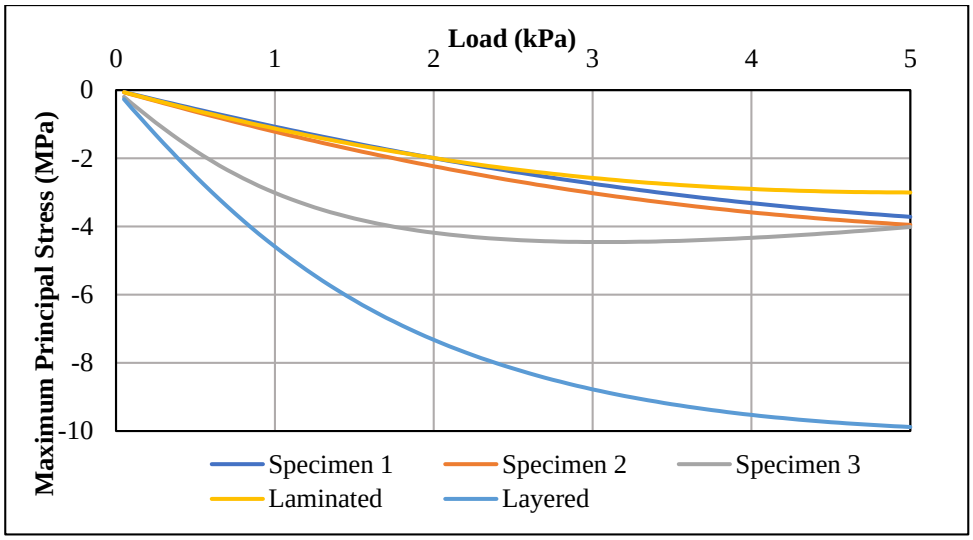

Figure 4.87. Maximum principal stresses on the top surface of the bottom glass.

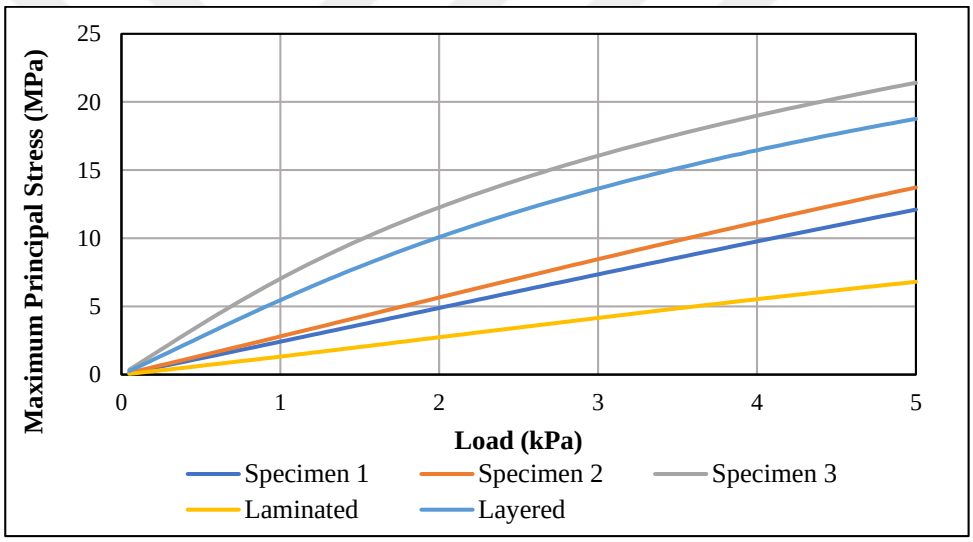

Figure 4.88. Maximum principal stresses on the bottom surface of the glass.

Figure 4.89-4.108 show the contours of the maximum and minimum principal stress values on the top and bottom surfaces of the simply supported quarter laminated glass plate. Maximum principal stress contours are given in Figure 4.89 for the top of Specimen 1 and in Figure 4.90 for the bottom of the unit. The maximum principal stress at the top surface is near the center of the quarter unit. It is observed as compression towards the center and tension towards the corners. The maximum principal stress at the bottom surface is near the center of the unit. It is observed as tension everywhere. Minimum principal stress contours are given in Figure 4.91 for the top of the unit (Specimen 1) and in Figure 4.92 for the bottom of the unit. The minimum principal stress on the top surface is at 0,3 meter of the

quarter unit. It is observed as compression everywhere. The minimum principal stress on the bottom surface is towards the center of the unit. It is observed as tension towards the center, while compression towards the corners.

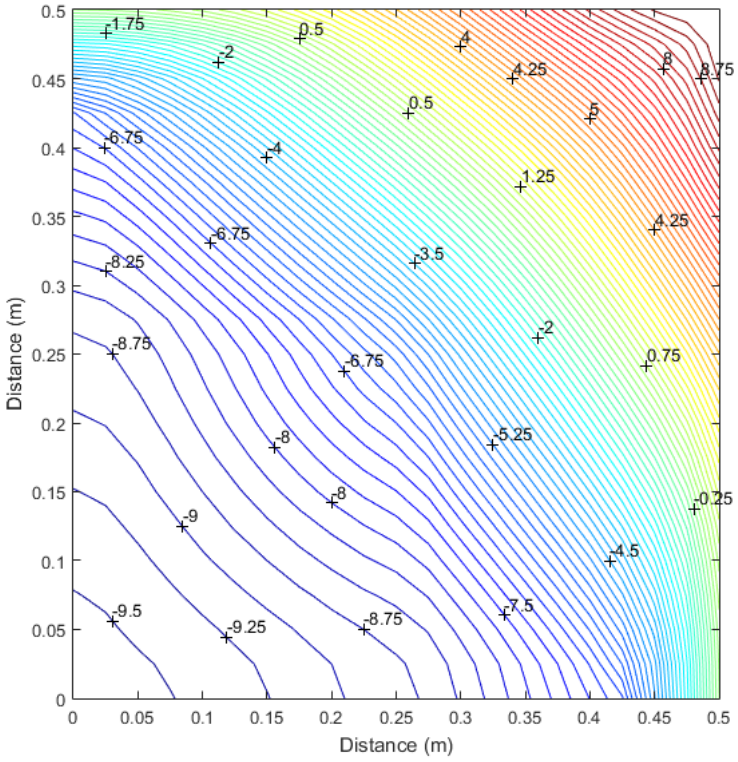

Figure 4.89. Contours of maximum principal stress on the top surface of Specimen 1.

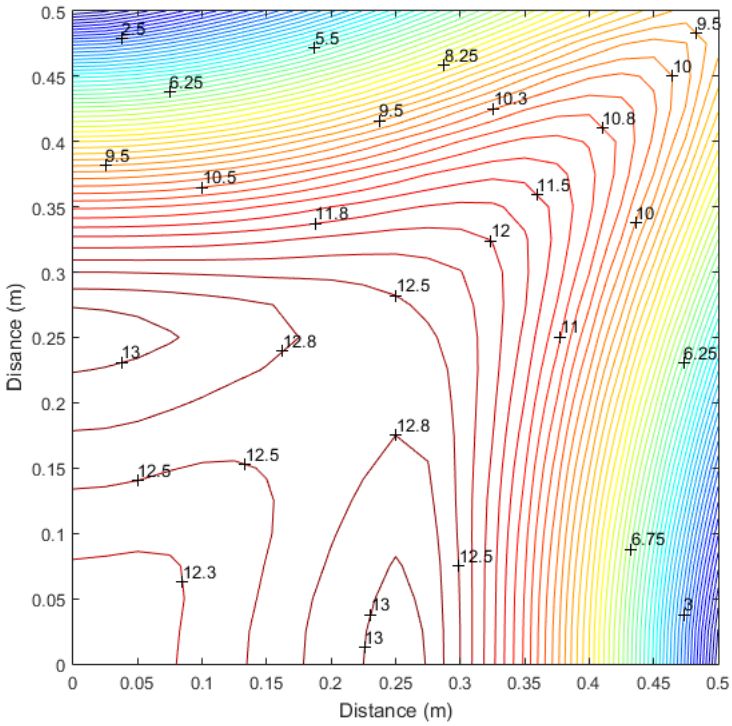

Figure 4.90. Contours of maximum principal stress on the bottom surface of Specimen 1.

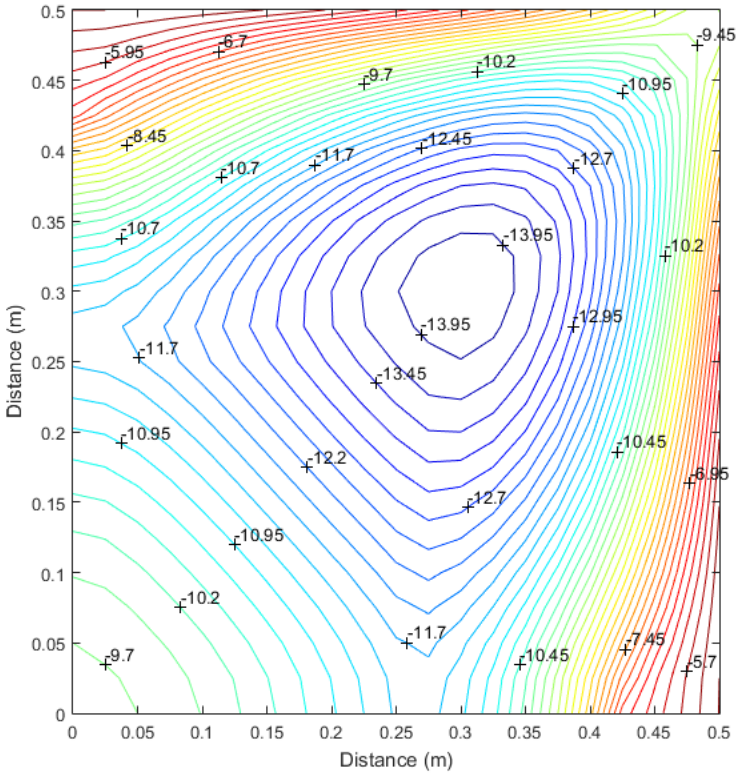

Figure 4.91. Contours of minimum principal stress on the top surface of Specimen 1.

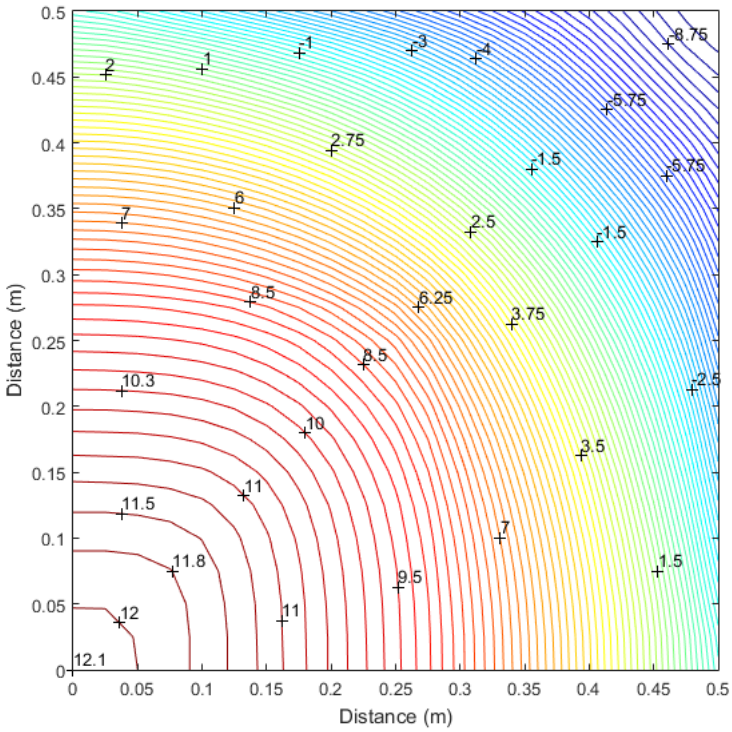

Figure 4.92. Contours of minimum principal stress on the bottom surface of Specimen 1.

Figure 4.93 symbolizes the maximum principal stress contours are given for the top unit (Specimen 2) and Figure 4.94 for the bottom unit. The maximum principal stress at the top surface is near the center of the quarter unit. It is observed as compression towards the center and tension towards the corners. The maximum principal stress at the bottom surface is near the center of the unit. It is observed as tension everywhere. The minimum principal stress contours of Specimen 2 are given in figure 4.95 and 4.96 for the top and bottom surface of the unit. The minimum principal stress on the top surface is towards the centers of the quarter of the unit. It is observed as compression everywhere. The minimum principal stress on the bottom surface is towards the center of the unit. It is observed as tension towards the center, while compression towards the corners.

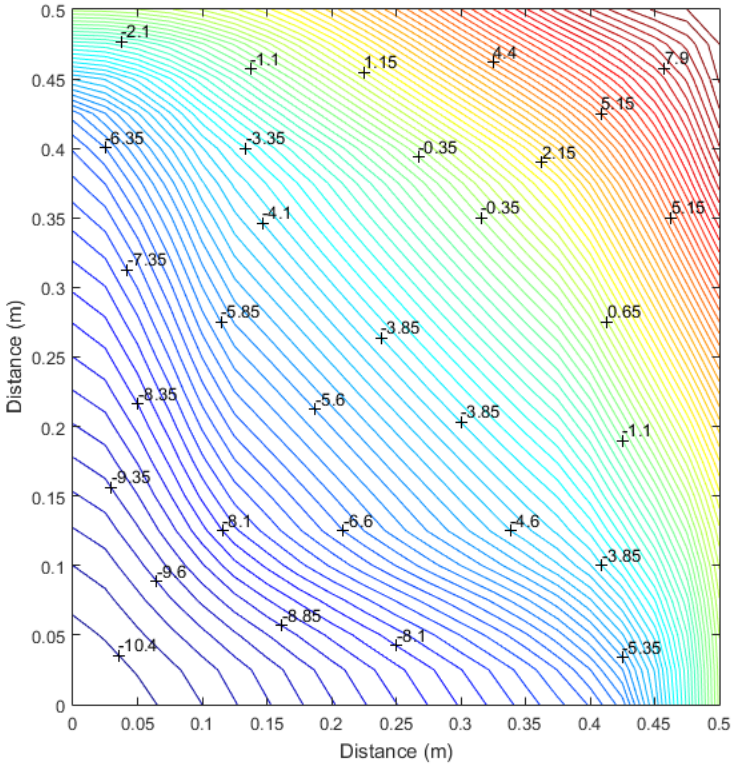

Figure 4.93. Contours of maximum principal stress on the top surface of Specimen 2.

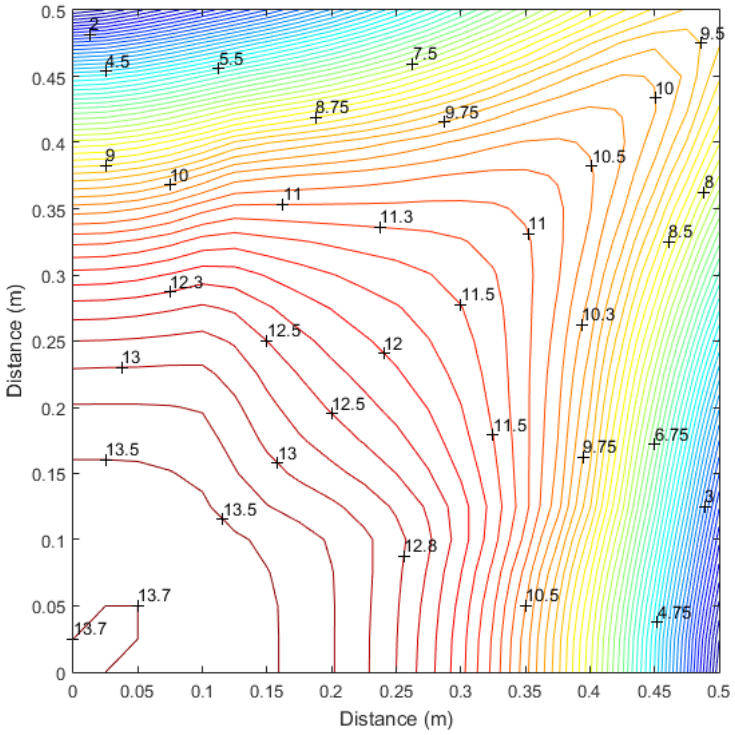

Figure 4.94. Contours of maximum principal stress on the bottom surface of Specimen 2.

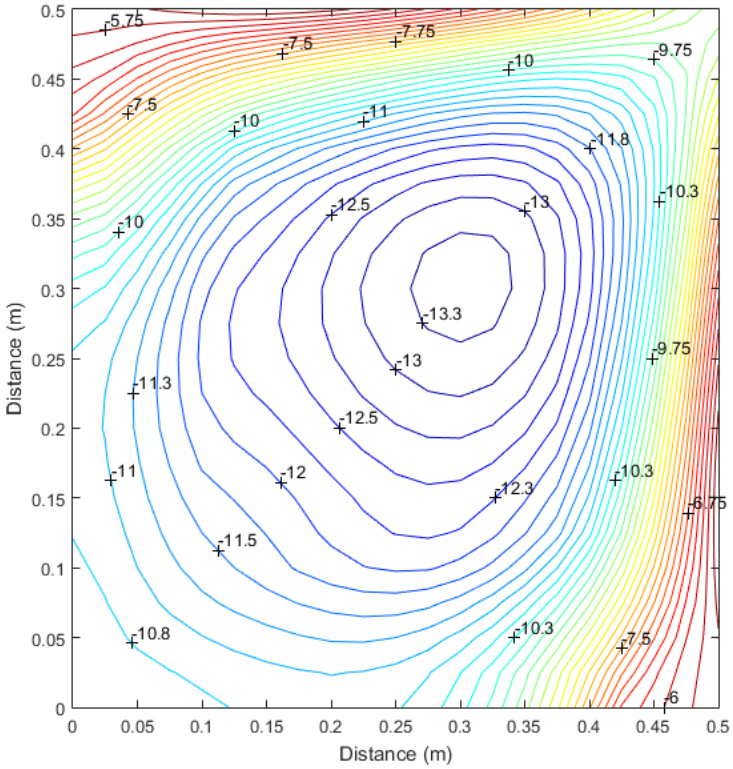

Figure 4.95. Contours of minimum principal stress on the top surface of Specimen 2.

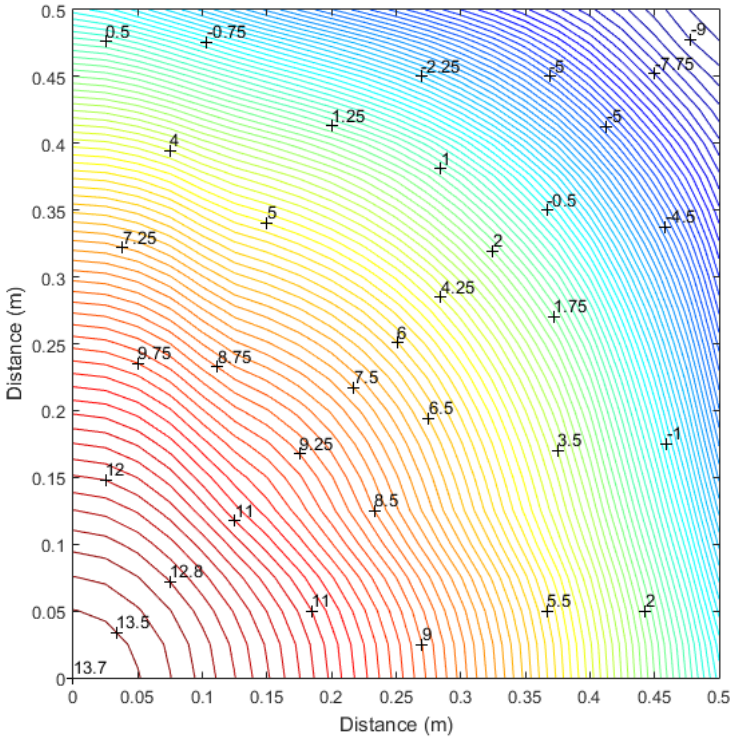

Figure 4.96. Contours of minimum principal stress on the bottom surface of Specimen 2.

Figure 4.97 symbolizes the maximum principal stress contours for top of the Specimen 3 and Figure 4.98 for the bottom unit. The maximum principal stress on the top surface is towards the corners of the unit. It is observed as compression towards the 0,1 point, while tension towards the corners. The maximum principal stress at the bottom surface is near the 0,23 meter of the unit. It is observed as tension everywhere. The minimum principal stress contours are given in Figure 4.99 for the top of the unit which has delamination at the boundary of unit (Specimen 3) and in Figure 4.100 for the bottom unit. The minimum principal stress on the top surface is towards the centers of the quarter unit. It is observed as compression everywhere. The minimum principal stress on the bottom surface is near the 0,13 meter of the unit. It is observed as tension towards the center and compression towards the corners.

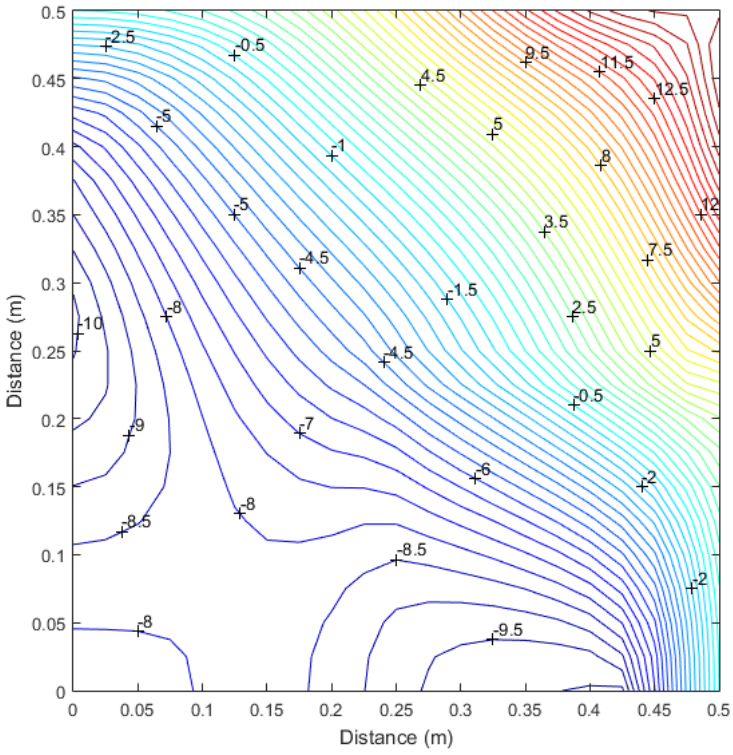

Figure 4.97. Contours of maximum principal stress on the top surface of Specimen 3.

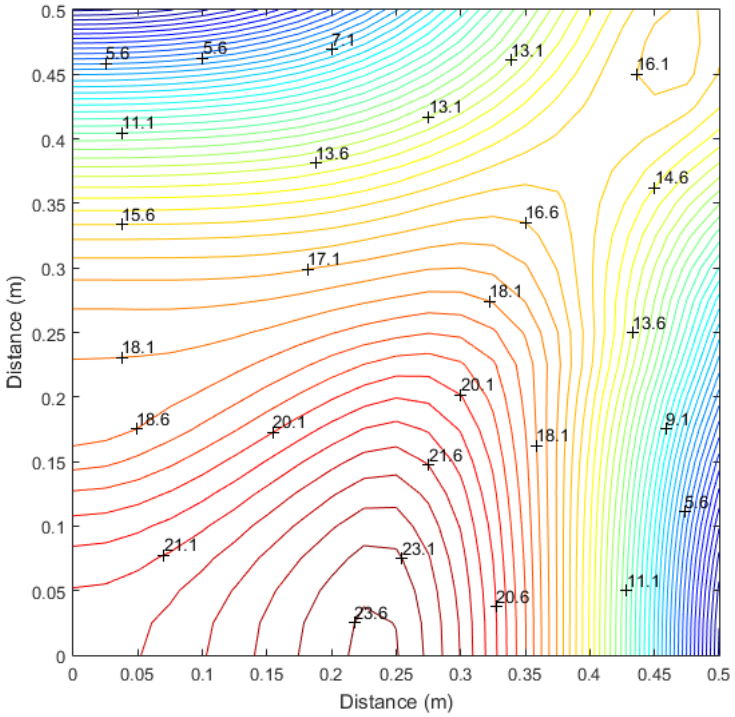

Figure 4.98. Contours of maximum principal stress on the bottom surface of Specimen 3.

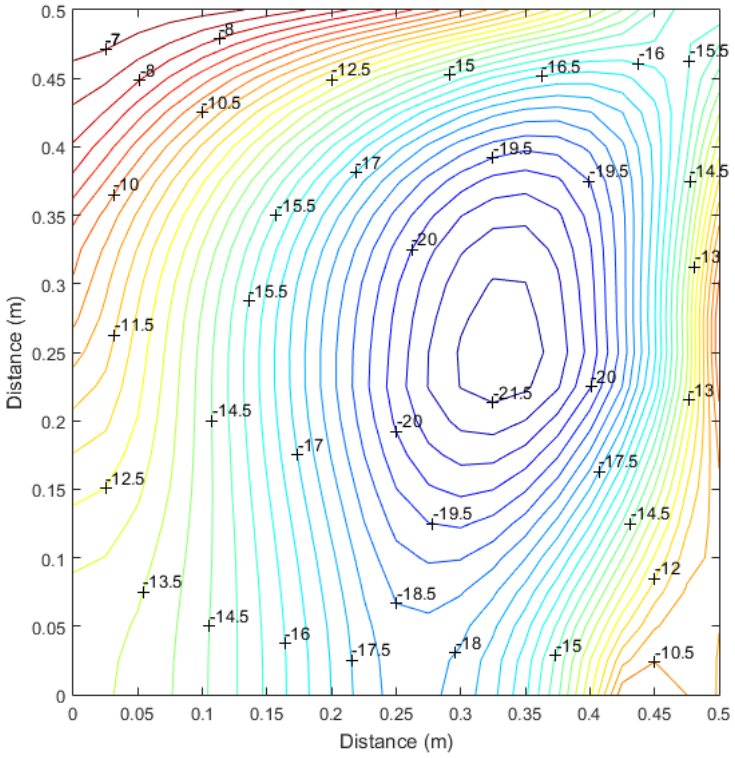

Figure 4.99. Contours of minimum principal stress on the top surface of Specimen 3.

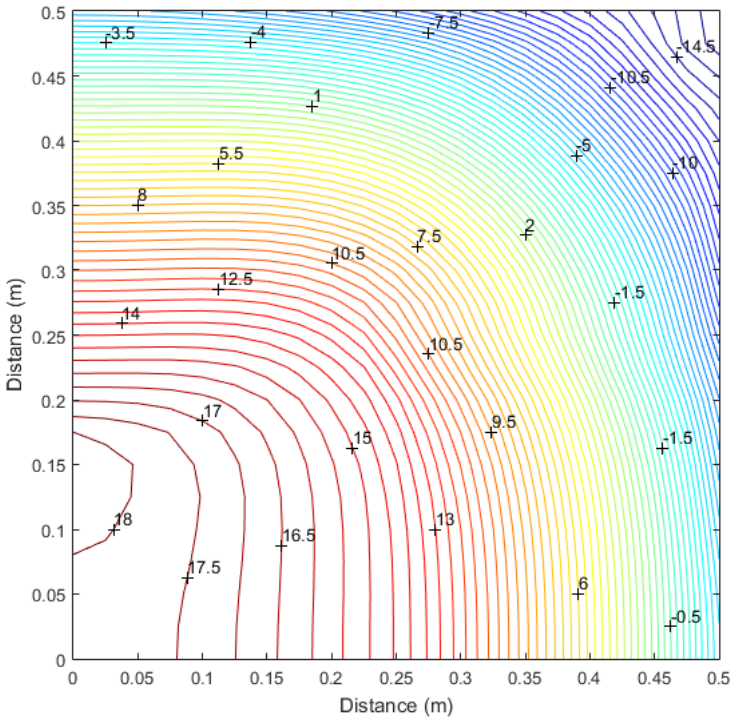

Figure 4.100. Contours of minimum principal stress on the bottom surface of Specimen 3.

Figure 4.101 symbolizes the maximum principal stress contours for the top of the laminated glass unit and Figure 4.102 for the bottom unit. The maximum principal stress at the top surface is at the center of the quarter plate. The maximum principal stress on the bottom surface of the laminated unit is located in the center of the unit.

The minimum principal stress contours are given in Figure 4.103 for the top of the laminated unit and Figure 4.104 for the bottom unit. The minimum principal stress on the bottom and top units of laminated unit are at the center of the quarter plate. The minimum principal stress take positive and negative values on both surface of laminated unit as seen in Figures 4.103 and 4.104.

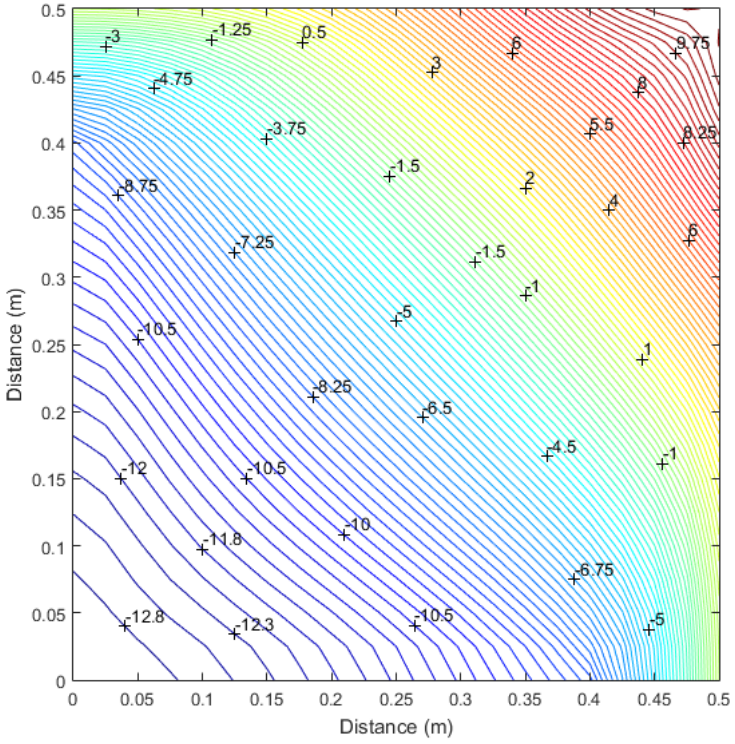

Figure 4.101. Contours of maximum principal stress on the top surface of the laminated glass unit.

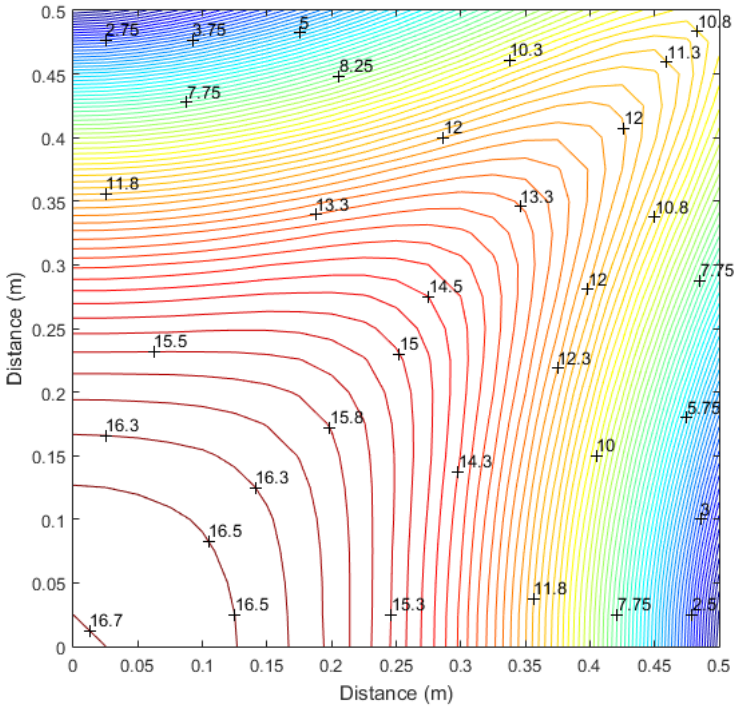

Figure 4.102. Contours of maximum principal stress on the bottom surface of the laminated glass unit.

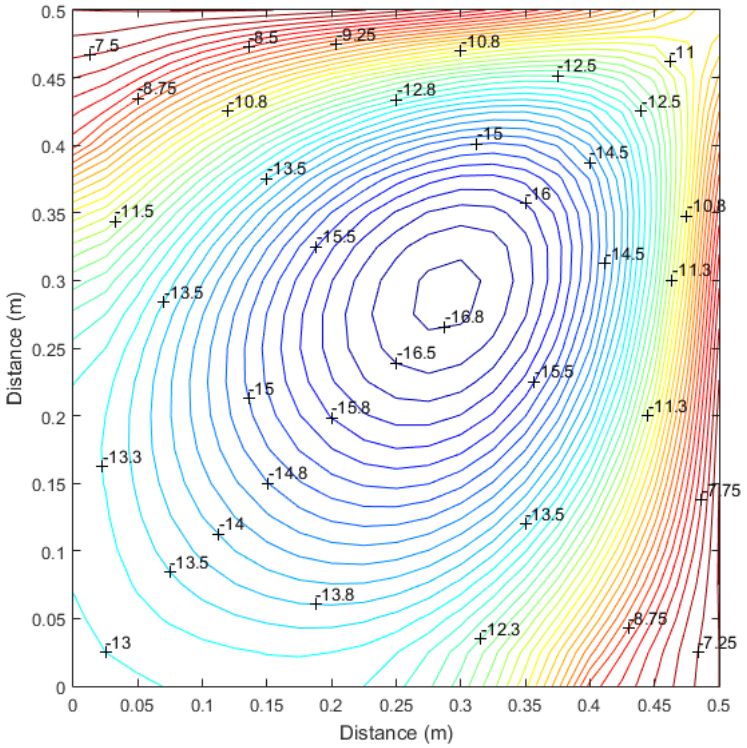

Figure 4.103. Contours of minimum principal stress on the top surface of the laminated glass unit.

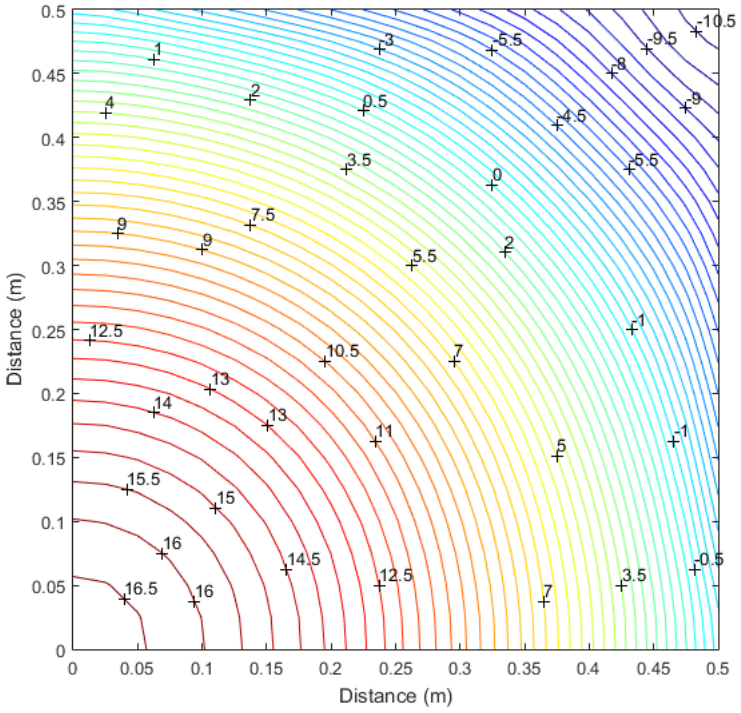

Figure 4.104. Contours of minimum principal stress on the bottom surface of the laminated glass unit.

The contours of the lateral displacements is given for a quarter laminated glass plate unit. Lateral displacement contours are plotted in Figures 4.105-4.108. The maximum lateral displacements is at the center of the unit. Below figures show that displacements are maximum for Specimen 3 which has delamination at the boundary of unit while they are minimum for Specimen 1 which has central delamination.

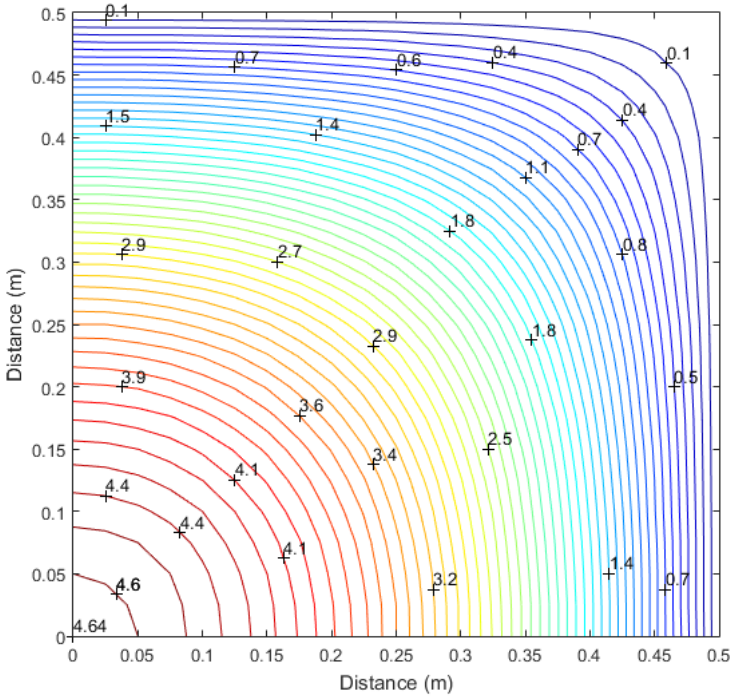

Figure 4.105. Contours of lateral displacement of Specimen 1.

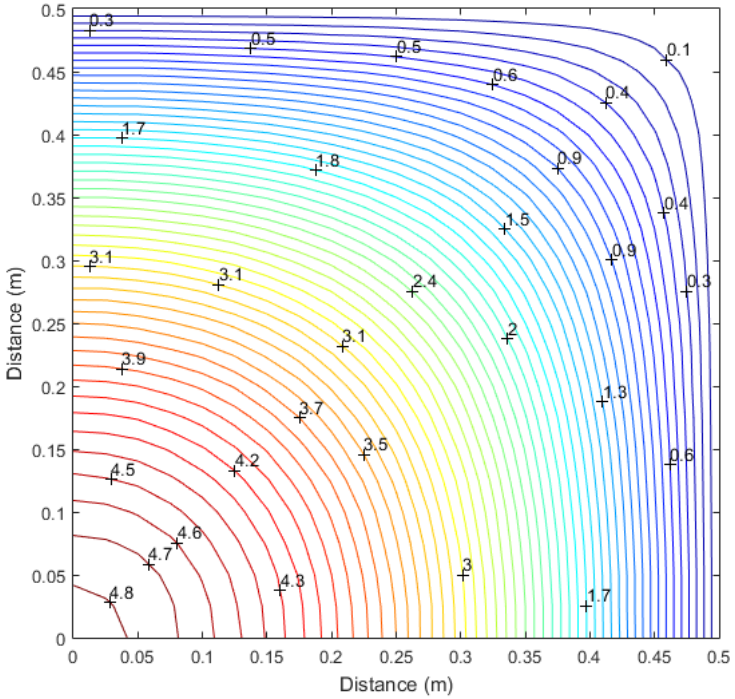

Figure 4.106. Contours of lateral displacement of Specimen 2.

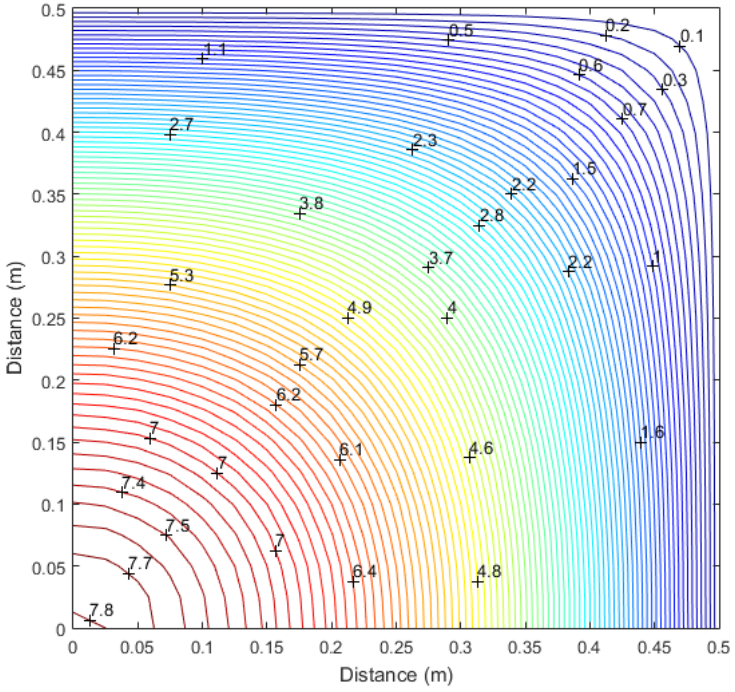

Figure 4.107. Contours of lateral displacement of Specimen 3.

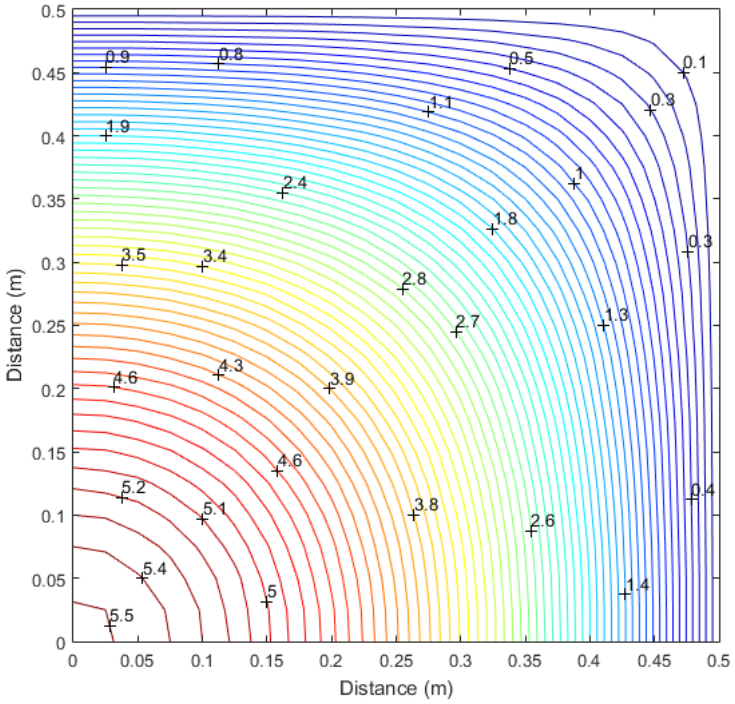

Figure 4.108. Contours of lateral displacement laminated glass unit.

5. CONCLUSION AND RECOMMENDATIONS

Purpose of this chapter is to show the results of improved mathematical model. Nonlinear bending theory developed for laminated glass plate by Aşık (2005) is modified for laminated glass unit subjected to delamination. The Aşık's model includes nonlinear theory of plates. It was developed using variational calculus and minimum potential energy theorem and five nonlinear partial differential equations were had.

In this research, mentioned field equations and boundary conditions of laminated glass unit are rearranged in the delaminated region of the plate. Obtained field equations are transformed into nonlinear algebraic equation systems for delaminated and undelaminated regions of unit. To obtain convergent solution equations are solved iteratively using interpolation parameters. Developed model is capable of solving the problem for different plate geometries, different delamination locations and ratios. In the analysis, based on the field equations a computer program has been developed for the analysis of delaminated glass unit. Obtained solutions are crosschecked with the improved finite element model. The finite element model is solved and generated using the ABAQUS finite element program. The results of the improved model agree with the finite element results.

Delamination analysis of laminated glass plate units was performed using a new mathematical model and finite difference method. The model contains nonlinear plate theory. The minimum potential energy theorem and calculus of variation are used to derive five nonlinear partial differential equations with simply and fixed supported boundary conditions. Obtained field equations are transformed into nonlinear algebraic equation systems for delaminated and undelaminated regions of unit. To obtain convergent solution equations are solved iteratively using interpolation parameters. Developed model is capable of solving the problem for different plate geometries, different delamination locations and ratios. A computer program was developed for the analysis of glass plates with delamination in different regions. A number of state problems for displacements, stresses and strength factors have been solved and acceptable results have been obtained.

The current model is capable of predicting the linear or nonlinear response of delaminated glass plate under different load values and boundary conditions. It may be observed that the level of delaminated units are lower than nonlinearity level of laminated unit. Seperation between lineer and nonlineer solutions starts for smaller load values for delaminated units. This means to make better observations about the behavior of delaminated units nonlinearity should be considered in the analysis.

Displacement and stress values for glass plate subjected to delamination in different regions are obtained for the use of engineers. Strength of simply and fixed supported delaminated glass plates are obtained and compared. Evaluating the obtained results, it is deduced that while the response of laminated unit enclosed by the responses of layered and monolithic units the situation is different for delaminated glass plates.According to the loaction of delaminated region, strength of laminated glass plate could increase or decrease and it can be concluded that the delamination zone has a significant effect on the behavior of laminated glass plates. Plates with delamination in the center has lower stress values than the other delaminated units.

Analysis of laminated and monolithic glass units provides additional information on the behavior of the laminated glass units subjected to uniform lateral pressure using the strength factor analyzes. It can be concluded that strength factors of laminated glass unit vary according to the location of delamination zones. The strength factors of laminated glasses except Specimen 3 are very close to each other and this values varies between 0.7 and 0.8 for fixed support unit. The strength factor for Specimen 3 is observed between 0.4-0.5 for different load values.

5.1. Suggestions for Future Studies

Existing software and solution can be modified for different boundary conditions. Further investigation can be done for different laminated glass plate thicknesses and different delamination zones and different delamination ratios. Delamination analysis of laminated glass plate units can be performed and compared to layered glass units. Temperature influence, delamination size and location, interlayer thickness and aspect ratios can be discussed for future studies.

REFERENCES

Aşık, M.Z. Laminated glass plate: revealing of nonlinear behavior *Computers and Structures*. 2003; 81, 2659-2671.

Aşık, M.Z.; Tezcan, S. A. mathematical model for the behavior of laminated glass beams. *Computers and Structures.* 2005; 83,1742-1753.

Behr, R.A., Minor, J.E., Linden M.P., Vallabhan, C.V.G. Laminated glass units under uniform lateral pressure. *Journal of Structural Engineering.* 1985;111(5):1037e50.

Behr, R.A.; Linden, M.P.; Minor J.E. Load duration and interlayer thickness effects on laminated glass. *Journal of Structural Engineering.* 1986;112(6), 1441-1453.

Coutellier, D., Walrick, J. C., & Geoffroy, P. (2006). Presentation of a methodology for delamination detection within laminated structures. *Composites science and technology*, 66(6), 837-845.

Davies, P., & Cadwallader, R. (1984). Delamination Issues with Laminated Glass–Causes and Prevention. *Glass Processing Days*. Vol Session, 16, 427-430.

Del Linz, P., Hooper, P. A., Arora, H., Wang, Y., Smith, D., Blackman, B. R., & Dear, J. P. (2017). Delamination properties of laminated glass windows subject to blast loading. *International Journal of Impact Engineering*, 105, 39-53.

Dural, E. (2016). Analysis of delaminated glass beams subjected to different boundary conditions. *Composites Part B: Engineering*, 101, 132-146.

Foraboschi, P. (2012). Analytical model for laminated glass plate. *Composites Part B: Engineering*, 43(5), 2094-2106.

Foraboschi, P. Analytical model for laminated glass plate. *Composites Part B: Engineering.* 43 (5), 2094-2106.

Foraboschi, P. Behavior and Failure Strength of Laminated Glass Beams. *Journal of Engineering Mechanics.* 2007; 133 (12), 1290-1301.

Galuppi, L., & Royer-Carfagn, G. (2012). Laminated beams with viscoelastic interlayer. *International Journal of Solids and Structures*, 49(18), 2637-2645.

Hooper, J.A. On the bending of architectural laminated glass. *Int. J. Mech. Sci*.1973: 15; 309-323.

La Saponara, V., Muliana, H., Haj-Ali, R., & Kardomateas, G. A. (2002). Experimental and numerical analysis of delamination growth in double cantilever laminated beams. Engineering Fracture Mechanics, 69(6), 687-699.

Paul, A. (1989). Chemistry of glasses. *Springer Science & Business Media.*

Saxe, T. J., Behr, R. A., Minor, J. E., Kremer, P. A., & Dharani, L. R. (2002). Effects of missile size and glass type on impact resistance of "sacrificial ply" laminated glass. *Journal of Architectural Engineering*, 8(1), 24-39.

Shen, F., Lee, K. H., & Tay, T. E. (2001). Modeling delamination growth in laminated composites. *Composites Science and Technology*, 61(9), 1239-1251.

Vallabhan, C.V.G. Iterative analysis of rectangular glass plates. *Journal of Structural Engineering.* 1983;109(2):489–502.

Vallabhan, C.V.G.; Das, Y.C.; Magdi, M.; Aşık, M.Z.; Bailey J.R. Analysis oflaminated glass units. *Journal of Structural Engineering.* 1993;119(5),1572-1585.

Zhao, S., Dharani, L. R., Chai, L., & Barbat, S. D. (2006). Analysis of damage in laminated automotive glazing subjected to simulated head impact. Engineering Failure Analysis, 13(4), 582-597.

Zou, Z., Reid, S. R., & Li, S. (2003). A continuum damage model for delaminations in laminated composites. *Journal of the Mechanics and Physics of Solids*, 51(2), 333-356.

Zou, Z., Reid, S. R., Li, S., & Soden, P. D. (2002). Application of a delamination model to laminated composite structures. *Composite Structures*, 56(4), 375-389.

T.C.

AYDIN ADNAN MENDERES UNIVERSITY

GRADUATE SCHOOL OF NATURAL AND APPLIED SCIENCE

SCIENTIFIC ETHICAL STATEMENT

I hereby declare that I composed all the information in my master's thesis entitled "DELAMINATION ANALYSIS OF LAMINATED GLASS PLATE STRUCTURES" within the framework of ethical behavior and academic rules, and that due references were provided and for all kinds of statements and information that do not belong to me in this study in accordance with the guide for writing the thesis. I declare that I accept all kinds of legal consequences when the opposite of what I have stated is revealed.

Fulya OYAR

21/01/2022